

DISSERTATION

AN INVESTIGATION OF THE NOVIKOV–VESELOV EQUATION: NEW
SOLUTIONS, STABILITY AND IMPLICATIONS FOR THE INVERSE SCATTERING
TRANSFORM

Submitted by

Ryan P. Croke

Department of Mathematics

In partial fulfillment of the requirements

For the Degree of Doctor of Philosophy

Colorado State University

Fort Collins, Colorado

Spring 2012

Doctoral Committee:

Advisor: Jennifer Mueller

Mark Bradley

Patrick Shipman

Yongcheng Zhou

Copyright by Ryan Patrick Croke 2012

All Rights Reserved

ABSTRACT

AN INVESTIGATION OF THE NOVIKOV–VESELOV EQUATION: NEW SOLUTIONS, STABILITY AND IMPLICATIONS FOR THE INVERSE SCATTERING TRANSFORM

Integrable systems in two spatial dimensions have received far less attention by scholars than their one-dimensional counterparts. In this dissertation the Novikov–Veselov (NV) equation, a (2+1)–dimensional integrable system that is a generalization of the famous Korteweg de–Vries (KdV) equation is investigated. New traveling wave solutions to the NV equation are presented along with an analysis of the stability of certain types of soliton solutions to transverse perturbations. To facilitate the investigation of the qualitative nature of various types of solutions, including solitons and their stability under transverse perturbations, a version of a pseudo-spectral numerical method introduced by Feng [*J. Comput. Phys.*, 153(2), 1999] is developed. With this fast numerical solver some conjectures related to the inverse scattering method for the NV equation are also examined. The scattering transform for the NV equation is the same as the scattering transform used to solve the inverse conductivity problem, a problem useful in medical applications and seismic imaging. However, recent developments have shed light on the nature of the long-term behavior of certain types of solutions to the NV equation that cannot be investigated using the inverse scattering method. The numerical method developed here is used to research these exciting new developments.

TABLE OF CONTENTS

1.	<i>Introduction</i>	1
2.	<i>Current Knowledge of the Novikov–Veselov Equation</i>	7
2.1	Dispersion, Nonlinearity and a Lax Representation	7
2.1.1	Symmetries and Scaling	12
2.1.2	Conservation Laws for the NV equation	16
3.	<i>Closed–Form Solutions to the Novikov–Veselov equation</i>	19
3.1	Traveling Wave Solutions to the NV Equation	20
3.2	General Solution Methods	24
3.2.1	Solutions Using Hirota’s Method	26
3.2.2	Modified Extended Tanh–Function Method	31
3.2.3	Multi–Linear Variable Separation Approach	37
3.2.4	Extended Mapping Approach	39
4.	<i>A Numerical Solver for the NV Equation</i>	51
4.1	A Pseudo–Spectral Method for Solving (2+1) Nonlinear Wave Equations	51
4.2	Implementing the Spectral Method for the NV Equation	52
4.2.1	Linear Numerical Stability Analysis	55
4.2.2	Preservation of the L_2 Norm for the Linear NV Equation	58
4.2.3	Numerical Simulations of Soliton Initial Conditions	59
5.	<i>Instability of Traveling–Wave Solutions of the NV Equation to Transverse Perturbations</i>	63
5.1	Introduction	63
5.1.1	History of the \mathbf{K} –Expansion Method	65
5.2	The Direct \mathbf{K} –Method Applied to the NV Equation	66
5.2.1	Setting up the NV System for Analysis	66
5.2.2	Perturbation Analysis, $k = 0$	68
5.2.3	Perturbation Analysis, $k = 1$	76
5.3	Numerical Estimation of the Growth Rate γ	78
5.4	Numerical Results Concerning the Instabilities of Soliton Solutions to the NV Equation	81
6.	<i>The Inverse Scattering Method for the NV Equation</i>	90
6.1	Numerical Verification of Recent Results Concerning the ISM for the NV Equation	90

6.1.1	Comparing Two Types of Numerical Evolutions of Solutions to the NV Equation	95
6.2	Numerical Experiments Regarding the Soliton Conjecture of the IST for the NV Equation	105
7.	<i>Conclusions</i>	112
	<i>Bibliography</i>	114

LIST OF FIGURES

2.1	A two–soliton solution of the KdV equation. The intersection of the traveling waves shows a phase shift as the only change in the wave after interaction	8
2.2	Two views of the dispersion relation $\omega(k)$ for the NV equation	11
3.1	One–soliton solution to the NV equation using Hirota’s method with parameters $k = 3, t = 1, C = 1,$	28
3.2	Evolution of 2-Soliton solution with $k_1 = 1, k_2 = 2$	29
3.3	Time snapshots of a two–soliton solution with choices $k_1 = 1, k_2 = 2$ from a view perpendicular to the direction of motion	30
3.4	A solution of the NV Equation found using the extended tanh–function method. It corresponds to Case 2 (pg. 35), $\lambda = 3, k = 4, l = 2, t = 0$	36
3.5	A static solution to the NV equation	47
3.6	Time snapshots of a breather solution derived using the EMA.	48
3.7	Two Views of the two–soliton solution derived using the EMA. Left: Interacting solitons, Right: Contour view of the same interaction	49
4.1	Computed L^2 norms of the numerical evolutions for $u(x, y, 0) = -2\text{sech}^2x$, left: $\ u(t)\ _{L^2}$, with time ranging $0 \leq t \leq 10$, right: $\ u(t)\ _{L^2}$, with time ranging $0 \leq t \leq 40$	60
4.2	Three views comparing the initial condition u_0 and its numerical evolution at $t = 10$	61
4.3	Three views comparing the initial condition u_0 and its numerical evolution at $t = 40$	62
5.1	Numerical Approximation for the Growth Rate γ	80
5.2	A profile of the initial condition $u_{IC}(x, y, 0) = -2 \text{sech}^2(x)$ in the yz -plane	81
5.3	A profile of the perturbed initial condition $u_p(x, y, 0) = \left(1 - \epsilon \cos\left(\frac{2\pi}{W_y}y\right)\right) \cdot (-2 \text{sech}^2x)$ in the yz -plane	81
5.4	Initial Condition, $u_{IC}(x, y, 0) = -2 \text{sech}^2(x)$, used in the numerical evolution to study transverse stability	83
5.5	Perturbed IC, $u_p(x, y, t) = \left(1 - \epsilon \cos\left(\frac{2\pi}{W_y}y\right)\right) (-2 \text{sech}^2x)$ at $t = 30.48$. This figure shows a singularity forming.	84
5.6	Contour View of $u_p(x, y, t) = \left(1 - \epsilon \cos\left(\frac{2\pi}{W_y}y\right)\right) (-2 \text{sech}^2x)$ at $t = 30.48$. This figure shows a singularity forming.	85
5.7	$u_P(x, y, 70)$ with restricted amplitude throughout the evolution “capped” at -5.	86

5.8	$u_P(x, y, 70)$ with restricted amplitude throughout the evolution “capped” at -5, contour view.	86
5.9	Contour view, $t = 5$ with amplitude capping.	87
5.10	Contour view, $t = 10$ with amplitude capping.	87
5.11	Contour view, $t = 15$ with amplitude capping.	87
5.12	Contour view, $t = 20$ with amplitude capping.	87
5.13	Contour view, $t = 25$ with amplitude capping.	88
5.14	Contour view, $t = 30$ with amplitude capping.	88
5.15	Contour view, $t = 35$ with amplitude capping.	88
5.16	Contour view, $t = 40$ with amplitude capping.	88
5.17	Contour view, $t = 45$ with amplitude capping.	89
5.18	Contour view, $t = 50$ with amplitude capping.	89
6.1	The initial condition of conductivity type, equation (6.1.17)	96
6.2	Comparison of the Spectral Method with the ISM for times $\tau = 0.0001,$ $0.0002, 0.0003, 0.0004$	97
6.3	Comparison of the Spectral Method with the ISM for times $\tau = 0.0005,$ $0.0006, 0.0007, 0.0008$	98
6.4	Comparison of the Spectral Method with the ISM for times $\tau = 0.0009, 0.001$	99
6.5	Comparison of the Spectral Method with the ISM for times $\tau = 0.0001,$ 0.0002 using contour plots	100
6.6	Comparison of the Spectral Method with the ISM for times $\tau = 0.0003,$ 0.0004 using contour plots	101
6.7	Comparison of the Spectral Method with the ISM for times $\tau = 0.0005,$ $0.0006,$ using contour plots	102
6.8	Comparison of the Spectral Method with the ISM for times $\tau = 0.0007,$ 0.0008 using contour plots	103
6.9	Comparison of the Spectral Method with the ISM for times $\tau = 0.0009,$ $0.001,$ using contour plots	104
6.10	Evolution of equation (6.2.5), $q_{NC}, t=0,0.05,0.1$	108
6.11	Evolution of equation (6.2.5), $q_{NC}, t=0.15,0.2,0.25,$	109
6.12	Evolution of equation (6.2.5), $q_{NC}, t=0.3,0.35,0.4$	110
6.13	Evolution of equation (6.2.5), $q_{NC}, t=0.45,0.5$	111

1. INTRODUCTION

Mathematicians have a zeal for finding solutions to differential equations, equations that involve unknown functions and the derivatives of the unknown functions. Linear differential equations have been studied for hundreds of years and there exists a great base of knowledge regarding how to solve them. However, a greater challenge is to find solutions to Nonlinear Partial Differential Equations (NLPDE). It is a struggle because there are very few general methods for finding solutions. In fact, until the early 1970's, there were almost no general methods for solving NLPDE.

NLPDE are also of great practical and theoretical interest to mathematicians, physicists, and any scientist hoping to be able to both solve complex equations and model interesting and possibly chaotic physical phenomena. While all differential equations are simple approximations to observed phenomena, linear differential equations are generally a more simplistic approximation than nonlinear differential equations.

An important subset of NLPDE are those equations with soliton solutions, solutions that can be characterized by their rather counter-intuitive behavior. The fundamental characteristic of solitons is their stability. When solitons pass through each other, they retain their identity after the interaction. This is in contrast to one's everyday experience. We do not expect to see waves on the ocean crash into each other violently and come out of the interaction unchanged. But, this is exactly what soliton waves do, and indeed, it is seen most famously in water waves.

The first recognized soliton was observed by the Scottish naval engineer John Scott-Russell in 1834. While observing the motion of a boat in a narrow channel he observed what he called a "Wave of Translation." His key observation was that this wave "continued

its course along the channel apparently **without change of form or diminution of speed.**” Besides Russell, not much work was done on this until 1895 when Korteweg and De-Vries derived an equation [38] to model this phenomena, which is known as the Korteweg De-Vries equation (KdV):

$$u_t + 6uu_x + u_{xxx} = 0. \quad (1.0.1)$$

The canonical traveling wave solution to the KdV [1] is

$$u(x, t) = \frac{c}{2} \operatorname{sech}^2 \left[\frac{\sqrt{c}}{2}(x - ct - a) \right]$$

where c and a are constants.

The development of the soliton, and soliton theory, was cited by Griffiths [73] in a discussion of mathematics as we entered the new millennium: “One of the most remarkable achievements of mathematics of the latter half of the 20th century is the theory of solitons...” In particular, this quote refers to the *inverse scattering method* (ISM), a generalization of Fourier transforms to NLPDE that was developed while studying soliton equations.

Soliton NLPDE are often referred to as integrable systems because of their solvability by the ISM. The ISM was originally developed by Gardner, Greene, Kruskal and Muira [27] in 1967 in an effort to solve the Korteweg De–Vries (KdV) equation, the most famous soliton equation.

This was a tremendous breakthrough in nonlinear mathematics, and the field developed quickly. The landmark accomplishments began with Peter Lax suggesting there are more equations like KdV in 1968 [45]. After that, there was the impressive discovery of the integrability of the nonlinear Schrödinger equations by Zakharov and Shabat in 1972 [74]. The most notable accomplishment was the general outline of the ISM by Ablowitz, Kaup, Newell, and Segur (AKNS) in 1974 [2].

The ISM is a very powerful method for solving nonlinear PDE’s because it turns a

nonlinear PDE into a system of decoupled linear ordinary differential equations through transformations called *inverse scattering transformations*. AKNS generalized this method to a class of nonlinear equations that included the KdV equation, the Sine-Gordon equation and the nonlinear Schrödinger equation. If an inverse scattering transformation exists for a given NLPDE, the equation is said to be *integrable*. It is conjectured that NLPDE have inverse scattering transformations if and only if the PDE admits soliton solutions. All of the results mentioned so far are for (1+1)-dimensional equations, that is, equations that have one spatial dimension and one temporal dimension. The study of soliton equations has led to deep mathematical and physical results since the late 1960's but the extensions of these results to multidimensional soliton equations came post 1970.

The first widely studied (2 + 1)-dimensional soliton equation was the Kadomtsev-Petviashvili equation (KP) [34], derived in 1970,

$$(u_t + uu_x + u_{xxx})_y + \lambda u_{yy} = 0, \quad \lambda = \pm 1. \quad (1.0.2)$$

Kadomtsev and Petviashvili were considering the problem of the stability of solitons of the KdV equation with respect to transverse perturbations, and in this context they derived a two-dimensional generalization of the KdV equation that became known as the KP equation.

The equation of interest in this work is the Novikov–Veselov (NV) equation, another (2 + 1)-dimensional generalization of the KdV equation first discussed in the periodic setting by Novikov and Veselov [54, 55] in 1984. It was very recently proved (2012) that the NV equation is an integrable system [43, 56]. Solving the NV equation using the ISM was first discussed in 1987 [12] for a certain class of initial values and has been generalized further by Mueller et. al. [43, 42]. The NV equation was originally stated as a D-bar equation for $u(z, t)$ with $z = x + iy \in \mathbb{C}$,

$$u_t = \partial^3 u + \bar{\partial}^3 u + 3\partial(u\nu) + 3\bar{\partial}(u\bar{\nu}), \quad (1.0.3)$$

$$\bar{\partial}\nu = \partial u, \quad (1.0.4)$$

with $\bar{\partial} = \frac{1}{2}(\partial_x + i\partial_y)$ and $\partial = \frac{1}{2}(\partial_x - i\partial_y)$. If we consider real solutions, $u(t) \in \mathbb{R}$ for all t , and let $\nu(x, y, t) = v(x, y, t) + iw(x, y, t)$, the NV equation has an equivalent representation in (x, y) -space,

$$0 = 4u_t + u_{xxx} - 3u_{xyy} - 3(uv)_x - 3(uw)_y, \quad (1.0.5)$$

$$u_x = v_x - w_y, \quad (1.0.6)$$

$$u_y = -w_x - v_y. \quad (1.0.7)$$

While the KP equation is derived by looking at transverse perturbations to the KdV equation, the NV equation is derived algebraically from a Lax triple, which will be discussed later, and from this point of view is considered the most natural generalization of the KdV equation [10]. There are other (2+1)-dimensional generalizations of KdV, most notably the Nizhnik–Novikov–Veselov (NNV) equation,

$$0 = u_t + au_{xxx} + bu_{yyy} - 3a(uv)_x - 3b(uw)_y, \quad (1.0.8)$$

$$u_x = v_y, \quad (1.0.9)$$

$$u_y = w_x. \quad (1.0.10)$$

Equations 1.0.8 – 1.0.10 are very similar to the NV equation and have applications such as a model for an incompressible fluid [20].

The goal of this dissertation is to help increase the general knowledge of (2+1) soliton equations by presenting various results related to the NV equation.

Particular attention will be paid to four areas: new traveling wave solutions, a numeri-

cal solver, stability of soliton solutions, and numerical experiments relating to conjectures regarding the relationship between certain types of soliton solutions and the ISM.

First, new traveling wave solutions were derived by applying the extended mapping approach, a general method that extends separation of variables to NLPDE. Some new multisoliton solutions were also derived using Hirota's method that will enable investigation into the stability of multisoliton solutions. Using the extended tanh-function method some traveling wave solutions with finite time blow-up were also derived.

Next, we show soliton solutions to (1.0.5) – (1.0.7) are unstable to long wavelength transverse perturbations and verify these results numerically. A numerical solver has been developed to detail this result and investigate the long term behavior of the perturbed solitons. This is the first application of a spectral numerical method to a system of nonlinear PDE's. To approximate the growth rate of the instability as a function of the wave vector of the perturbation, a different numerical scheme was created and implemented.

Lastly, some conjectures concerning the inverse scattering method are investigated using the numerical scheme developed here. As will be discussed in detail in Chapter 6, an important class of functions that is used as initial data to solve the Cauchy problem for the NV equation is called *functions of conductivity-type*. In Chapter 6, evolutions of initial data of conductivity-type are compared to evolutions of functions that are not of conductivity type in an effort to elucidate some conjectures regarding the existence of solitons (of non-plane wave type). The results presented here can lead to future paths of research including multisoliton stability and stability of all types of perturbations, not simply transverse ones.

In this thesis I show the existence of various types of soliton solutions to the NV equation, and develop methods to help find soliton solutions that may be of use in the development of the ISM for the NV equation. I perform an analytical stability analysis for plane wave soliton solutions of KdV type of the NV equation. The nature of the instability is examined using numerical methods.

The numerical code developed in this thesis is used in conjunction with the pre-existing

numerical implementation of the ISM to investigate the validity of more general sets of initial conditions than those introduced in [42] and [43]. In particular, I consider initial conditions of non conductivity-type that are rapidly decaying and computed their evolutions and have found strong numerical evidence of soliton solutions, supporting the conjecture of their existence, explained in Chapter 6.

The work in this dissertation is significant because it is the first thorough study of soliton solutions to the NV equation, an important equation because it is a soliton equation that is a system of PDE's and it is a generalization of KdV. The numerical spectral method presented here is the first implementation for a NLPDE system. There is no study of soliton stability for NV in the literature, and this work applies the K-method to a NLDPE system (NV). It provides visual insight into the nature of solutions through numerical computations, and it provides a means to study conjectures about the integrability of NV and the ISM. We compute the evolution by the ISM and check if it agrees with the results of the numerical code for the NV equation evolutions developed in this thesis.

2. CURRENT KNOWLEDGE OF THE NOVIKOV–VESELOV EQUATION

2.1 Dispersion, Nonlinearity and a Lax Representation

Solitons form when there is a ‘balance’ between nonlinearity and dispersion. In general, one would expect waves in a nonlinear system to become incoherent in the sense that the nonlinearity would cause shocks and waves to break. Moreover, the higher order derivative terms of odd order bigger than three will cause dispersion, which, for a linear equation, has the effect of pulling waves apart. Even order derivatives cause dissipation, a phenomena not considered here. A soliton wave can be characterized by three properties [17]; They are of permanent form, they are localized within a region and they can interact with other solitons, and emerge from the collision unchanged, except for a phase shift. Figure (2.1) is a graph of the evolution of a two–soliton solution to the KdV equation and shows the interaction of two solitons where the phase shift can be seen after the collision. This amazing balance between dispersion and nonlinearity was found in many applications, but it was the work done at Los Alamos National Laboratory in the 1950’s that catapulted the KdV equation and solitons to high level of interest.

In 1955, Enrico Fermi’s team at Los Alamos began looking at the equipartition of energy in a lattice that modeled atomic interaction using vibrating strings [26]. They added small nonlinear terms between the atoms and simulated the dynamics numerically. This setup yielded a curious result. The expectation was that there would be a thermalization of the energy, that there would be an ergodic end state. But, what they found was that the energy states became periodic, a totally unexpected result. The model they built can be

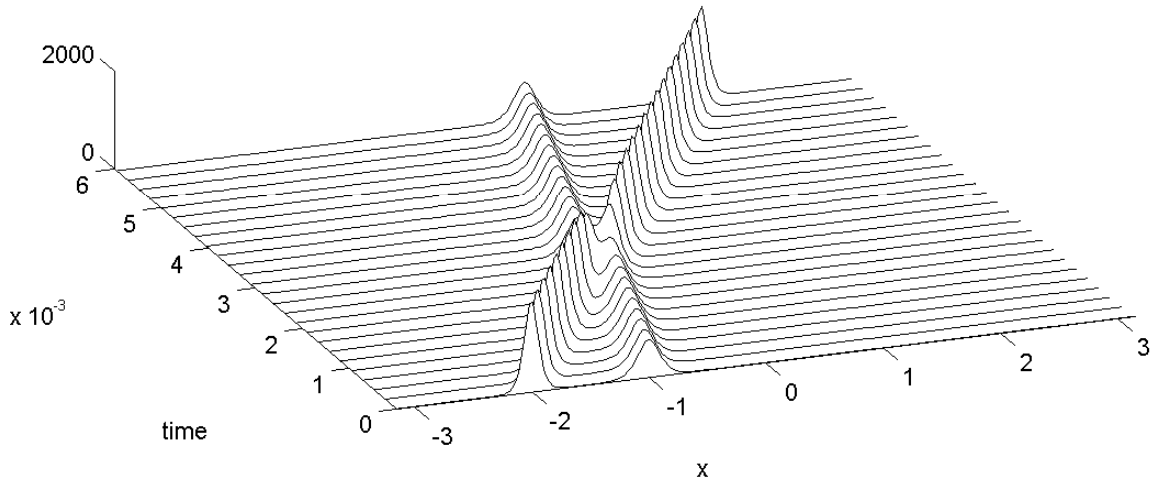


Fig. 2.1: Two-soliton interaction for the KdV equation

reduced to the KdV equation, and thus contains soliton solutions. The solitons were propagating the energy periodically. These permanent waves of translation would not allow for thermalization. This problem is now known as the Fermi-Pasta-Ulam (FPU) problem and was the genesis of contemporary soliton research.

Another milestone occurred in the late 1960's when the KdV equation was found to have an infinite number of conserved quantities. This observation drew a considerable amount of attention and research into NLPDE and soliton equations. This result was codified in 1968 with Peter Lax's publication deriving the conservation laws for the KdV equation using an algebraic formalism. To do this, let the evolution equation be written as $u_t = K(u)$ where K is the nonlinear operator. Let the function u be in a closed (under the evolution of $u(t)$) space, and associate with it a self-adjoint operator L in a suitable Hilbert space, $u \rightarrow L_u$ such that the following holds: If u changes with t subject to the equation $u_t = K(u)$ the operator $L(t)$ remains unitary equivalent as it changes with t . If this is the case, then the eigenvalues of L are the integrals, or conserved quantities, of u .

The unitary equivalence of L means there is a one-parameter family of operators $U(t)$ such that the quantity $U(t)^{-1}L(t)U(t)$ is independent of t . A one-parameter family of unitary operators satisfies the differential equation $U_t = BU$ where B is an antisymmetric

operator. Using these facts, we see that

$$L_t = [B, L]$$

where $[\cdot, \cdot]$ is the commutator. If one has the operator L , then it is a simple game to find B . The drawback is that the relationship between u and L is not obvious. In the case of the KdV equation, L is the Schrödinger operator,

$$L = D^2 + \frac{1}{6}u.$$

Once we have the operators, we can find the eigenvalues, and the conserved quantities follow.

The NV equation (1.0.3) has a operator representation, called an L-A-B triple or a Shabat representation, that generalizes the derivation of the KdV equation to two spatial dimensions. From this point of view the NV equation is a more natural generalization of the KdV than the Kadomtsev-Petviashvili equation [10]. For clarity, the KP equation is presented as equation (2.1.1),

$$(u_t + uu_x + u_{xxx})_y + \lambda u_{yy} = 0, \lambda = \pm 1. \quad (2.1.1)$$

Whereas the KP equation is derived from physical considerations consistent with KdV, the NV is a natural algebraic generalization of KdV. We can ask the question, ‘what would be a $(2 + 1)$ generalization of the Lax pair?’ The answer is the L-A-B triple,

$$L = \partial \bar{\partial} + u, \quad A = \partial^3 + \bar{\partial}^3 + v\partial + w\bar{\partial}, \quad B = \partial v + \bar{\partial}w. \quad (2.1.2)$$

It can be shown then that

$$[L, A + \partial_t] = BL$$

if and only if u is a solution to the NV equation,

$$u_t = \partial^3 u + \bar{\partial}^3 u + 3\partial(u\nu) + 3\bar{\partial}(u\bar{\nu}) \quad (2.1.3)$$

$$\bar{\partial}\nu(x, y, t) = \partial u(x, y, t) \quad (2.1.4)$$

where

$$\partial = \frac{1}{2} \left(\frac{d}{dx} - i \frac{d}{dy} \right), \quad \bar{\partial} = \frac{1}{2} \left(\frac{d}{dx} + i \frac{d}{dy} \right), \quad \text{and } \nu = v + iw.$$

Recovering KdV via the L-A-B triple

Using (2.1.2) we can recover the KdV equation. Assume the functions in question are only functions of x and t . Then we can ignore the y -derivative operators in the $L - A - B$ triple above. We find the following

$$\begin{aligned} 0 = [L, A + \partial_t] - BL &= \left(-\frac{u_{xxx}}{4} - u_t - \frac{wu_x}{2} - \frac{vu_x}{2} - \frac{w_x u}{2} - \frac{v_x u}{2} \right) \\ &+ \left(\frac{v_{xx}}{8} + \frac{w_{xx}}{8} - \frac{3}{4}u_{xx} \right) \frac{\partial}{\partial x} \\ &+ \left(\frac{v_x}{8} + \frac{w_x}{8} - \frac{3}{4}u_x \right) \frac{\partial^2}{\partial x^2} \end{aligned} \quad (2.1.5)$$

The last two coefficients must be zero to make the operator multiplicative, i.e.

$$6u_x = v_x + w_x$$

and upon integrating we have

$$6u = v + w + \phi(t)$$

where ϕ is a function of time alone. Using this we find

$$0 = [L, A + \partial_t] - BL$$

if and only if

$$u_t = -\frac{1}{4}u_{xxx} - 3uu_x. \quad (2.1.6)$$

A trivial change of variables transforms (2.1.6) to the classic form of the KdV equation, $u_t = -u_{xxx} - 6uu_x$.

Dispersion, Phase Velocity and Group Velocity

The *dispersion relation* is the relation that gives the frequency as a function of the wave vector $\mathbf{k} = (k_1, k_2)$. To find the dispersion relation, we consider the linear NV equation,

$$u_t = -\frac{1}{4}u_{xxx} + \frac{3}{4}u_{xyy} \equiv -Au. \quad (2.1.7)$$

Consider plane wave solutions of the form $u(x, y, t) = e^{k_1x + k_2y - \omega t}$. Substituting this plane wave solution into equation (2.1.7), we find the dispersion relation for NV is

$$\omega = -\frac{1}{4}k_1^3 + \frac{3}{4}k_1k_2^2. \quad (2.1.8)$$

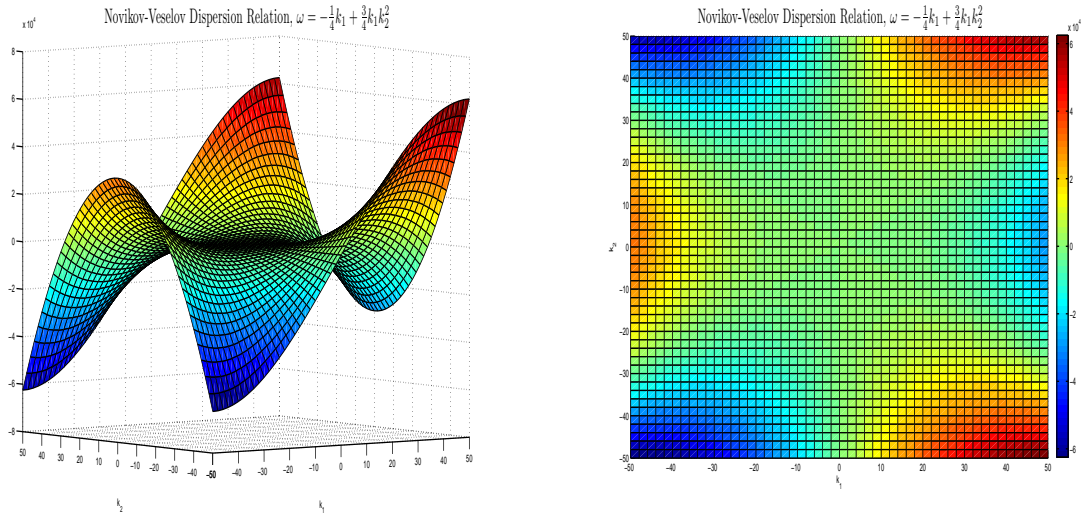


Fig. 2.2: Two views of the dispersion relation $\omega(k)$ for the NV equation

The *phase velocity* \mathbf{c}_p , gives the velocity of the wavefronts of the sinusoidal mode [16],

is defined by $\mathbf{c}_p = \frac{\omega(\mathbf{k})}{|\mathbf{k}|^2}(k_1, k_2)$ and for the NV equation is

$$\mathbf{c}_p = \frac{k_1^3 - 3k_1k_2^2}{4(k_1^2 + k_2^2)^{3/2}} \langle k_1, k_2 \rangle. \quad (2.1.9)$$

Having established the dispersion relation $\omega(\mathbf{k})$ and the phase velocity \mathbf{c}_p for the NV equation, we turn our attention to the *group velocity*. The group velocity is a vector defined componentwise as [69]

$$C_j(\mathbf{k}, \mathbf{x}, t) = \frac{\partial \omega}{\partial k_j}.$$

The group velocity gives the velocity of the wave packet, that is, a group of waves with nearly the same length $2\pi/|\mathbf{k}|$. The group velocity for NV is

$$\mathbf{c}_g \equiv \nabla \omega = \frac{3}{4} \langle -k_1^2 + k_2^2, 2k_1k_2 \rangle.$$

The magnitudes of the phase velocity is $|\mathbf{c}_p| = \frac{1}{4|\mathbf{k}|^2}(k_1^3 - 3k_1k_2^2)$ and the magnitude of the group velocity is $|\mathbf{c}_g| = \frac{3}{4}|\mathbf{k}|^2$. Thus, the group velocity is bounded below by 0, and the sign of the phase velocity depends on $\text{sgn}(k_1^3 - 3k_1k_2^2)$.

2.1.1 Symmetries and Scaling

We would like to find how scaling of the dependent and independent variables change the NV equation. For this effort let us first consider the D-bar equation presented in equation (1.0.4),

$$\bar{\partial} \nu = \partial u.$$

Replace the function ν with r by

$$r(x, y, t) = \gamma \nu(\alpha t, \beta x, \beta y).$$

Then

$$\frac{\partial}{\partial x} r(x, y, t) = \beta\gamma \frac{\partial}{\partial x} \nu(\alpha t, \beta x, \beta y) \quad (2.1.10)$$

$$\frac{\partial}{\partial y} r(x, y, t) = \beta\gamma \frac{\partial}{\partial y} \nu(\alpha t, \beta x, \beta y) \quad (2.1.11)$$

Similarly, let

$$s(x, y, t) = \gamma u(\alpha t, \beta x, \beta y).$$

With these choices of scalings the D-bar equation (1.0.4) remains unchanged,

$$\bar{\partial} \nu = \partial u \quad \iff \quad \bar{\partial} r = \partial s.$$

Now, we examine the main equation as presented in equation (1.0.5). For what follows let us define \vec{r} as $\vec{r}(x, y, t) = r_1(x, y, t) + ir_2(x, y, t)$. We find the following transformations,

$$\begin{aligned} \frac{d}{dt} s(x, y, t) &= \alpha\gamma \frac{d}{dt} u(\alpha t, \beta x, \beta y), \\ \frac{\partial^3}{\partial x^3} s(x, y, t) &= \beta^3\gamma \frac{\partial^3}{\partial x^3} u(\alpha t, \beta x, \beta y), \\ \frac{\partial^3}{\partial x \partial y^2} s(x, y, t) &= \beta^3\gamma \frac{\partial^3}{\partial x \partial y^2} u(\alpha t, \beta x, \beta y), \\ \frac{\partial}{\partial x}(uv) + \frac{\partial}{\partial y}(uw) &= \gamma^2\beta \left(\frac{\partial}{\partial x}(sr_1) + \frac{\partial}{\partial y}(sr_2) \right) \end{aligned}$$

Assuming u and \vec{z} is a solution to the NV equation (1.0.5), we find

$$\begin{aligned} 4u_t &= -u_{xxx} + 3u_{xyy} + 3(uv)_x + 3(uy)_y \\ \implies \frac{4}{\alpha\gamma} s_t &= -\frac{1}{\beta^3\gamma} s_{xxx} + \frac{3}{\beta^3\gamma} s_{xyy} + \frac{3}{\beta\gamma^2} (sr_1)_x + \frac{3}{\beta\gamma^2} (sr_2)_y. \end{aligned}$$

Multiplying by $\alpha\gamma$ leads to

$$4s_t = -\frac{\alpha}{\beta^3} s_{xxx} + \frac{3\alpha}{\beta^3} s_{xyy} + \frac{3\alpha}{\beta\gamma} ((sr_1)_x + (sr_2)_y). \quad (2.1.12)$$

The table below shows the possible sign conventions possible for each term of the right hand side of equation (2.1.12).

α	β	γ	Signs in (2.1.12)		
+	+	+	-	+	+
-	-	+	-	+	+
-	+	+	+	-	-
+	-	+	+	-	-
+	+	-	-	+	-
-	-	-	-	+	-
-	+	-	+	-	+
+	-	-	+	-	+

We conclude:

1. There is a fixed ratio of -3 of the coefficients of the linear spatial terms, and
2. Any other coefficient is possible by proper rescaling of independent and dependent variables.

We also consider under what rotations the Novikov-Veselov is invariant. Recall the NV equation

$$u_t = -\partial^3 u - \bar{\partial}^3 u + 3\partial(u\nu) + 3\bar{\partial}(u\bar{\nu}), \quad (2.1.13)$$

$$\bar{\partial}\nu = \partial u. \quad (2.1.14)$$

If u is real at time t_0 , then

$$\begin{aligned} \bar{u}_t &= \overline{-\partial^3 u - \bar{\partial}^3 u + 3\partial(u\nu) + 3\bar{\partial}(u\bar{\nu})}, \\ &= -\bar{\partial}^3 u - \partial^3 u + 3\bar{\partial}(u\bar{\nu}) + 3\partial(u\nu), \\ &= u_t, \end{aligned}$$

thus

$$\frac{d}{dt} \operatorname{Im} u = \frac{1}{2i} (u_t - \bar{u}_t) = 0,$$

and so u remains real.

To consider rotations let

$$x = x' \cos(\theta) - y' \sin(\theta) \quad (2.1.15)$$

$$y = x' \sin(\theta) + y' \cos(\theta). \quad (2.1.16)$$

Then

$$\frac{\partial}{\partial x} = \frac{\partial}{\partial x'} \cos(\theta) - \frac{\partial}{\partial y'} \sin(\theta) \quad (2.1.17)$$

$$\frac{\partial}{\partial y} = \frac{\partial}{\partial x'} \sin(\theta) + \frac{\partial}{\partial y'} \cos(\theta) \quad (2.1.18)$$

and so

$$\begin{aligned} \partial_z &= \frac{\partial}{\partial x} - i \frac{\partial}{\partial y} = (\cos \theta - i \sin \theta) \frac{\partial}{\partial x'} - (\sin \theta + i \cos \theta) \frac{\partial}{\partial y'} \\ &= e^{-i\theta} \left(\frac{\partial}{\partial x'} - i \frac{\partial}{\partial y'} \right), \end{aligned}$$

i.e. $\partial_z = e^{i\theta} \bar{\partial}_{z'}$. The operator ∂_z is the same as the operator ∂ defined in Chapter 1, however, in order to make the rotations clearer we needed to introduce the notation ∂_z .

Equation (2.1.13) becomes

$$u_t = e^{i\theta} \partial_{z'} (\nu' u) + e^{i\theta} \bar{\partial}_{z'} (\bar{\nu}' u) - e^{-3i\theta} \bar{\partial}_{z'}^3 u - e^{-3i\theta} \partial_{z'}^3 u \quad (2.1.19)$$

where $\nu' = e^{-i\theta} \nu$. The auxiliary equation becomes

$$e^{i\theta} \bar{\partial}_{z'} \nu = e^{i\theta} \partial_{z'} u$$

or

$$\bar{\partial}_{z'} v' = e^{-3i\theta} \partial_{z'} u$$

so we have invariant solutions under rotations of $2\pi/3$ and $4\pi/3$. This shows that if a solution to the NV equation has this symmetry, it must be preserved under the evolution. It does not mean that all solutions will display this type of symmetry.

2.1.2 Conservation Laws for the NV equation

Recently, it was shown the NV equation (1.0.3) can be solved using the inverse scattering method of Ablowitz, Newall, Kaup and Segur for a certain class of initial data [56]. In order to present the conservation laws we need to recall some ideas from the inverse scattering method.

The scattering data, or *scattering transform* $\mathbf{t} : \mathbb{C} \rightarrow \mathbb{C}$ of u is defined by

$$\mathbf{t}(k) = \int_{\mathbb{R}^2} e^{i\bar{k}\bar{x}} u(x) \psi(x, k) dx \quad (2.1.20)$$

where we are using the notation $x = x_1 + ix_2$ and $k = k_1 + ik_2$. The function ψ is the exponentially growing solution of the Schrödinger equation

$$(-\Delta + u)\psi(\cdot, k) = 0 \quad (2.1.21)$$

as established by Faddeev [21] and Nachman [52] with asymptotic behavior $\psi(x, k) \sim e^{ikx}$ in the sense that

$$e^{-ikx} \psi(x, k) - 1 \in L^{\tilde{p}} \cap L^\infty(\mathbb{R}^2) \quad \text{for fixed } k \in \mathbb{C} \setminus 0, \quad \text{where } 1/\tilde{p} = 1/p - 1/2. \quad (2.1.22)$$

Thus, we seek solutions of the form $\psi = \mu(x, t; k)e^{ikx}$ where μ has the asymptotic behavior

$\mu \approx 1$ for large $|k|$. The evolution of \mathbf{t} is then given by

$$\mathbf{t}(k, \tau) = \mathbf{m}(k, \tau)\mathbf{t}(k, 0), \quad (2.1.23)$$

where $\mathbf{m}(k, \tau) = \exp(i\tau(k^3 + \bar{k}^3))$.

Under suitable assumptions on u , the Schrödinger potential u can be recovered using the D-bar method of Beals and Coifman [6] and Nachman [52]. There are many results in the literature concerning this scattering transform but the one of interest to us is the result of Nachman [52]. Nachman solved the inverse problem of determining the Schrödinger potential in equation (2.1.21) from knowledge of the Dirichlet-to-Neumann map. This work was in the context of the inverse conductivity problem. In his constructive proof, he needed to determine a class of potentials for which there were no exceptional points. That is, points at which there fails to be a unique solution of equation (2.1.21). He proved that this class is potentials of conductivity-type. In chapter 6, this is discussed and numerical results are presented concerning evolutions of conductivity-type and non conductivity-type potentials.

We can derive a set of conservation laws for the NV equation by using an expansion method. Expand the function $\mu(x, k)$ as a series

$$\mu(x, k) = 1 + \sum_{j=1}^{\infty} \frac{a_j(x)}{k^j}. \quad (2.1.24)$$

Substitute equation (2.1.24) into $(-\Delta - 4ik\partial + u)(\mu - 1) = -u$ and solve the resulting system for the coefficients a_j ,

$$-\sum_{j=1}^{\infty} \frac{\Delta a_j(x)}{k^j} - \sum_{j=1}^{\infty} \frac{4i\partial a_j(x)}{k^{j-1}} + u \sum_{j=1}^{\infty} \frac{a_j(x)}{k^j} = -u. \quad (2.1.25)$$

We find

$$a_1 = \frac{1}{4i} \bar{\partial}^{-1} u.$$

A recursion formula can then be derived,

$$a_{j+1} = \frac{1}{4i} \bar{\partial}^{-1} (-4\bar{\partial}\partial a_j + ua_j) = i\partial a_j + \frac{1}{4i} \bar{\partial}^{-1}(ua_j). \quad (2.1.26)$$

Substituting the series (2.1.25) into (2.1.26) yields an infinite set of conserved quantities. The first three are presented here:

$$\begin{aligned} I_0 &= \int_{\mathbb{R}^2} u(x) dx, \\ I_1 &= \int_{\mathbb{R}^2} u(x)(\bar{\partial}^{-1}u)(x) dx, \\ I_2 &= \int_{\mathbb{R}^2} \left(\frac{1}{3}u(x)v(x) - \frac{1}{4}\bar{\partial}^{-1}(u\bar{\partial}^{-1}u)(x) \right) dx. \end{aligned}$$

We define

$$(\bar{\partial}^{-1}u)(x) = \frac{1}{\pi} \int_{\mathbb{R}^2} \frac{u(y)dy}{x-y}$$

where $x = x_1 + ix_2$ and $y = y_1 + iy_2$.

While the NV equation represents a natural generalization of the widely applicable KdV equation, there is no known derivation of the full equation from physical principles. The dispersionless NV equation has been shown to have applications in hydrodynamics [11], nonlinear optics [37, 36], and as a model for the propagation of light in the limit of geometrical optics through a particular class of nonlinear media [37]. In particular, the dispersionless NV equation is derived from Maxwells equations in the context of nonlinear media with a Cole-Cole dependence of the dielectric function and the magnetic permeability on frequency. They assume the medium is anisotropic and consider the propagation of monochromatic (single frequency, time harmonic) electromagnetic waves with high frequency.

3. CLOSED-FORM SOLUTIONS TO THE NOVIKOV-VESELOV EQUATION

There are various powerful methods to find solutions of nonlinear evolution equations, most notably the inverse scattering method mentioned in the introduction. However, the inverse scattering method is not readily useful for finding closed-form solutions to the NV equation. This is due to the complicated functions involved and that only recently has it been shown that the NV equation is solvable by the inverse scattering method [56, 43].

In this chapter we will apply other methods to the NV equation that have produced new and interesting solutions for other (2+1) evolution equations such as the KP equation, the ZK equation and the NNV equation. The methods presented here include Hirota's method, the extended tanh-function method, and the extended mapping approach (EMA). There are some general themes that tie these methods together.

The first theme is the idea of using expansion methods. Most, if not all, soliton equations admit traveling waves solutions that involve the hyperbolic secant function, which can be written in terms of the hyperbolic tangent function. Moreover, the hyperbolic tangent function is a solution to the Riccati equation, $\phi' = l_0 + \phi^2$, for $l_0 < 0$ for certain initial conditions. The ubiquity of the hyperbolic functions as traveling wave solutions naturally lead to the idea of expansion methods for solving soliton equations. There are many other modern methods including the F -expansion method [67], the Jacobi elliptic function method [71], general perturbation methods, Backlund transformations, the tanh-function method [41] and the Exp-function method [9] to name just a few. Because of the vast number of 'different' solution methods, a common criticism is that some of them are equivalent, or at

least find the same solutions.

Recently, in an excellent paper [39], these criticisms were expunged in an effort to elucidate some common errors researchers make when looking for new traveling-wave solutions to nonlinear partial differential equations. Alas, the NV equation is well under-studied, and at the time of this publication the only solutions in the literature are the solutions from the inverse scattering transform [42, 43, 44, 55], the classic hyperbolic secant and cnoidal solutions [53], and rational solutions derived using Darboux transformations that lead to finite time blow-up [59]. *This chapter presents a vast number of new, and qualitatively different, traveling wave solutions to the NV equation.*

3.1 Traveling Wave Solutions to the NV Equation

We seek solutions with arguments of one variable of the form $\theta := k_1x + k_2y - ct$. Here, k_1, k_2 and c are constants. The parameter c is referred to as the wave speed and k_1 and k_2 are the dispersive components of the wave vector.

For example, the KdV equation $u_t - 6uu_x + u_{xxx} = 0$, can be parametrized by letting the argument be $\theta = x - ct$ and let $u(x, t) = f(\theta)$. This reduces the partial differential equation to an ordinary differential equation,

$$-cf' - 6ff' + f''' = 0. \quad (3.1.1)$$

The solution to (3.1.1) critically depends on the constants of integration. If we assume the wave has the asymptotic behavior that $f, f', f'' \rightarrow 0$ as $|\theta| \rightarrow \infty$ the solution is

$$f(\theta) = -\frac{1}{2}c \operatorname{sech}^2 \left(\frac{1}{2}\sqrt{c}(\theta - \theta_0) \right)$$

for any constants $c \geq 0$ and θ_0 .

Dropping the assumption that the solution f and its derivatives decay to 0 in the limit,

one obtains the classic cnoidal solutions. These are periodic waves whose appearance are similar to a squared sinusoid. For the sake of brevity the cnoidal solutions to the KdV will not be presented. It is worth noting the cnoidal solutions to the NV equation are derived in [53]. Referring to equation (3.1.11) below we can find cnoidal solutions to the NV equation in terms of the Jacobi Elliptic function in the same manner outlined in Drazin [16]. Even though these are important solutions historically, there are no new results concerning these solutions in this work, and so the derivation and presentation of these important solutions are omitted.

Theorem 3.1.1. *If $u := u(\theta, ct)$, $\theta := k_1x + k_2y$, then any solution to the NV equation is a solution to a KdV-type equation ($'$ denotes $\partial/\partial\theta$),*

$$\frac{4}{\kappa}u_t = -u''' + \frac{6uu'}{k_1^2 + k_2^2}$$

where $\kappa = k_1^3 - 3k_1k_2^2$ is the linear dispersion relation. In particular, if $k_2 = 0$ and $k_1 = 1$ we recover a one-dimensional KdV-type soliton solution,

$$u = -2c \operatorname{sech}^2(\sqrt{c}(x - ct + x_0)).$$

Proof. Define u, v and w to be functions of θ and relabel the solutions as f, g and h , respectively,

$$u(x, y, t) = f(\theta),$$

$$v(x, y, t) = g(\theta),$$

$$w(x, y, t) = h(\theta).$$

The NV equation and its auxiliary equations become

$$0 = -4cf' + k_1^3 f''' - 3k_1 k_2^2 f''' - 3k_1 (fg)' - 3k_2 (fh)', \quad (3.1.2)$$

$$k_1 f' = k_1 g' - k_2 h', \quad (3.1.3)$$

$$k_2 f' = -k_2 g' - k_1 h' \quad (3.1.4)$$

Equations (3.1.2) – (3.1.4) can be integrated,

$$0 = -4cf + k_1^3 f'' - 3k_1 k_2^2 f'' - 3k_1 (fg) - 3k_2 (fh) + D, \quad (3.1.5)$$

$$k_1 f = k_1 g - k_2 h + C_2, \quad (3.1.6)$$

$$k_2 f = -k_2 g - k_1 h + C_3, \quad (3.1.7)$$

and now equations (3.1.6) and (3.1.7) can be solved for g and h in terms of f ,

$$g = \frac{k_1^2 - k_2^2}{k_1^2 + k_2^2} f + D_1 \quad (3.1.8)$$

$$h = -\frac{2k_1 k_2}{k_1^2 + k_2^2} f + D_2. \quad (3.1.9)$$

Substituting equations (3.1.8) and (3.1.9) into (3.1.5) we find

$$0 = -f(4c + 3k_1 D_1 + 3k_2 D_2) + (k_1^3 - 3k_1 k_2^2) f'' - 3f^2 \left(\frac{k_1^3 - 3k_1 k_2^2}{k_1^2 + k_2^2} \right) + D. \quad (3.1.10)$$

Define $A = 4c + 3k_1 D_1 + 3k_2 D_2$, $B = k_1^3 - 3k_1 k_2^2$ and $C = k_1^2 + k_2^2$ and we have the simplified ODE

$$0 = -Af + Bf'' - \frac{3B}{C} f^2 + D. \quad (3.1.11)$$

Multiplying equation (3.1.11) by f' , integrating and after relabeling the constants, we

have

$$\frac{1}{2}(f')^2 = Cf^3 + Bf^2 + Df + E. \quad (3.1.12)$$

This is very close to the KdV solution presented in Drazin [16] on pg. 13. The remainder of this section follows the analysis presented there but applied to the NV equation.

If we impose the boundary conditions that $f, f', f'', g, h \rightarrow 0$ as $|\theta| \rightarrow \infty$ then the constants of integration D and E must be zero (along with D_1 and D_2 from above) and equation (3.1.12) becomes

$$\frac{1}{2}(f')^2 = Cf^3 + Bf^2 \quad (3.1.13)$$

which upon solving for f' gives

$$f' = \frac{df}{d\theta} \implies d\theta = \frac{df}{f'}$$

and so

$$\theta = \int \frac{df}{f'} = \frac{1}{\sqrt{2}} \int \frac{df}{f\sqrt{Cf + B}}.$$

Letting $f = -\frac{B}{C}\text{sech}^2\psi$ yields the solution

$$u(x, y, t) = f(\theta) = -\frac{B}{C}\text{sech}^2\left(\frac{\sqrt{B}}{\sqrt{2}}(\theta - \theta_0)\right).$$

If $k_2 = 0$ and $k_1 = 1$ (which corresponds to $\theta = x - ct$) our solution is the classic KdV-type solution

$$u(x - ct) = -2c \text{sech}^2(\sqrt{c}(x - ct + x_0)).$$

□

3.2 *General Solution Methods*

In this section we present new solutions to the NV equation using the extended tanh-function method, Hirota's method, and the extended mapping approach. The new solutions presented here are traveling wave solutions and go beyond the hyperbolic secant and cnoidal solutions to the NV equation. One method that was attempted but was not successful was the multi-linear variable separation approach (MLVSA). Even though that work was not fruitful it did inform the successful work using the extended mapping approach and so is outlined briefly.

An application of Hirota's method has proved very successful in finding multisoliton solutions that can be useful for studying the stability of solitons. An interesting question is whether instabilities are transferred from one soliton to another when they interact. Thus, the existence of multisolitons proves important not only for heuristic reasons but also for tangential research.

Lastly, two methods that generalize separation of variables are presented. The first, the multi-linear variable separation approach, has not produced solutions yet. This work is on-going and if successful should be very fruitful. However, the extended mapping approach has produced many interesting and complex solutions with many more to come. This method has proven quite effective.

Multisoliton Solutions

Since the NV equation is not linear, techniques such as Fourier transforms and superposition do not apply. However, there exists a notion of superposition of solutions for nonlinear partial differential equations that admit soliton solutions. This allows for construction of what are called multisoliton solutions, solutions that have more than one 'wave of permanent form.' We will describe a notion of superposition that allow for solutions with N distinct soliton waves, and present a two-soliton solution. Note, however, that the method

can be used to derive solutions with as many solitons as desired. Since the wave speed is related to the amplitude, the solitons are guaranteed to interact and their spectacular characteristics are easily seen.

Multisoliton solutions to the KdV equation can be found using the inverse scattering transform (IST) [15], a method sometimes referred to as the *nonlinear Fourier transform*. However, this computation can be difficult, and for the NV equation in particular, an initial condition is needed which one may not have. There is another way to find multisoliton solutions, Hirota's bilinear method.

Following the pioneering work of Hirota [29], we can derive multisoliton solutions to the NV equation using what is known as *Hirota's bilinear method*. The main idea behind Hirota's bilinear method is that many nonlinear evolution equations can be reduced to a bilinear form through a transformation involving the logarithm function. This allows for another way to find multisoliton solutions different from those found by the ISM. However, the transformations that give the bilinear form can be very hard to find.

As an example, consider the KdV equation,

$$u_t - 6uu_x + u_{xxx} = 0.$$

We want to find a transformation for u involving a function f such that $f, f_x, f_{xx}, \dots \rightarrow 0$ as $|x| \rightarrow \infty$. Let

$$u = -2 \frac{\partial^2}{\partial x^2} \log f. \tag{3.2.1}$$

After substituting this into the KdV equation and a little manipulation involving an integration in x , we get

$$f f_{xt} - f_x f_t + f f_{xxxx} - 4 f_x f_{xxx} + 3 f_{xx}^2 = 0.$$

Now the problem is how to solve this bilinear form.

Hirota introduced the *bilinear operator*, $D_t^m D_x^n(a \cdot b)$, defined by

$$D_t^m D_x^n(a \cdot b) = \left(\frac{\partial}{\partial t} - \frac{\partial}{\partial t'} \right)^m \left(\frac{\partial}{\partial x} - \frac{\partial}{\partial x'} \right)^n a(x, t) b(x', t') \Big|_{x'=x, t'=t}.$$

Using Hirota's operator, and the transformation (3.2.1), the KdV equation is represented by

$$D_x(D_t + D_x^3)(f \cdot f) = 0$$

The ansatz solution is that u is a sum of exponentials. *Hirota's method gives soliton solutions as a sum of polynomials of exponentials.* To generate a single soliton solution, the sum is reduced to a single term. A two-soliton solution has two terms, a three-soliton solution has three terms, etc. The number of terms kept is the number of solitons generated.

3.2.1 Solutions Using Hirota's Method

Following the work in [68] we can find multisoliton solutions to NV using the Hirota bilinear method. Assume u is a plane wave solution, that is, $u(x, y, t) = e^{kx+ky-Ct}$. This is done in order to express the wave velocity c in terms of the dispersive coefficients. To make the analysis easier we have set $k_1 = k_2 = k$.

Substituting the plane wave solution into the linear part of (2.1.7) we find

$$c = -\frac{k^3}{2}.$$

Thus, $u(x, y, t) = e^{kx+ky+\frac{k^3}{2}t}$. The ansatz for f is

$$f(x, y, t) = 1 + C e^{kx+ky+\frac{k^3}{2}t}$$

where C is an arbitrary constant. The one-soliton solution can be defined by the transfor-

mations

$$u = R(\ln(f))_{xx} \quad (3.2.2)$$

$$v = R(\ln(f))_{xy} \quad (3.2.3)$$

$$w = R(\ln(f))_{yy} \quad (3.2.4)$$

The transformations (3.2.2) – (3.2.4) are Bäcklund-type transformations. When the transformations are put into the NV system, we can algebraically solve for R . This is algebraically intensive and is omitted. We find that $R = 2$. Thus,

$$u(x, y, t) = v(x, y, t) = w(x, y, t) = \frac{2Ck^2 e^{k(2x+2y+k^2t)/2}}{(1 + e^{k(2x+2y+k^2t)/2})^2} \quad (3.2.5)$$

is a soliton solution to the NV equation.

A two-soliton solution can be found if we redefine f to be

$$f(x, y, t) = 1 + e^{\theta_1} + e^{\theta_2} + a_{12}e^{\theta_1+\theta_2} \quad (3.2.6)$$

where $\theta_i = k_i x + k_i y + \frac{1}{2}k_i^3 t, i = 1, 2$.

Substituting the transformations (3.2.2) – (3.2.4) along with our new ansatz for f , equation (3.2.6), into the NV equation we are able to solve for a_{12} in terms of the wave numbers k_1 and k_2

$$a_{12} = \frac{(k_1 - k_2)^2}{(k_1 + k_2)^2}.$$

This gives us a two-soliton solution

$$u(x, y, t) = \frac{2 \left(k_1^2 e^{\theta_1} + k_2^2 e^{\theta_2} + (k_1 - k_2)^2 e^{\theta_1 + \theta_2} \right)}{1 + e^{\theta_1} + e^{\theta_2} + \frac{(k_1 - k_2)^2}{(k_1 + k_2)^2} e^{\theta_1 + \theta_2}} - \frac{2 \left(k_1 e^{\theta_1} + k_2 e^{\theta_2} + \frac{(k_1 - k_2)^2}{k_1 + k_2} e^{\theta_1 + \theta_2} \right)^2}{\left(1 + e^{\theta_1} + e^{\theta_2} + \frac{(k_1 - k_2)^2}{(k_1 + k_2)^2} e^{\theta_1 + \theta_2} \right)^2}. \quad (3.2.7)$$

This method can be generalized to find N -soliton solutions. For example, to find a three-soliton solution we use as the ansatz for f ,

$$f(x, y, t) = 1 + C_1 e^{\theta_1} + C_2 e^{\theta_2} + C_3 e^{\theta_3} + C_1 C_2 a_{12} e^{\theta_1 + \theta_2} + C_1 C_3 a_{13} e^{\theta_1 + \theta_3} + C_2 C_3 a_{23} e^{\theta_2 + \theta_3} + C_1 C_2 C_3 b_{123} e^{\theta_1 + \theta_2 + \theta_3}$$

Figure 3.1 shows the one-soliton solution derived above. Figure 3.2 shows the evolution of the two-soliton interaction, while Figure 3.3 shows the evolution and interaction of the two-soliton solution from the a view perpendicular to the direction of propagation.

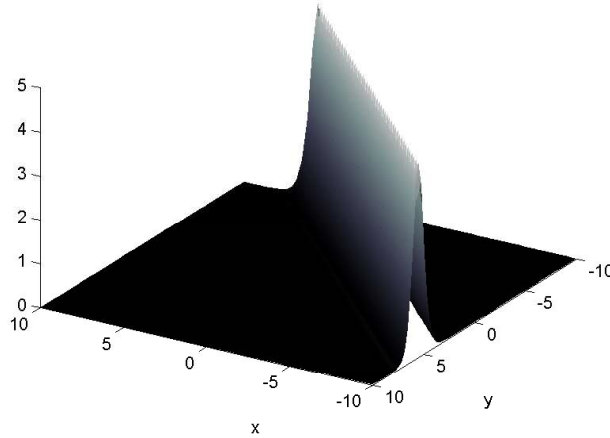


Fig. 3.1: One-soliton solution to the NV equation using Hirota's method with parameters $k = 3$, $t = 1$, $C = 1$,

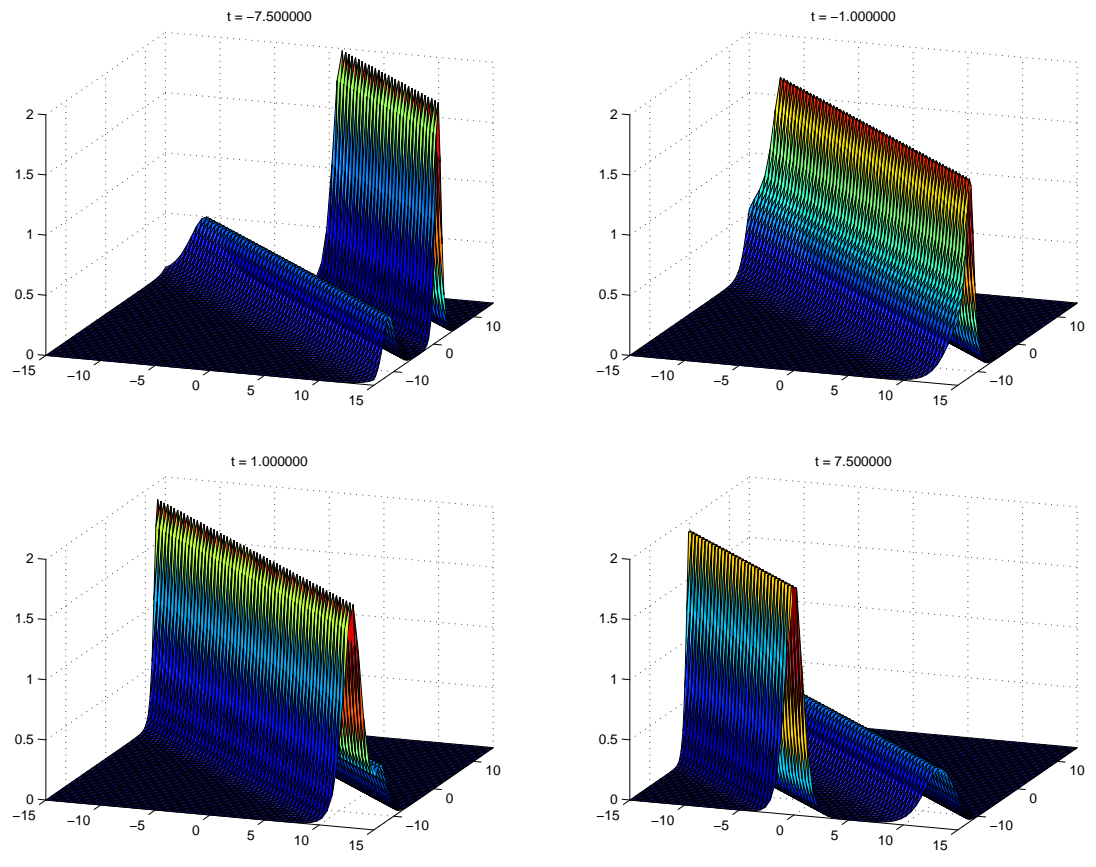


Fig. 3.2: Evolution of 2-Soliton solution with $k_1 = 1, k_2 = 2$

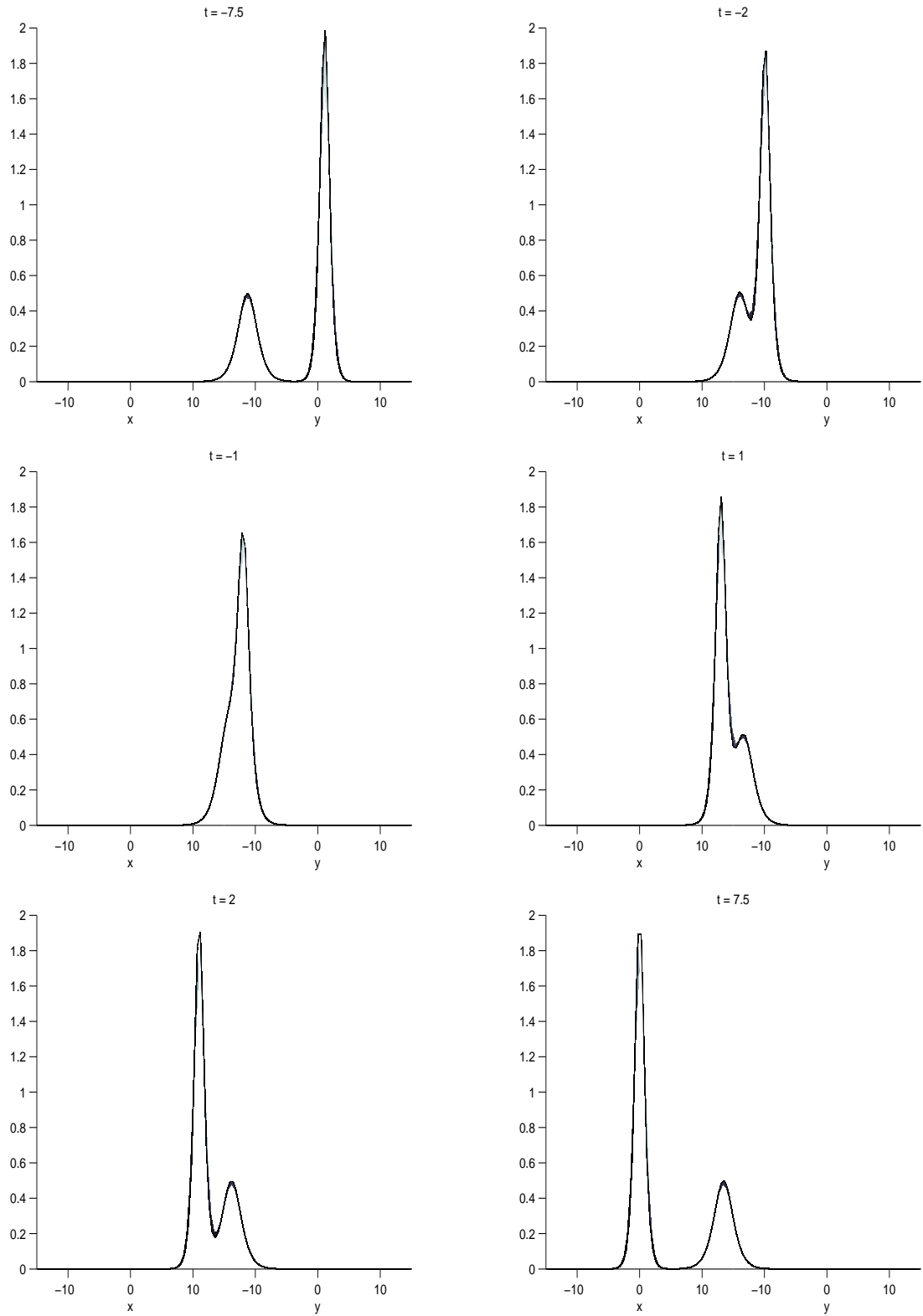


Fig. 3.3: Time snapshots of a two-soliton solution with choices $k_1 = 1$, $k_2 = 2$ from a view perpendicular to the direction of motion

3.2.2 Modified Extended Tanh–Function Method

Using the extended tanh–function method described in [18, 19] we find new multiple traveling wave solutions to the NV equation. This is another expansion method, but this time our expansion variable is allowed to have negative exponents. It broadens the number of solutions by including more terms in its expansion methods than the original tanh–function method.

In an effort to find more traveling wave solutions to the NV equation make the assumption that

$$u(x, y, t) = u(\theta),$$

$$v(x, y, t) = v(\theta),$$

$$w(x, y, t) = w(\theta)$$

where this time $\theta := k(x + ly + \lambda t)$. The NV equations and its auxiliary equations become

$$0 = 4k\lambda u' + k^3 u''' - 3k^3 l^2 u''' - 3k(uv)' - 3kl(uw)', \quad (3.2.8)$$

$$0 = -ku' + kv' - lkw', \quad (3.2.9)$$

$$0 = lku' + klv' + kw'. \quad (3.2.10)$$

In all three equations we can factor out a k, and integrating yields

$$0 = 4\lambda u + k^2 u'' - 3k^2 l^2 u'' - 3uv - 3lww, \quad (3.2.11)$$

$$0 = -u + v - lw, \quad (3.2.12)$$

$$0 = lu + lv + w. \quad (3.2.13)$$

Equations (3.2.12) – (3.2.13) can be solved for v and w in terms of u ,

$$v = u \frac{1 - l^2}{1 + l^2}, \quad (3.2.14)$$

$$w = -\frac{2ul}{1 + l^2}. \quad (3.2.15)$$

Substituting equations (3.2.14) – (3.2.15) into equation (3.2.11) from above we have

$$0 = 4\lambda u + k^2 u'' - 3k^2 l^2 u'' - 3u^2 \frac{1 - 3l^2}{1 + l^2} \quad (3.2.16)$$

Now we can make our expansion assumption

$$u = a_0 + a_1 z + a_2 z^2 + b_1 z^{-1} + b_2 z^{-2} \quad (3.2.17)$$

where z satisfies the Riccati equation

$$\frac{dz}{d\theta} = b + z^2, \quad z := z(\theta). \quad (3.2.18)$$

The solutions to equation (3.2.18) are

(a) If $b < 0$

$$z = -\sqrt{-b} \tanh(\sqrt{-b}\theta),$$

$$z = -\sqrt{-b} \coth(\sqrt{-b}\theta)$$

(b) If $b = 0$

$$z = -1/\theta$$

(c) If $b > 0$

$$z = \sqrt{b} \tan(\sqrt{b}\theta),$$

$$z = -\sqrt{b} \cot(\sqrt{b}\theta)$$

Substituting the expansion (3.2.17) into (3.2.16) and using the Riccati equation, we can

equate coefficients of z equal to 0 to get an algebraic system of equations

$$0 = 9l^2 a_2^2 - 3a_2^2 - 12k^2 l^2 a_2 - 18k^2 l^4 a_2 + 6k^2 a_2 \quad (3.2.19)$$

$$0 = 2k^2 b_1 b^2 - 6k^2 l^4 b_1 b^2 + 18l^2 b_1 b_2 - 4k^2 l^2 b_1 b^2 - 6b_1 b_2, \quad (3.2.20)$$

$$0 = 18l^2 a_1 a_2 - 4k^2 l^2 a_1 - 6a_1 a_2 - 6k^2 l^4 a_1 + 2k^2 a_1 \quad (3.2.21)$$

$$0 = -18k^2 l^4 b_2 b^2 - 12k^2 l^2 b_2 b^2 + 9l^2 b_2^2 - 3b_2^2 + 6k^2 b_2 b^2 \quad (3.2.22)$$

$$0 = -4\lambda a_2 - 6a_0 a_2 - 24k^2 l^4 a_2 b - 16k^2 l^2 a_2 b + 18l^2 a_0 a_2 - 3a_1^2 + 8k^2 a_2 b - 4\lambda l^2 a_2 + 9l^2 a_1^2 \quad (3.2.23)$$

$$0 = -6b_1 a_2 - 4k^2 l^2 a_1 b - 4\lambda a_1 - 4\lambda l^2 a_1 - 6k^2 l^4 a_1 b - 6a_0 a_1 + 18l^2 b_1 a_2 + 2k^2 a_1 b + 18l^2 a_0 a_1 \quad (3.2.24)$$

$$0 = 18l^2 a_1 b_2 - 4\lambda l^2 b_1 - 4k^2 l^2 b_1 b + 18l^2 a_0 b_1 - 6a_0 b_1 - 4\lambda b_1 + 2k^2 b_1 b - 6k^2 l^4 b_1 b - 6a_1 b_2 \quad (3.2.25)$$

$$0 = -4\lambda l^2 a_0 + 2k^2 a_2 b^2 + 2k^2 b_2 + 9l^2 a_0^2 - 4k^2 l^2 b_2 - 6a_2 b_2 - 4\lambda a_0 - 3a_0^2 + 18l^2 a_2 b_2 + 18l^2 a_1 b_1 - 6k^2 l^4 a_2 b^2 - 6a_1 b_1 - 4k^2 l^2 a_2 b^2 - 6k^2 l^4 b_2 \quad (3.2.26)$$

$$0 = 8k^2 b_2 b - 4\lambda l^2 b_2 - 16k^2 l^2 b_2 b - 6a_0 b_2 - 3b_1^2 + 9l^2 b_1^2 - 4\lambda b_2 - 24k^2 l^4 b_2 b + 18l^2 a_0 b_2 \quad (3.2.27)$$

Solving equations (3.2.19) – (3.2.27) we get a few nontrivial cases to consider:

Case1 :

$$a_0 = \frac{4\lambda(l^2 + 1)}{3(3l^2 - 1)}, \quad a_1 = 0, \quad a_2 = 0, \quad (3.2.28)$$

$$b = b, \quad b_1 = 0, \quad b_2 = 0 \quad (3.2.29)$$

Case2 :

$$a_0 = -\frac{2\lambda(l^2 + 1)}{3(3l^2 - 1)}, a_1 = 0, a_2 = 2k^2l^2 + 2k^2, \quad (3.2.30)$$

$$b = -\frac{\lambda}{k^2(3l^2 - 1)}, b_1 = 0, b_2 = 0 \quad (3.2.31)$$

Case3 :

$$a_0 = \frac{2\lambda(l^2 + 1)}{3l^2 - 1}, a_1 = 0, a_2 = 2k^2l^2 + 2k^2, \quad (3.2.32)$$

$$b = \frac{\lambda}{k^2(3l^2 - 1)}, b_1 = 0, b_2 = 0 \quad (3.2.33)$$

Case4 :

$$a_0 = \frac{2\lambda(l^2 + 1)}{3l^2 - 1}, a_1 = 0, a_2 = 0, \quad (3.2.34)$$

$$b = \frac{\lambda}{k^2(3l^2 - 1)}, b_1 = 0, b_2 = \frac{2\lambda^2(l^2 + 1)}{k^2(3l^2 - 1)^2} \quad (3.2.35)$$

Case5 :

$$a_0 = -\frac{2\lambda(l^2 + 1)}{3(3l^2 - 1)}, a_1 = 0, a_2 = 0, \quad (3.2.36)$$

$$b = -\frac{\lambda}{k^2(3l^2 - 1)}, b_1 = 0, b_2 = \frac{2\lambda^2(l^2 + 1)}{k^2(3l^2 - 1)^2} \quad (3.2.37)$$

Case6 :

$$a_0 = \frac{\lambda(l^2 + 1)}{3(3l^2 - 1)}, a_1 = 0, a_2 = 2k^2(l^2 + 1), \quad (3.2.38)$$

$$b = -\frac{\lambda}{4k^2(3l^2 - 1)}, b_1 = 0, b_2 = \frac{\lambda^2(l^2 + 1)}{8k^2(3l^2 - 1)^2} \quad (3.2.39)$$

Case7 :

$$a_0 = \frac{\lambda(l^2 + 1)}{3l^2 - 1}, \quad a_1 = 0, \quad a_2 = 2k^2(l^2 + 1), \quad (3.2.40)$$

$$b = \frac{\lambda}{4k^2(3l^2 - 1)}, \quad b_1 = 0, \quad b_2 = \frac{\lambda^2(l^2 + 1)}{8k^2(3l^2 - 1)^2} \quad (3.2.41)$$

For each case assume $\frac{\lambda}{3l^2 - 1} > 0$.

Case 2 We have $b < 0$. Then u becomes

$$u(x, y, t) = -\frac{2\lambda(l^2 + 1)}{3(3l^2 - 1)} \left[1 - 3 \tanh^2 \left(k(x + ly - \lambda t) \sqrt{\frac{\lambda}{k^2(3l^2 - 1)}} \right) \right] \quad (3.2.42)$$

Case 3 We have $b > 0$. Then u becomes

$$u(x, y, t) = \frac{2\lambda(l^2 + 1)}{3l^2 - 1} \left[1 + 3 \tanh^2 \left(k(x + ly - \lambda t) \sqrt{\frac{\lambda}{k^2(3l^2 - 1)}} \right) \right] \quad (3.2.43)$$

Case 4 We have $b > 0$. Then u becomes

$$u(x, y, t) = \frac{2\lambda(l^2 + 1)}{3l^2 - 1} \left[1 + \cot^2 \left(k(x + ly - \lambda t) \sqrt{\frac{\lambda}{k^2(3l^2 - 1)}} \right) \right] \quad (3.2.44)$$

Case 5 We have $b < 0$. Then u becomes

$$u(x, y, t) = -\frac{2}{3} \frac{\lambda(l^2 + 1)}{3l^2 - 1} \left[1 - 3 \coth^2 \left(k(x + ly - \lambda t) \sqrt{\frac{\lambda}{k^2(3l^2 - 1)}} \right) \right] \quad (3.2.45)$$

Case 6 We have $b < 0$. Then u becomes

$$u(x, y, t) = \frac{\lambda(l^2 + 1)}{6(3l^2 - 1)} \left[2 + 3 \tanh^2 \left(k(x + ly - \lambda t) \sqrt{\frac{\lambda}{4k^2(3l^2 - 1)}} \right) + 3 \coth^2 \left(k(x + ly - \lambda t) \sqrt{\frac{\lambda}{4k^2(3l^2 - 1)}} \right) \right] \quad (3.2.46)$$

Case 7 We have $b > 0$. Then u becomes

$$u(x, y, t) = \frac{\lambda(l^2 + 1)}{2(3l^2 - 1)} \left[2 + \tan^2 \left(k(x + ly - \lambda t) \sqrt{\frac{\lambda}{4k^2(3l^2 - 1)}} \right) + \cot^2 \left(k(x + ly - \lambda t) \sqrt{\frac{\lambda}{4k^2(3l^2 - 1)}} \right) \right] \quad (3.2.47)$$

The only solution without singularities is Case 2, which is presented in figure (3.4).

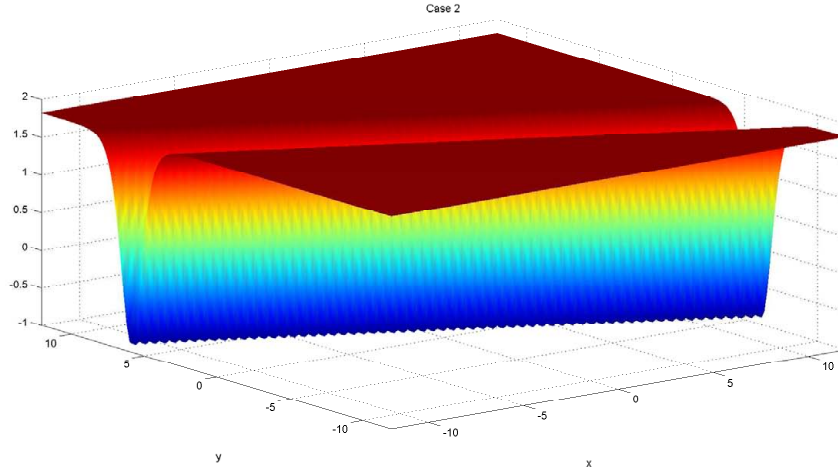


Fig. 3.4: Case 2, with $\lambda = 3$, $k = 4$, $l = 2$, $t = 0$

3.2.3 Multi-Linear Variable Separation Approach

Two techniques have been developed over the last two decades that enable one to generate an infinite number of qualitatively different solutions beginning with arbitrary functions or a seed solution. The first method is the multi-linear variable separation approach (MLVSA) and the other is called the extended mapping approach (EMA). They both rely on expanding the solutions in terms of functions that satisfy a Riccati equation. The solutions of the particular Riccati equations are either sinusoidal, hyperbolic or rational, and thus lend themselves to soliton equations. These methods seem to generate a universal formula for an integrable NLPDE which to this point has been found for all integrable systems solved in this manner [62, 61]. This formula is

$$u = \frac{2(a_1 a_2 - a_3 a_0) p_x q_y}{(a_0 + a_1 p + a_2 q + a_3 p q)^2} \quad (3.2.48)$$

where $a_0, a_1, a_2,$ and a_3 are arbitrary constants and $p(x, t)$ and $q(y, t)$ are arbitrary functions. This formula is a solution for many soliton PDE's including KP, higher dimensional Sine-Gordon, and Nizhnik-Novikov-Veselov (NNV) to name a few [62].

It is conjectured that possessing this universal formula is another sense of integrability. The NV has not been solved in this way and another goal would be to derive this universal formula for NV.

The multi-linear variable separation approach (MLVSA) was originally proposed in 1996 by Lou et. al. [47] to study the Davey-Stewartson (DS) equation. The method was originally an extension of Hirota's bilinear method. This method has already been used to solve a large number of (2+1) nonlinear systems including the NNV equation [75], dispersive long-range system [61], the (3+1) Jimbo Miwa system [60], the Davey-Stewartson system [47], the 2D Sine-Gordon equation and a (2+1)-dimensional (M+N) ANKS system [46].

As work has progressed, this method of finding solutions has been credited as a "soliton

factory” which can produce a variety of coherent nonlinear structures, such as dromion, solitoff, curved line and surface soliton, soliton lattice, ring soliton, peakon, compacton, foldon, chaotic soliton, fractal soliton, bubble soliton, tire soliton, ghost soliton, and so on, and various soliton interaction modes, such as soliton fission and fusion, soliton reconnection and reflection [63, 48, 28].

Given a (2+1)-dimensional nonlinear system, $F(u, u_t, u_x, u_y, \dots) = 0$, where u is a function of x, y , and t , we outline the general algorithm for finding solutions using the MLVSA. The first step is to multi-linearize the nonlinear system. Using Painleve analysis we know the system can be written as

$$u = \tilde{u}(f, f_x, \dots) + u_0, \quad (3.2.49)$$

where \tilde{u} is constructed by an expansion function $f(x, y, t)$ and its derivatives with respect to x, y, t , and u_0 is a seed solution (possibly 0) remaining as arbitrary as possible. The function \tilde{u} is essentially a Backlund transformation and has a homogeneous property, $\tilde{u}(\lambda f) = \lambda^k \tilde{u}(f)$ for a nonzero constant λ and integer k .

Substitution of (3.2.49) into our original system yields a multi-linearized system in f ,

$$\tilde{F}(f, f_t, f_x, f_y, \dots) = 0. \quad (3.2.50)$$

which is homogeneous and k -linear for some $k \in \mathbb{Z}$.

The second step is to make a variable separation assumption on f . This can be found using the Darboux transformation [62], but it is generally some variant of

$$f = a_0 + a_1 p + a_2 q + A p q, \quad (3.2.51)$$

where $p = p(x, t)$, $q = q(y, t)$ and a_0, a_1, a_2 and A are constants. Substitution of (3.2.51)

into (3.2.50) yields a new system

$$G(p, p_t, p_x, \dots, q, q_t, q_y, \dots) = 0. \quad (3.2.52)$$

Next, separate the functions p and q in (3.2.52),

$$G_1(p, p_t, p_x, \dots) = 0 \quad \text{and} \quad G_2(q, q_t, q_x, \dots) = 0. \quad (3.2.53)$$

The last step is to solve G_1 and G_2 for p and q . This last step is nontrivial, but, if possible, can yield many of the nonlinear structures cited above due to p and q being arbitrary.

Many variants on this algorithm exists, the most obvious being to try alternative forms of (3.2.51).

For the NV equation we have found the correct Painleve transformation, and we will either find a sufficient form of f or separate the system (3.2.53) using (3.2.51). The transformations are

$$u = a(\ln f)_{xx} + c(\ln f)_{yy} + u_0, \quad (3.2.54)$$

$$v = a(\ln f)_{xx} - c(\ln f)_{yy} + v_0, \quad (3.2.55)$$

$$w = -2a(\ln f)_{xy} + w_0, \quad (3.2.56)$$

for constants a and c . Using (3.2.51) the NV equation becomes a 5-linear form in f with 65 terms and has yet to be solved. A successful method of finding arbitrary solutions for the NV equation is the extended mapping approach and is presented next.

3.2.4 Extended Mapping Approach

The extended mapping approach (EMA) was presented formally by Zheng [77] and extends results by Lou and Ni [72]. The method is designed to find mappings between nonlinear PDE's. Through this mapping more solutions could be found algebraically, similar to a

Bäcklund transformation.

This work has led to a rather general result for finding solutions to soliton PDE's. Given a PDE, $F(u, Du, \dots) = 0$, where D refers to a derivative operator, assuming there exists a universal formula (3.2.48) for the solution $u(x, y, t)$, we can derive a family of such formulas with no restrictions on a_i and p and q , besides simple domain restrictions.

The extended mapping approach relies on expanding all quantities (u, v and w in the case of NV) by

$$u(x, y, t) = \sum_{i=0}^n a_i \phi^i, \quad (3.2.57)$$

$$v(x, y, t) = \sum_{i=0}^m b_i \phi^i, \quad (3.2.58)$$

$$w(x, y, t) = \sum_{i=0}^k c_i \phi^i. \quad (3.2.59)$$

The function ϕ satisfies the Riccati equation

$$\frac{d\phi}{dR} = l_0 + \phi^2, \quad (3.2.60)$$

where $R := R(x, y, t)$. The values of n, m and k are determined by balancing the highest-order derivative terms with the nonlinear terms of the PDE. The method is described nicely in [58]. The balancing method informs us that $n = k = m = 2$, and thus, $a_i := a_i(x, y, t)$, $b_i := b_i(x, y, t)$, and $c_i := c_i(x, y, t)$, ($i = 0, 1, \dots, n$) are arbitrary functions and l_0 is an arbitrary constant.

Substitute the expansions (3.2.57) - (3.2.59) into our original PDE and equate coefficients of the resulting polynomial in ϕ . For the NV equation this yields a system of thirteen PDE's. We need to solve this system for the coefficients a_i, b_i and c_i . Once this is done we have solutions for the original PDE. A key component to this method is that we have control over R , and can therefore manipulate the resulting system. We follow the separa-

tion most widely used, $R(x, y, t) = p(x, t) + q(y, t)$. When using this separation technique for R it is possible to generate a number of interesting coherent structures: ring solitons, lump solitons, dark solitons, dromions, foldons and compact solitons to name a few. For instance, many of these types of solutions were derived for the NNV equation [76], and it is an ongoing task to find all of these solutions for the NV equation. *In this work, we present a number of new solutions for the NV equation that were found using the EMA including breathers and bounded traveling wave solutions.*

EMA Applied to the Real-Valued NV Equation

Recall the NV equation is given by

$$\begin{aligned} 0 &= 4u_t + u_{xxx} - 3u_{xyy} - 3(uv)_x - 3(uw)_y, \\ u_x &= v_x - w_y, \\ u_y &= -w_x - v_y. \end{aligned} \tag{3.2.61}$$

Assume the solutions have the form

$$u = \sum_{i=1}^n a_i \phi^i, \tag{3.2.62}$$

$$v = \sum_{i=1}^m b_i \phi^i, \tag{3.2.63}$$

$$w = \sum_{i=1}^k c_i \phi^i \tag{3.2.64}$$

where $\phi = \phi(R)$, $R = R(x, y, t)$ and ϕ satisfies the Riccati equation

$$\frac{d\phi}{dR} = l_0 + \phi^2. \tag{3.2.65}$$

The reason for this choice of ϕ is because the solutions of the Riccati equation are traveling

wave solutions

$$\phi = \begin{cases} -\tanh(R), & l_0 = -1 \\ -\coth(R), & l_0 = -1 \\ \tan(R), & l_0 = 1 \\ -\cot(R), & l_0 = 1 \\ -R^{-1} & l_0 = 0 \end{cases} \quad (3.2.66)$$

Using these relations in the NV equation and its auxiliary relations, by using Maple we get the following system of partial differential equations

$$0 = -a_{0,x} - a_1 R_x l_0 + b_{0,x} + b_1 R_x l_0 - c_{0,y} - c_1 R_y l_0 \quad (3.2.67)$$

$$0 = -a_{1,x} - 2 a_2 R_x l_0 + b_{1,x} + 2 b_2 R_x l_0 - c_{1,y} - 2 c_2 R_y l_0 \quad (3.2.68)$$

$$0 = a_{0,y} + a_1 R_y l_0 + b_{0,y} + b_1 R_y l_0 + c_{0,x} + c_1 R_x l_0 \quad (3.2.69)$$

$$0 = a_{1,y} + 2 a_2 R_y l_0 + b_{1,y} + 2 b_2 R_y l_0 + c_{1,x} + 2 c_2 R_x l_0 \quad (3.2.70)$$

$$0 = a_1 R_y + a_{2,y} + b_1 R_y + b_{2,y} + c_1 R_x + c_{2,x} \quad (3.2.71)$$

$$0 = -a_1 R_x - a_{2,x} + b_1 R_x + b_{2,x} - c_1 R_y - c_{2,y} \quad (3.2.72)$$

$$0 = -72 a_2 R_y^2 R_x - 12 b_2 R_x a_2 - 12 c_2 R_y a_2 + 24 a_2 R_x^3 \quad (3.2.73)$$

$$0 = -2 a_2 R_x + 2 b_2 R_x - 2 c_2 R_y \quad (3.2.74)$$

$$0 = 2 a_2 R_y + 2 b_2 R_y + 2 c_2 R_x \quad (3.2.75)$$

$$\begin{aligned} 0 = & -6 c_2 R_y a_0 - 3 a_{1,y} c_2 - 3 a_{2,x} b_1 - 3 c_{1,y} a_2 + 2 a_2 R_{x,x,x} - 6 b_1 R_x a_1 \\ & - 3 b_{1,x} a_2 - 6 c_1 R_y a_1 - 3 a_{2,y} c_1 - 3 b_{2,x} a_1 - 6 a_{2,x} R_{y,y} \\ & - 6 a_{1,x} R_y^2 - 12 a_{2,x,y} R_y + 6 a_{1,x} R_x^2 - 6 a_{2,y,y} R_x - 12 b_2 R_x l_0 a_2 + 8 a_2 R_t \\ & - 6 a_2 R_{x,y,y} + 6 a_{2,x} R_{x,x} - 6 a_2 R_y c_0 - 6 b_2 R_x a_0 - 6 a_2 R_x b_0 - 12 a_1 R_y R_{x,y} \\ & - 120 a_2 R_y^2 R_x l_0 - 3 c_{2,y} a_1 - 12 a_{1,y} R_y R_x + 6 a_1 R_x R_{x,x} + 40 a_2 R_x^3 l_0 \\ & - 6 a_1 R_{y,y} R_x - 3 a_{1,x} b_2 + 6 a_{2,x,x} R_x - 12 a_{2,y} R_{x,y} - 12 c_2 R_y l_0 a_2 \end{aligned} \quad (3.2.76)$$

$$\begin{aligned}
0 = & -18 a_{2,x} R_y^2 - 3 a_{2,y} c_2 - 3 c_{2,y} a_2 + 6 a_1 R_x^3 + 18 a_{2,x} R_x^2 - 36 a_{2,y} R_y R_x \\
& - 18 a_2 R_{y,y} R_x - 36 a_2 R_y R_{x,y} - 18 a_1 R_y^2 R_x + 18 a_2 R_x R_{x,x} - 9 b_1 R_x a_2 \\
& - 9 b_2 R_x a_1 - 9 c_2 R_y a_1 - 9 c_1 R_y a_2 - 3 b_{2,x} a_2 - 3 a_{2,x} b_2 \tag{3.2.77}
\end{aligned}$$

$$\begin{aligned}
0 = & 24 a_{2,x} R_x^2 l_0 - 3 b_1 R_x a_0 + 4 a_{2,t} - 9 b_2 R_x l_0 a_1 + 8 a_1 R_x^3 l_0 - 3 a_{1,x} R_{y,y} \\
& + a_{2,x,x,x} - 3 a_{2,x,y,y} - 3 c_1 R_y a_0 - 24 a_{2,x} R_y^2 l_0 - 6 a_{1,y} R_{x,y} - 24 a_1 R_y^2 R_x l_0 \\
& - 3 a_1 R_y c_0 - 9 b_1 R_x l_0 a_2 + 3 a_{1,x} R_{x,x} - 3 a_1 R_{x,y,y} - 6 a_{1,x,y} R_y - 3 c_{2,y} a_0 - 3 b_{2,x} a_0 \\
& - 3 b_{0,x} a_2 - 3 a_{1,y} c_1 - 3 a_{0,y} c_2 - 3 a_{0,x} b_2 - 3 a_{1,x} b_1 - 3 c_{0,y} a_2 - 3 a_{2,x} b_0 - 3 a_{2,y} c_0 \\
& - 3 c_{1,y} a_1 - 48 a_2 R_y R_{x,y} l_0 + 3 a_{1,x,x} R_x + a_1 R_{x,x,x} + 24 a_2 R_x R_{x,x} l_0 - 9 c_2 R_y l_0 a_1 \\
& - 48 a_{2,y} R_y R_x l_0 + 4 a_1 R_t - 3 a_{1,y,y} R_x - 9 c_1 R_y l_0 a_2 - 24 a_2 R_{y,y} R_x l_0 - 3 b_{1,x} a_1 \\
& - 3 a_1 R_x b_0 \tag{3.2.78}
\end{aligned}$$

$$\begin{aligned}
0 = & -6 a_1 R_{y,y} R_x l_0 + a_{1,x,x,x} + 6 a_1 R_x R_{x,x} l_0 + 4 a_{1,t} - 3 a_{1,x,y,y} - 6 b_2 R_x l_0 a_0 \\
& - 12 a_{1,y} R_y R_x l_0 - 6 a_{2,x} R_{y,y} l_0 - 12 a_{2,x,y} R_y l_0 - 12 a_1 R_y R_{x,y} l_0 - 12 a_{2,y} R_{x,y} l_0 \\
& + 2 a_2 R_{x,x,x} l_0 + 6 a_{1,x} R_x^2 l_0 - 48 a_2 R_y^2 R_x l_0^2 - 6 a_{2,y,y} R_x l_0 - 3 a_{0,y} c_1 - 3 a_{1,y} c_0 \\
& - 3 c_{0,y} a_1 - 3 b_{0,x} a_1 - 3 a_{0,x} b_1 - 3 b_{1,x} a_0 - 6 a_2 R_y l_0 c_0 - 6 c_2 R_y l_0 a_0 - 6 a_{1,x} R_y^2 l_0 \\
& + 16 a_2 R_x^3 l_0^2 + 8 a_2 R_t l_0 + 6 a_{2,x,x} R_x l_0 - 6 a_2 R_x l_0 b_0 - 6 a_2 R_{x,y,y} l_0 - 3 c_{1,y} a_0 \\
& - 6 b_1 R_x l_0 a_1 - 3 a_{1,x} b_0 - 6 c_1 R_y l_0 a_1 + 6 a_{2,x} R_{x,x} l_0 \tag{3.2.79}
\end{aligned}$$

Assuming $a_2 \neq 0$, equations (3.2.73) – (3.2.75) can be solved algebraically for a_2 , b_2 , and

c_2 . We find

$$a_2 = 2R_x^2 + 2R_y^2 \quad (3.2.80)$$

$$b_2 = -2R_y^2 + 2R_x^2 \quad (3.2.81)$$

$$c_2 = -4R_y R_x. \quad (3.2.82)$$

Substituting equations (3.2.80) – (3.2.82) into the PDE system we have reduced the number of equations to ten, and we can now use equations (3.2.71), (3.2.72) and (3.2.77) to solve for a_1 , b_1 and c_1 .

$$a_1 = 2R_{xx} + 2R_{yy}, \quad (3.2.83)$$

$$b_1 = 2R_{xx} - 2R_{yy}, \quad (3.2.84)$$

$$c_1 = -4R_{xy}. \quad (3.2.85)$$

So far the general solutions for a_0 , b_0 and c_0 have been elusive. However, by choosing specific $R(x, y, t)$ the system becomes solvable using Maple. Many of these solutions will be presented below. I have some conjectures for certain choices of $R(x, y, t)$ that seem to be consistent when solving using Maple. For instance, when we assume $R(x, y, t) = p(x) + q(y)$, a spatial separation and no t dependence, $c_0 = -4l_0 R_x R_y$, but this is not proven rigorously yet. A quick outline of some conjectures are given.

If we make the separation assumption $R(x, y, t) = p(x, t) + q(y, t)$ and attempt to solve for a_0 , b_0 and c_0 , we can say a few things that will aid in future work. Equations (3.2.69) and (3.2.70) become

$$c_{0,y} = -a_{0,x} - 4p_x l_0 q_{y,y} + b_{0,x} \quad (3.2.86)$$

$$c_{0,x} = -a_{0,y} - 4p_{x,x} l_0 q_y - b_{0,y} \quad (3.2.87)$$

Integrating equation (3.2.86) with respect to y and equation (3.2.87) with respect to x

we find

$$c_0 = \int (-a_{0,x} + b_{0,x}) dy - 4p_x l_0 q_y + F_1(t, x) \quad (3.2.88)$$

$$c_0 = \int (-a_{0,y} - b_{0,y}) dx - 4p_x l_0 q_y + F_2(t, y) \quad (3.2.89)$$

where F_1 and F_2 are arbitrary functions from the integration. For the moment, let's assume these are 0. If $c_0 = -4l_0 p_x q_y$ we can conclude that

$$b_0 - a_0 = f_1(t, y), \text{ and } b_0 + a_0 = f_2(t, x).$$

If this is the case, we conjecture

$$b_0 = \frac{f_1 + f_2}{2} \quad (3.2.90)$$

$$a_0 = \frac{f_2 - f_1}{2}. \quad (3.2.91)$$

This gives us structure on what a_0 and b_0 can look like. We should see this in any results given by Maple.

Sech² Solutions

If we let $l_0 = -1$ and $R(x, y, t) = x - t$ we have $u(x, y, t) = a_0 + 2 \tanh^2(x - t)$. This particular choice of R allows the system to be solved by Maple and we find a solution is

$$a_0(x, y, t) = -4 - F(y),$$

$$b_0(x, y, t) = F(y),$$

$$c_0(x, y, t) = 0.$$

Choosing $F(y) = -2$ we obtain

$$\begin{aligned} u(x, y, t) &= -2 + 2 \tanh^2(x - t) \\ &= -2 \operatorname{sech}^2(x - t) \end{aligned}$$

This is the solution found in section in on page 23 in section 3.1 with $c = 1$ and $x_0 = 0$.

This also serves as evidence for the conjectures in equations (3.2.90) and (3.2.91) with $f_1(t, y) = 2F(y) + 4$ and $f_2(t, x) = -4$, and we have $c_0 = 0$ which is consistent with the conjectures above.

Static Solutions

Here we consider some cases where $R(x, y, t) = p(x) + q(y)$. For example, let $R(x, y, t) = x + y^2$ and $l_0 = -1$. For this choice of R the coefficients a_0, b_0 and c_0 are

$$a_0(x, y, t) = \frac{-1728y^6 + (-96 + 1728C)y^4 + (-40 + 288C)y^2 - 36C + 5}{432y^4 - 36y^2}$$

$$b_0(x, y, t) = \frac{144y^4 + (-12 + 432C)y^2 - 36C + 5}{36y^2}$$

$$c_0(x, y, t) = 8y$$

with solutions

$$\begin{aligned} u(x, y, t) &= \frac{-1728y^6 + (-96 + 1728C)y^4 + (-40 + 288C)y^2 - 36C + 5}{432y^4 - 36y^2} \\ &\quad - 4 \tanh(x + y^2) + (2 + 8y) \tanh^2(x + y^2) \end{aligned} \tag{3.2.92}$$

$$\begin{aligned} v(x, y, t) &= \frac{144y^4 + (-12 + 432C)y^2 - 36C + 5}{36y^2} \\ &\quad + 4 \tanh(x + y^2) + (2 - 8y) \tanh^2(x + y^2) \end{aligned} \tag{3.2.93}$$

$$w(x, y, t) = 8y - 8y \tanh^2(x + y^2), \tag{3.2.94}$$

where C is an arbitrary constant. There is a picture of the solution u with $C = 1$ in figure 3.5.

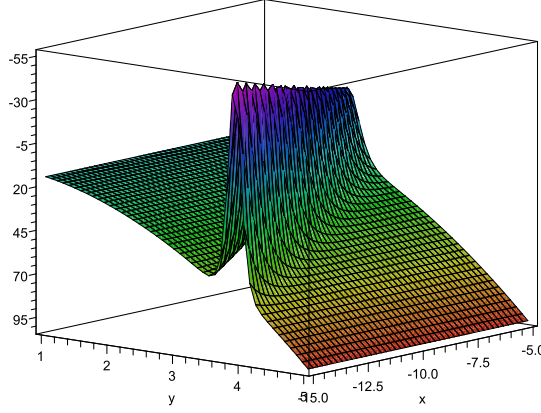


Fig. 3.5: A static solution to the NV equation

The solutions for a_0 , b_0 and c_0 are consistent with the conjectures in the previous section if we do not assume F_1 and F_2 are 0. Notice that $-4l_0p_xq_y = -4(-1)(1)(2y) = 8y = c_0$.

Breather

Breather solutions are solutions that have a respiratory action, that is, a periodic motion in time that resembles breathing. Let $R(x, y, t) = 1 + x + y^2 + 4 \cos(t)$ and $l_0 = -1$. With this choice of R and l_0 we obtain breather solutions:

$$u(x, y, t) = \frac{-1728y^6 + (-96 + 1728C)y^4 + (-40 + 288C)y^2 - 36C + 5}{432y^4 - 36y^2} - 4 \tanh(1 + x + y^2 + 4 \cos t) + (2 + 8y^2) \tanh^2(1 + x + y^2 + 4 \cos t) \quad (3.2.95)$$

$$v(x, y, t) = \frac{-192 \sin(t)y^2 + 144y^4 + (-12 + 432C)y^2 - 36C + 5}{36y^2} + 4 \tanh(1 + x + y^2 + 4 \cos t) + (2 - 8y^2) \tanh^2(1 + x + y^2 + 4 \cos t) \quad (3.2.96)$$

$$w(x, y, t) = 8y - 8y \tanh^2(1 + x + y^2 + 4 \cos t). \quad (3.2.97)$$

Again, notice that $-4l_0 p_x q_y = 8y = c_0$ which again affirms the conjecture that $c_0 = -4l_0 p_x q_y$. Several time snapshots are shown in Figure (3.6):

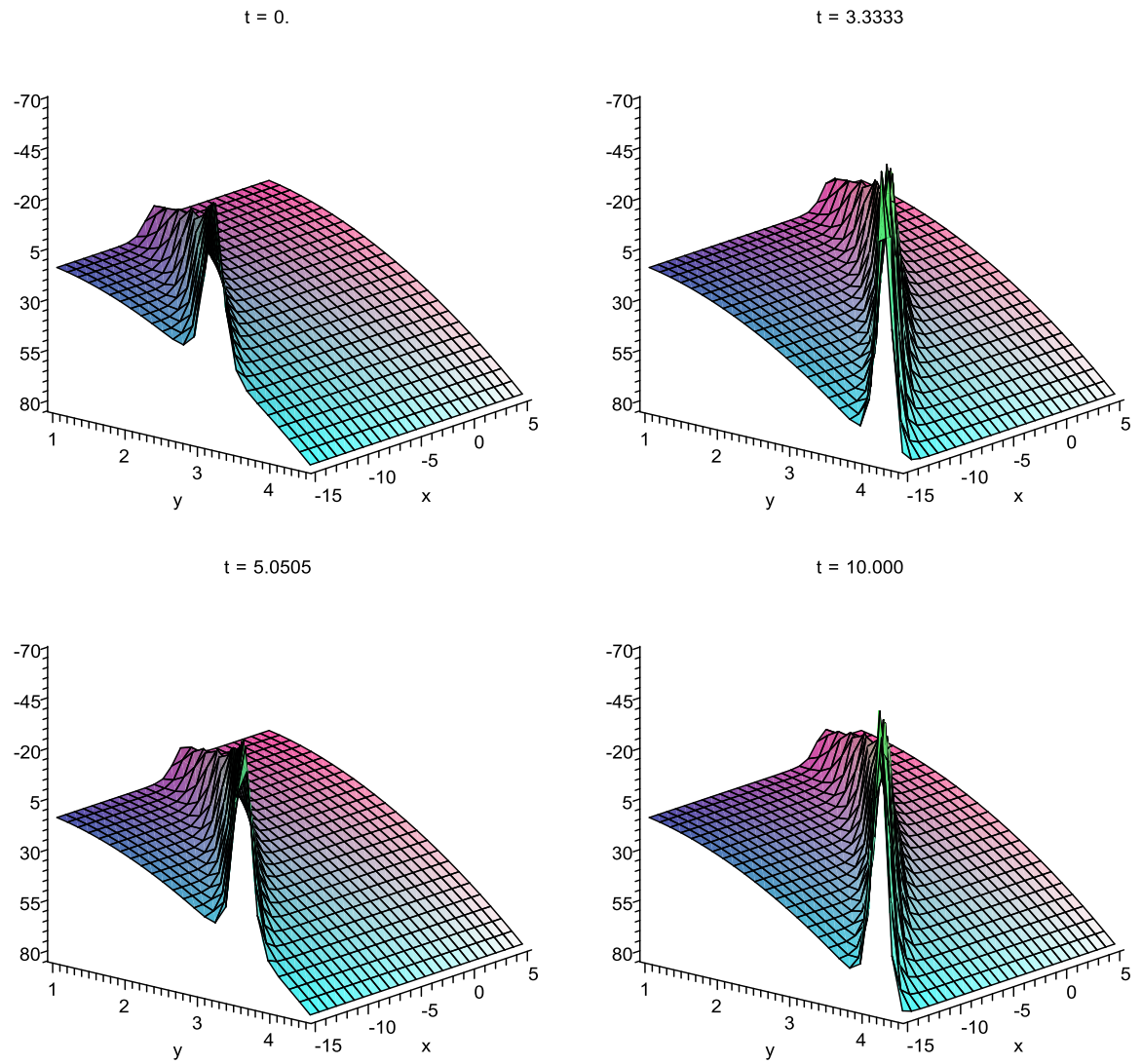


Fig. 3.6: Time snapshots of a breather solution derived using the EMA.

Multisolitons

Let $R(x, y, t) = x + y - t$. The resulting solution for $u(x, y, t)$ is

$$u(x, y, t) = \frac{3 \cosh^2(1 + y - x + t) - 12}{3 \cosh^2(1 + y - x + t)} + 4 \tanh^2(-x - y + t). \quad (3.2.98)$$

The result is the classic two-soliton interaction

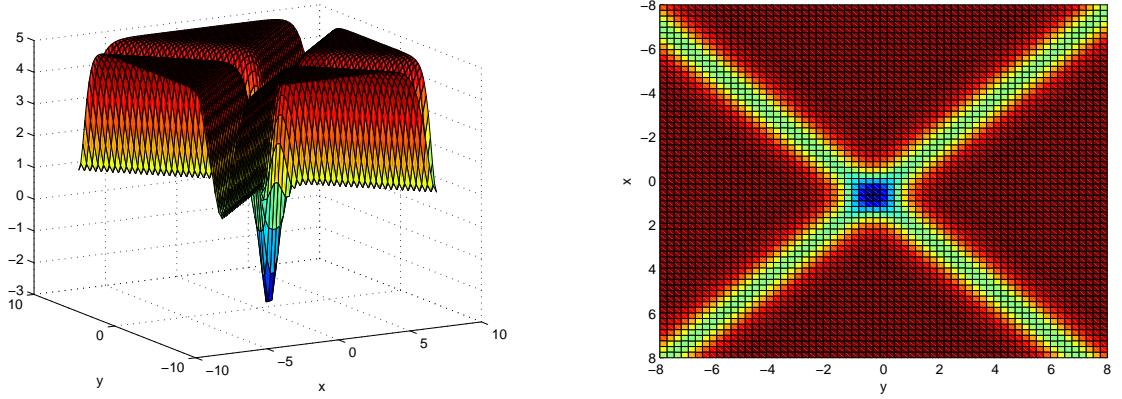


Fig. 3.7: Two Views of the two-soliton solution derived using the EMA. Left: Interacting solitons, Right: Contour view of the same interaction

Bounded Solutions

Let $l_0 = 0$. This is the case where we may be able to derive peakons, foldons, and compactons [76], if they exist. An example of a bounded solution is given for $R(x, y, t) = y^2 - x + e^t$. The solution for $u(x, y, t)$ is

$$\begin{aligned} u(x, y, t) &= \frac{192y^4 + 20y^2 - 3}{48y^4 - 4y^2} - \frac{4}{y^2 - x + e^t} + \frac{-8y^2 + 2}{(y^2 - x + e^t)^2} \\ v(x, y, t) &= -\frac{4e^t}{3} - \frac{1 - 12y^2}{y^2} + \frac{4}{y^2 - x + e^t} + \frac{-8y^2 + 2}{(y^2 - x + e^t)^2} \\ w(x, y, t) &= \frac{8y}{(y^2 - x + e^t)^2} \end{aligned}$$

Note here that $c_0 = 0$ which again confirms the conjecture that $c_0(x, y, t) = -4l_0p_xq_y$ since $l_0 = 0$ in this case. For choices of $R(x, y, t)$ that Maple can solve for a_0 , b_0 , and c_0 there has not been a c_0 that contradicts the conjecture $c_0(x, y, t) = -4l_0p_xq_y$.

Away from the singularities, $u \rightarrow 4$ as $t \rightarrow \infty$. A simple modification on R , $R(x, y, t) = y^2 - x^2 + e^t + 3$ yields a solution that goes to 0 in the limit,

$$u(x, y, t) = \frac{8x^2 + 8y^2}{(y^2 - x^2 + e^t + 3)^2}.$$

So far, I have not been able to find solutions that are bounded or decay to 0 in all directions that do not have singularities. A major goal is to find closed-form solutions of the NV equation that are of conductivity-type, and this will be pursued further in the future.

Movies and still pictures of everything discussed in this work can be found at my website: <http://www.math.colostate.edu/~croke/Research/>

4. A NUMERICAL SOLVER FOR THE NV EQUATION

4.1 *A Pseudo–Spectral Method for Solving (2+1) Nonlinear Wave Equations*

To verify analytical results presented in this dissertation and in order to help with conjectures involving the inverse scattering transform, a numerical solution to the NV equation was developed that is based on a general scheme created by Feng et. al. [22]. A semi-implicit numerical solver was already in existence [44] that uses finite differences in the spatial variables, Crank-Nicolson in time, and fast Fourier transforms for the auxiliary D-bar equation. However, the finite difference solver is slow compared to this spectral solver and requires more computational memory allocation.

In [3] Allen applied the method of Feng et.al. to the KP equation in order to investigate the stability of soliton solutions. Here, a numerical solution to the Cauchy problem for (1.0.5) – (1.0.7) is presented and is used in two capacities: to study the stability of soliton solutions to the NV equation, and to help with conjectures involving the evolution of initial data that are of non conductivity-type.

The original idea was considered in 1999 [22] and is applicable to many wave equations but *this is the first implementation for a NLPDE system*. We are restricting ourselves to a finite spatial domain with periodic boundary conditions where the periodic domain is $\Omega = [0, W_x] \times [0, W_y]$. Our computational domain must be sufficiently large to avoid reflections from the boundaries. This chapter will describe the spectral method, while its applications and uses will be in subsequent chapters.

The idea is to use the fast Fourier transform (FFT) and the discrete Fourier transform

(DFT) to compute the spatial evolution and a three-level difference scheme to advance the solution in time. For the linear terms, a free parameter θ is used, and for the nonlinear terms a leapfrog scheme is used. This is in contrast to the finite difference scheme, which uses an implicit finite-difference method in the spatial variables, and only takes advantage of the FFT for equation (1.0.3), the auxiliary D-bar equation. The main advantage of the spectral method is that it avoids solving nonlinear algebraic equations and avoids memory intensive operations such as LU decomposition.

The method can be summarized by first making the following definitions. Assume the intervals for x and y are both equidiscretized, $x_0 = 0, x_1 = \Delta x, x_2 = 2\Delta x, \dots, x_{L-1} = (L-1)\Delta x$ where $\Delta x = W_x/L$, and $y_0 = 0, y_1 = \Delta y, y_2 = 2\Delta y, \dots, y_{M-1} = (M-1)\Delta y$ where $\Delta y = W_y/M$. The parameters L and M should both be powers of 2 in order to use the FFT. The grid points are $(x_l, y_m) = (l\Delta x, m\Delta y)$ where $l \in \{0, \dots, L-1\}$ and $m \in \{0, \dots, M-1\}$. We denote the solution at time t and point (x_l, y_m) as $u_{l,m}(t)$. Let the corresponding spectral variables be denoted by $\xi_p = 2\pi p/W_x$ and $\eta_q = 2\pi q/W_y$, where $p \in \{-L/2, \dots, -1, 0, 1, \dots, L/2\}$, and $q \in \{-M/2, \dots, -1, 0, 1, \dots, M/2\}$. The DFT and its inverse are given by

$$\hat{u}_{p,q} = \mathcal{F}[u_{l,m}] = \sum_{l=0}^{L-1} \sum_{m=0}^{M-1} u_{l,m} e^{-i(\xi_p x_l + \eta_q y_m)} \quad (4.1.1)$$

$$u_{l,m} = \mathcal{F}^{-1}[\hat{u}_{p,q}] = \frac{1}{LM} \sum_{p=-L/2}^{L/2-1} \sum_{q=-M/2}^{M/2-1} \hat{u}_{p,q} e^{i(\xi_p x_l + \eta_q y_m)} \quad (4.1.2)$$

4.2 Implementing the Spectral Method for the NV Equation

Using equations (4.1.1) and (4.1.2) we find that the Fourier transform of the system (1.0.5) – (1.0.7) is

$$0 = 4\hat{u}_t + (3i\xi\eta^2 - i\xi^3)\hat{u} - 3i\xi\mathcal{F}[(uv)] - 3i\eta\mathcal{F}[(uv)], \quad (4.2.1)$$

$$\xi\hat{u} = \xi\hat{v} - \eta\hat{w}, \quad (4.2.2)$$

$$\eta\hat{u} = -\eta\hat{v} - \nu\hat{w}. \quad (4.2.3)$$

Equations (4.2.2) and (4.2.3) can be solved in terms of \hat{u}

$$\hat{w} = \frac{-2\eta\xi}{\eta^2 + \xi^2}\hat{u} \quad (4.2.4)$$

$$\hat{v} = \frac{\xi^2 - \eta^2}{\xi^2 + \eta^2}\hat{u} \quad (4.2.5)$$

For the time integration we use a symmetric three-level difference method for the linear terms, and a leapfrog method for the nonlinear terms. The idea here is to treat the linear terms implicitly, while treating the nonlinear terms explicitly. We advance the nonlinear terms in time only by previous time levels. We do this by solving for w and v in terms of u at previous time steps and then solving the main equation. At this point we introduce superscripts on all functions that are evolving in time. For example, let the n^{th} time step of $u_{l,m}$ be denoted as $u_{l,m}^n$. Taking the inverse Fourier transform of equations (4.2.4) and (4.2.5), the n^{th} time step is given by

$$w^n = \frac{-2\eta\xi}{\eta^2 + \xi^2}\mathcal{F}^{-1}\hat{u}^n \quad (4.2.6)$$

$$v^n = \frac{\xi^2 - \eta^2}{\xi^2 + \eta^2}\mathcal{F}^{-1}\hat{u}^n. \quad (4.2.7)$$

The time evolution of equations (4.2.1) – (4.2.3) is given by the following

$$0 = 4 \frac{\hat{u}^{n+1} - \hat{u}^{n-1}}{2\Delta t} + (3i\xi\eta^2 - i\xi^3) (\theta(\hat{u}^{n+1} + \hat{u}^{n-1}) + (1 - 2\theta)\hat{u}^n) - 3i\xi\mathcal{F}[(u^n v^n)] - 3i\eta\mathcal{F}[(u^n w^n)] \quad (4.2.8)$$

$$\hat{w}^n = \frac{-2\eta\xi}{\eta^2 + \xi^2} \hat{u}^n \quad (4.2.9)$$

$$\hat{v}^n = \frac{\xi^2 - \eta^2}{\xi^2 + \eta^2} \hat{u}^n \quad (4.2.10)$$

In this semi-implicit scheme two FFT's are needed for each time step. Solving for \hat{u}^{n+1} we have

$$\hat{u}^{n+1} = \frac{2\Delta t}{4 + 2\Delta t \theta(3i\xi\eta^2 - i\xi^3)} \left(3i\xi\mathcal{F}[(u^n v^n)] + 3i\eta\mathcal{F}[(u^n w^n)] - (3i\xi\eta^2 - i\xi^3) ((1 - 2\theta)\hat{u}^n + \theta\hat{u}^{n-1}) \right) + \frac{4}{4 + 2\Delta t \theta(3i\xi\eta^2 - i\xi^3)} \hat{u}^{n-1} \quad (4.2.11)$$

As one can see from this formula, if we know the previous two time steps, we can compute the solution at the present time step. This has the advantage that there is not an extra computational step at every time step as there is with the Crank-Nicolson method. However, because there are three time steps, two initial approximation are needed.

This extra initial condition is attained by manually time stepping the given initial condition. If $u_{IC1}(x, y, 0)$ is the initial condition we would like to evolve numerically, we compute $u_{IC2}(x, y, 0 - dt)$ where dt is our time step. For example, later we show the evolution of the solution $u(x, y, t) = -2\text{sech}^2(x - t)$. To use the pseudo-spectral method we have as input $u_{IC1}(x, y, 0) = -2\text{sech}^2 x$ and $u_{IC2}(x, y, t) = -2\text{sech}^2(x - dt)$.

The next section will address the issue of numerical stability. As in Feng et. al. we employ a linear numerical stability analysis to get necessary conditions for stability.

4.2.1 Linear Numerical Stability Analysis

To gain insight into the stability of the spectral method, a linear stability analysis is undertaken. To proceed we approximate the function u with a constant $\alpha = |u|_{max}$ in the nonlinear terms. The relevance of a stability analysis for a fundamentally different system can certainly be questioned. After all, a nonlinear system is quite different from a linear one. However, this issue was addressed by the authors in [22], in the context of stability of a spectral scheme for the KP and ZK equations,

“Although a linearized stability analysis is not sufficient for proving stability and convergence of the corresponding nonlinear schemes, the obtained stability conditions are often sufficient in practice.”

The authors argue that their linear stability analysis for the KP and ZK equations are validated by numerical results. I humbly defer to their arguments as validation for the similar analysis done here for the NV equation. To begin, let $\omega = \xi(3\eta^2 - \xi^2)$ be the linear dispersion relation given in terms of the spectral parameters. We can use definitions (4.2.6) – (4.2.7) to linearize equation (4.2.8) and rewrite (4.2.8) as

$$0 = \frac{\hat{u}^{n+1} - \hat{u}^{n-1}}{(1/2)\Delta t} + i\omega (\theta(\hat{u}^{n+1} + \hat{u}^{n-1}) + (1 - 2\theta)\hat{u}^n) + \frac{3i\alpha\omega}{\xi^2 + \eta^2}\hat{u}^n \quad (4.2.12)$$

where $\alpha = |u|_{max}$. This leads to the characteristic polynomial

$$\phi_{NV}(z) = b_1 z^2 + b_2 z - \bar{b}_1 \quad (4.2.13)$$

where

$$b_1 = [1 + (1/2)i\Delta t\omega\theta], \quad (4.2.14)$$

$$b_2 = \frac{i\Delta t\omega}{2} \left[(1 - 2\theta) + \frac{3\alpha}{\xi^2 + \eta^2} \right]. \quad (4.2.15)$$

Let $\beta_{1,2} = (-b_2 \pm \sqrt{b_2^2 + 4|b_1|^2})/2b_1$ be the two distinct zeros of the characteristic polynomial $\phi_{NV}(z)$. To avoid instability we need that both $|\beta_1| \leq 1$ and $|\beta_2| \leq 1$. However,

$$\begin{aligned} \beta_1\beta_2 &= \frac{(-b_2 + \sqrt{b_2^2 - 4b_1\bar{b}_1})(-b_2 - \sqrt{b_2^2 - 4b_1\bar{b}_1})}{4b_1^2} \\ &= \frac{b_2^2 - (b_2^2 - 4b_1\bar{b}_1)}{4b_1^2} \\ &= \frac{4b_1\bar{b}_1}{4b_1^2} \\ &= \frac{\bar{b}_1}{b_1} \end{aligned}$$

and so $|\beta_1\beta_2| = 1$ it follows $|\beta_1| = |\beta_2| = 1$. Since the roots of equation (4.2.13) are on the unit circle the numerical method is stable, or conservative. Therefore, it is required that $b_2^2 + 4|b_1|^2 > 0$. We compute

$$\begin{aligned} b_2^2 + 4|b_1|^2 &= -\frac{1}{4}(\Delta t)^2\omega^2 \left[(1 - 2\theta) + \frac{3\alpha}{\xi^2 + \eta^2} \right]^2 + 4 \left(1 + \frac{1}{4}(\Delta t)^2\omega^2\theta^2 \right) \\ &= (\Delta t)^2\omega^2 \left((\theta - (1/4)) - \frac{1}{4} \frac{6\alpha(1 - 2\theta)}{\eta^2 + \xi^2} - \frac{1}{4} \left(\frac{3\alpha}{\eta^2 + \xi^2} \right)^2 \right) + 4. \end{aligned}$$

Let $\gamma = \frac{3\alpha}{\eta^2 + \xi^2}$. Using that $1 - 2\theta = -2(\theta - (1/4)) + 1/2$ we now have

$$b_2^2 + 4|b_1|^2 = (\Delta t)^2 \omega^2 (\theta - (1/4)) \left(1 + \gamma - \frac{1}{4\theta - (1/4)} \frac{\gamma}{\theta - (1/4)} - \frac{1}{4(\theta - (1/4))} \gamma^2 \right) + 4 \quad (4.2.16)$$

Recall that $\gamma > 0$, and so a necessary condition that this quantity is positive is $\theta > 1/4$.

Equation (4.2.16) is linear in θ and thus is monotonic in θ . Analysis done by a collaborator, Andreas Strahel, has already shown $1/4 < \theta < 1$. So, in terms of theta, the maximum that equation (4.2.16) can be is at when θ is at its maximum, $\theta = 1$. For the analysis here, we can assume $\theta = 1$. This will lead to an estimate for Δt .

$$\begin{aligned} b_2^2 + 4|b_1|^2 &= -\frac{1}{4}(\Delta t)^2 \omega^2 \left[-1 + \frac{3\alpha}{\xi^2 + \eta^2} \right]^2 + 4 \left(1 + \frac{1}{4}(\Delta t)^2 \omega^2 \right) \\ &= (\Delta t)^2 \omega^2 \left(- \left[-1 + \frac{3\alpha}{\xi^2 + \eta^2} \right]^2 + 4 \right) + 16 \\ &= (\Delta t)^2 \omega^2 \left(- \left[1 - \frac{6\alpha}{\xi^2 + \eta^2} + 9 \left(\frac{\alpha}{\xi^2 + \eta^2} \right)^2 \right] + 4 \right) + 16 \\ &= (\Delta t)^2 \omega^2 \left(3 + \frac{6\alpha}{\xi^2 + \eta^2} - 9 \left(\frac{\alpha}{\xi^2 + \eta^2} \right)^2 \right) + 16 \\ &= 3(\Delta t)^2 \omega^2 \left(\left(1 + \frac{\alpha}{\xi^2 + \eta^2} \right)^2 - 4 \left(\frac{\alpha}{\xi^2 + \eta^2} \right)^2 \right) + 16 > 0 \quad (4.2.17) \end{aligned}$$

A sufficient condition to satisfy (4.2.17) is

$$\Delta t < \frac{2}{\sqrt{3}} \frac{\xi_{max}^2 + \eta_{max}^2}{\alpha \omega} \quad (4.2.18)$$

Recall that $\omega = \xi(3\eta^2 - \xi^2)$. For simplicity let's assume $\Delta x = \Delta y$ and $\xi = \eta$. Then inequality (4.2.17) becomes

$$\Delta t < \frac{2}{\sqrt{3}} \frac{2\xi_{max}^2}{\alpha\xi_{max}(2\xi_{max}^2)} = \frac{2}{\sqrt{3}} \frac{1}{\alpha\xi_{max}} = \frac{1}{\pi\sqrt{3}} \frac{\Delta x}{|u|_{max}} \quad (4.2.19)$$

We have proved the following theorem,

Theorem 4.2.1. *For the linear periodic initial value problem*

$$\begin{aligned} 0 &= 4u_t + u_{xxx} - 3u_{xyy} - 3(u\alpha)_x - 3(u\alpha)_y, & (x, y) \times t \in \Omega \times \mathbb{R}, \\ u(x, y, 0) &= u_0(x, y), & (x, y) \in \Omega, \\ u(x, y, t) &= u(x + W_x, y, t), & (x, y) \times t \in \mathbb{R}^3, \\ u(x, y, t) &= u(x, y + W_y, t), & (x, y) \times t \in \mathbb{R}^3, \end{aligned}$$

where $\Omega = [0, W_x] \times [0, W_y]$, $\alpha \in \mathbb{R}^+$, the spectral scheme

$$0 = \frac{\hat{u}^{n+1} - \hat{u}^{n-1}}{(1/2)\Delta t} + i\omega (\theta(\hat{u}^{n+1} + \hat{u}^{n-1}) + (1 - 2\theta)\hat{u}^n) + \frac{3i\alpha\omega}{\xi^2 + \eta^2} \hat{u}^n$$

is conservative and stable provided that $\theta > 1/4$ and $\Delta t \leq \frac{1}{\pi\sqrt{3}} \frac{\Delta x}{|u|_{max}}$.

4.2.2 Preservation of the L_2 Norm for the Linear NV Equation

Recall from chapter 3, the linear NV equation, equation (2.1.7), is

$$u_t = -\frac{1}{4}u_{xxx} + \frac{3}{4}u_{yyx} \equiv -Au \quad (4.2.20)$$

Defining the inner product as

$$\langle u, v \rangle = \int \int u(x, y, t)v(x, y, t)dA,$$

we see

$$\begin{aligned} \langle \frac{\partial^3}{\partial x^3} u, v \rangle &= \int \int \frac{\partial^3}{\partial x^3} u(x, y, t) v(x, y, t) dA \\ &= - \int \int u(x, y, t) \frac{\partial^3}{\partial x^3} v(x, y, t) dA. \end{aligned}$$

A similar calculation shows

$$\langle Au, v \rangle = - \langle u, Av \rangle .$$

Using that $\frac{d}{dt}u = -Au$,

$$\begin{aligned} \frac{d}{dt} \|u(t)\|_{L_2}^2 &= \frac{d}{dt} \langle u, u \rangle \\ &= - \langle Au, u \rangle - \langle u, Au \rangle \\ &= - \langle Au, u \rangle + \langle Au, u \rangle \\ &= 0 \end{aligned}$$

and so

$$\|u(t)\|_{L_2} = \|u(t, \cdot, \cdot)\|_{L_2} = \text{constant}.$$

In particular, for traveling wave solutions the L_2 norm should be preserved.

4.2.3 Numerical Simulations of Soliton Initial Conditions

In this section the results from numerical computations are presented for the traveling wave solution $u(x, y, t) = -2 \operatorname{sech}^2(x - t)$. All work was done in Matlab using the built-in routines FFT, IFFT, and ODE45. In chapter 6 the spectral scheme will be applied in the context of exploring conjectures related to the ISM for the NV equation. It will also be used when investigating transversely perturbed initial conditions to study stability in chapter 5

In figure (4.1) the L_2 norm of the numerically solution was computed for a sequence

of time steps and is seen to be extremely stable. In table (4.1) some statistics regarding the norm are presented. The maximum deviation from the norm for $t \in [0, 10]$ is 0.0176 and the maximum deviation from the norm for $t \in [0, 40]$ is 0.0323. Note that the scale of the vertical axis is very small in figure (4.1) and so the graph appears to be space filling.

Figures (4.2) and (4.3) compare the numerically computed evolution of $u_0(x, y, t) = -2c\operatorname{sech}^2(x - ct)$ to the initial condition, $u_0(x, y, 0)$. To compute these images, a 128x128 mesh was created on the grid $(x, y) \in ([0, 40], [0, 20])$ with $dt = 0.01$.

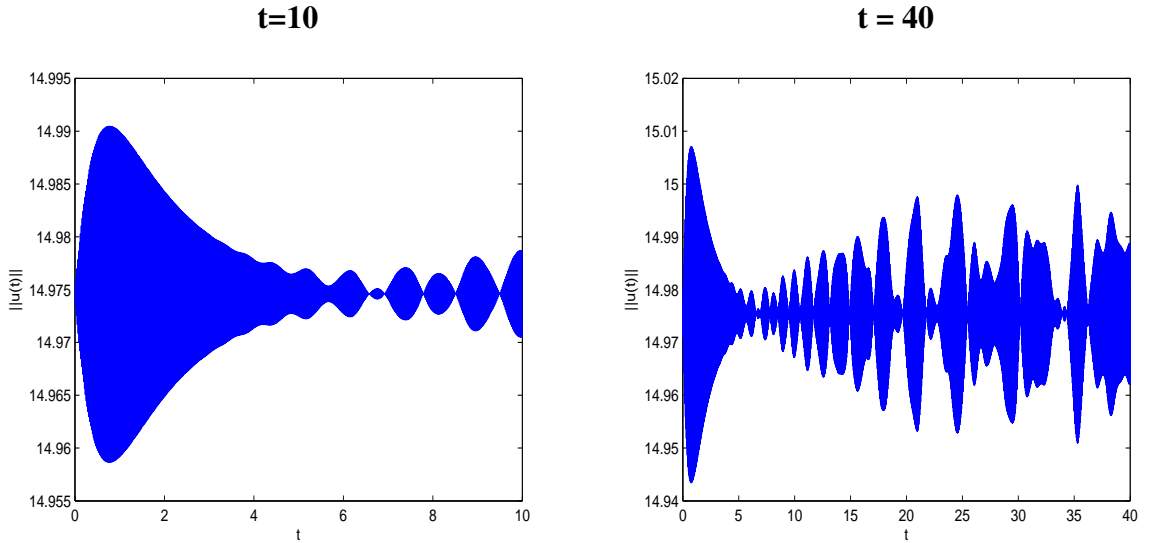


Fig. 4.1: Left: $\|u(t)\|_{L^2}$, with time ranging $0 \leq t \leq 10$, Right: $\|u(t)\|_{L^2}$, with time ranging $0 \leq t \leq 40$

Time	Mean	Min	Max
t = 10	14.9746	14.9586	14.9905
t = 40	14.9754	14.9431	15.0071

Tab. 4.1: Statistics of the norms computed in Figure 4.1

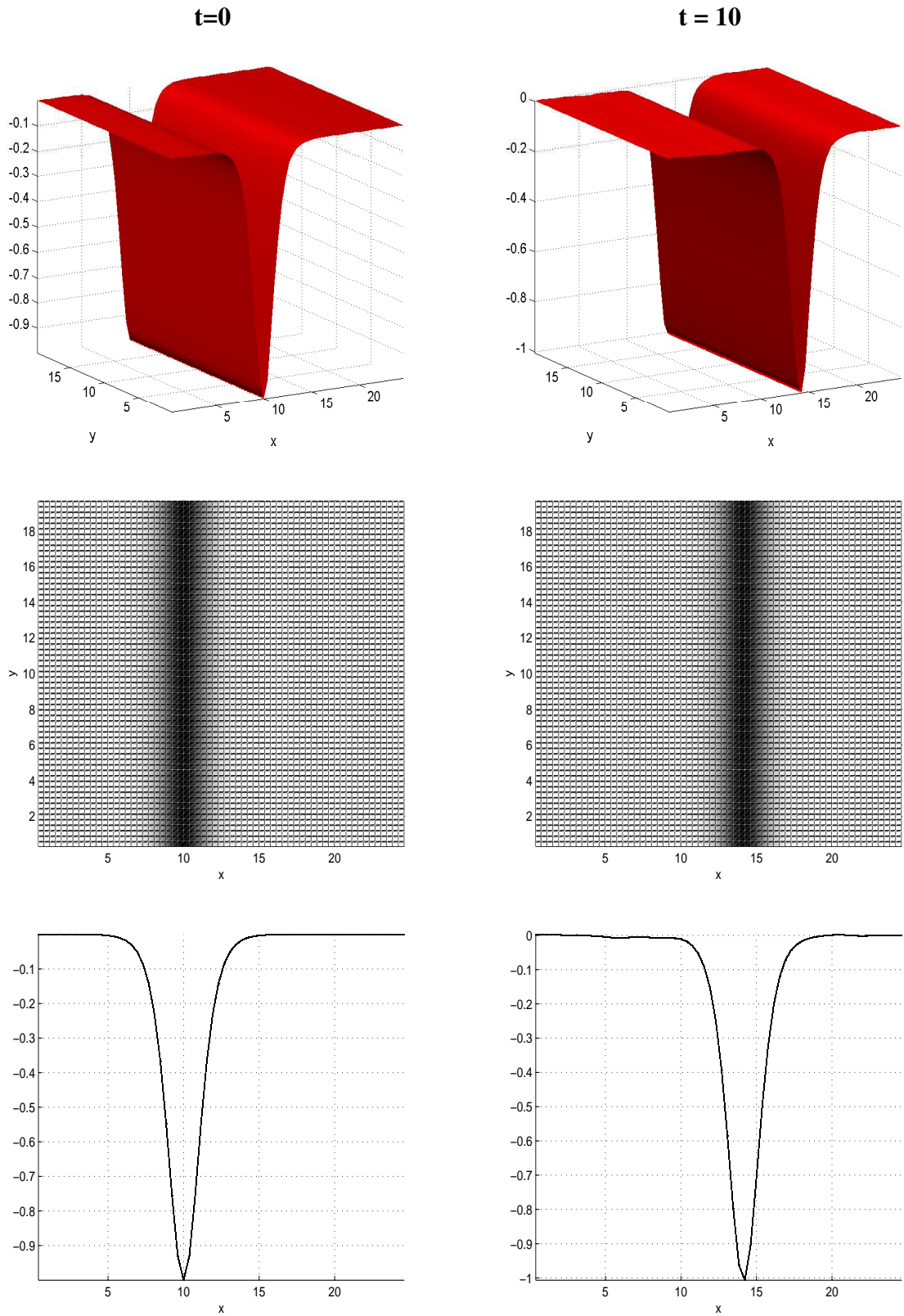


Fig. 4.2: Three views comparing the initial condition u_0 and its numerical evolution at $t = 10$.

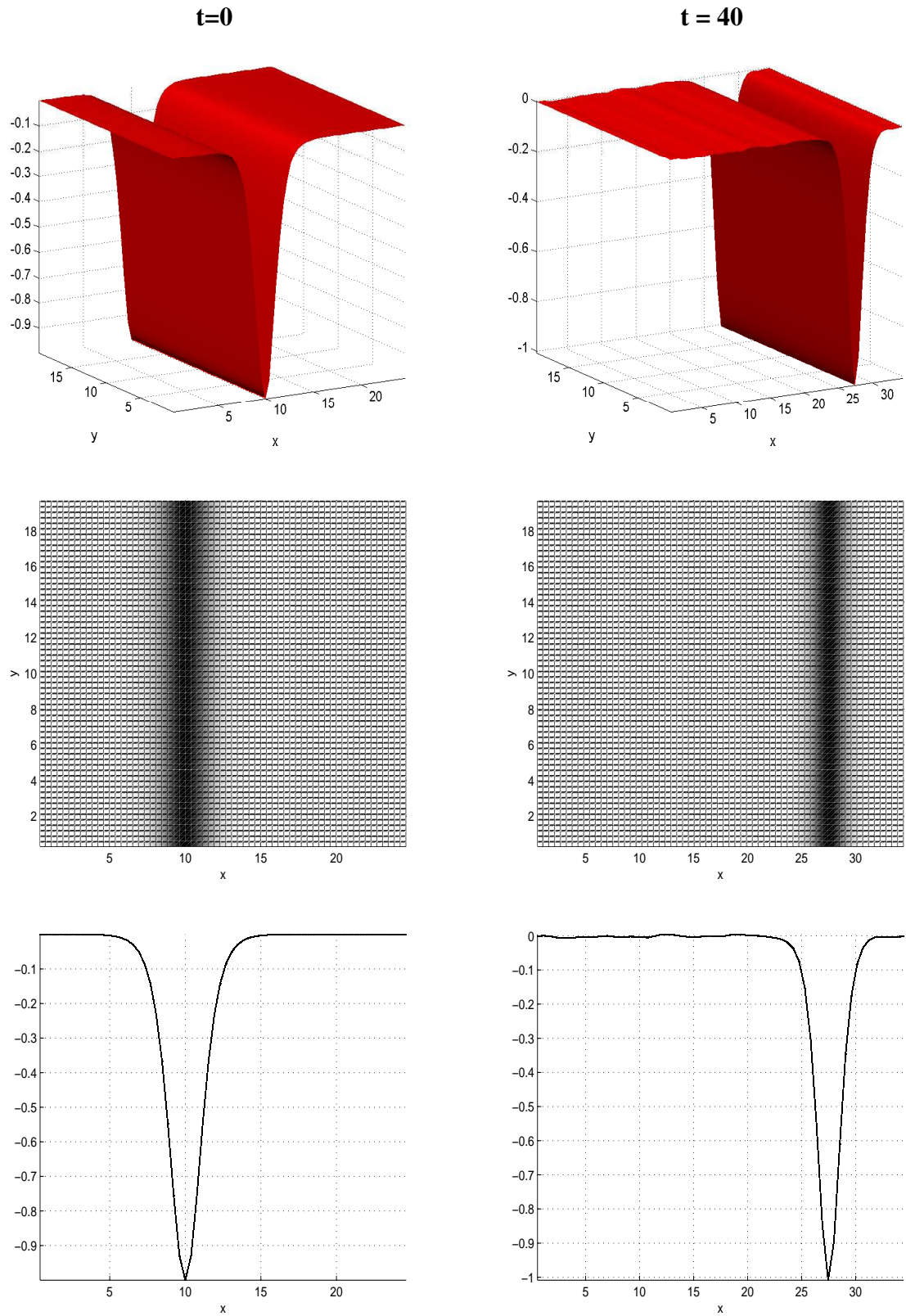


Fig. 4.3: Three views comparing the initial condition u_0 and its numerical evolution at $t = 40$.

5. INSTABILITY OF TRAVELING–WAVE SOLUTIONS OF THE NV EQUATION TO TRANSVERSE PERTURBATIONS

5.1 Introduction

In physical settings, verifying whether a wave exists or not can be quite simple. If you observe the wave or disturbance, it exists. For example, soliton solutions to the KdV equations certainly exist because we see them in many applications such as water waves, fiber optics and the Fermi–Pasta–Ulam problem. However, if a certain type of wave is not seen, it may still exist. It can simply mean that if the wave exists, it may not exist long enough to be detected.

For this reason the study of stability of solutions becomes important. If the wave is shown to be unstable it should not appear in applications or in a laboratory setting [57]. A question that can be asked is how is the wave unstable, that is, what type of disturbances cause the wave to disappear. In many applications there are perturbations acting transversely on a wave. This type of perturbation is one that occurs frequently in water waves, gravity waves, and plasmas [57, 5].

The problem of transverse stability has been studied for many of the classic soliton equations including the KP equation [33, 5, 3, 14], the Boussinesq equation [5], the ZK equation [4, 23, 31, 30], and most notably, the KdV equation [34]. In fact, Kadomstev & Petviashvili were considering the problem of the instability of the KdV equation to transverse perturbations when they derived the celebrated KP equation.

In order to understand the stability of one-dimensional soliton solutions of the NV equation we will carry out a linear stability analysis by considering sinusoidal perturbations

with wavevector perpendicular to the direction of propagation. In order to make conclusions about the stability of soliton solutions, as well as approximate the growth rate, the method chosen is the one developed by Rowlands, Infeld and Allen [32, 4].

Due to the complicated boundary conditions, we employ a geometric optics limit based on a scheme that assumes the nonlinear wave undergoes a long-wavelength perturbation. Thus, if the wave vector of the perturbation is \mathbf{k} , we assume $k \ll K$ where \mathbf{K} is the wave vector of the solution. This type of investigation is called the \mathbf{K} -expansion method.

To my knowledge, with the exception of the work of Bradley [13], this is the only known use of this method for a soliton system. In [13] equations are derived to model small amplitude, long waves traveling over the surface of a thin current-carrying metal film. His system can be reduced to the dimensionless form

$$u_t - 4u_x + \nabla^2 u_x + \frac{1}{2}uu_x = -\frac{1}{2}(\Psi_x u_x + \Psi_y u_y),$$

$$\nabla^2 \Psi = u_x.$$

In [13] it was necessary to use a multiscale perturbation technique, a much more intensive and technical method than an ordinary perturbation method, to prove the instability of transverse perturbations and to find an approximation to the linear growth rate of the instability.

In [32], the authors conjecture that to do a linear stability analysis using the \mathbf{K} -expansion method, a regular perturbation analysis is consistent only if the equation is an integrable system. If a multiscale analysis is necessary, the equation is not integrable. The ZK equation and Bradley equations are not integrable, and the ordinary perturbation analysis fails [4, 13]. So far this conjecture holds true for the KP and Boussinesq equations [5]. The results contained here back up their claim by showing only an ordinary perturbation analysis is needed for the NV equation.

5.1.1 History of the \mathbf{K} -Expansion Method

As the ubiquity of the KdV equation in physical applications became apparent, the question of the stability of its wave solutions became important. The first application where this was addressed was in water waves. In [7] Benjamin showed all soliton solutions to KdV are stable in the shallow water limit. However, in the deep water limit $h/\lambda \rightarrow \infty$, where h is the water depth and λ is the wavelength, Brooke-Benjamin and Feir [8] showed small amplitude solutions to be unstable by using expansion methods.

Answering the question of stability was next addressed using Lagrangian's and Hamiltonians by Whitham [70]. Whitham employed an averaging method that relies on Floquet's theorem, a theorem that relies on integrating over the period of a wave. If the wave is a soliton, the wavelength is taken to infinity after the integration has occurred. Infeld and Rowlands argue that this does not take into account the algebraic secular terms and can miss certain regimes of instability. For instance, the question of stability of one-dimensional nonlinear structures in the KP equation to two-dimensional perturbations was 'solved' by Kuznetsov *et. al.* [40]. However, the growth rates for certain limiting cases were not completed and were only tractable through numerical techniques. Infeld and Rowlands formalized a method to better handle the limiting cases missed for the KP equation. They eventually completed Kuznetsov's analysis [33] using the \mathbf{K} -expansion method described here.

In the \mathbf{K} -expansion method, the first step is make transformations so the solution that is being investigated becomes stationary in the system. This generally requires an affine transformation. The equation is then linearized around this stationary solution. Next, take perturbed quantities to be of the form $f(x)e^{i(\mathbf{k}x - \Omega t)}$ where f has wavelength equal to the solution u . Lastly, at each wavelength \mathbf{k} , remove the secular terms. This is a consistency condition. At this step the approximations for the growth rate are revealed.

There are some advantages to the \mathbf{K} -expansion method that make it a very practical method with which to study stability. The first is that it can be used when no Lagrangian

exists and when there are insufficient conservation laws to describe the system. This makes it ideal for use in the NV equation since the conservation laws are not easily calculated. The \mathbf{K} -expansion method also works on non-integrable systems such as the ZK equation. Lastly, it does not necessarily rely on periodicity of the solutions or periodicity of boundary conditions.

To circumvent using Floquet's theorem, Allen and Rowlands suggested [4] replacing Floquet's theorem with a condition on the asymptotics of the solutions in the space variables. Their suggestion was to enforce the boundary condition that the full solution must agree with the asymptotic solution at each order of \mathbf{K} .

5.2 The Direct \mathbf{K} -Method Applied to the NV Equation

5.2.1 Setting up the NV System for Analysis

We will work with the NV system in the form

$$0 = 4u_t + u_{xxx} - 3u_{xyy} - 3(uv)_x - 3(uw)_y, \quad (5.2.1)$$

$$u_x = v_x - w_y, \quad (5.2.2)$$

$$u_y = -w_x - v_y. \quad (5.2.3)$$

If the functions u , v and w are not dependent on y the NV equations (5.2.1) – (5.2.3) reduce to a KdV-type equation and admits soliton solutions of the form

$$u(x, y, t) = -2c \operatorname{sech}^2(\sqrt{c}(x - ct)), \quad (5.2.4)$$

$$v(x, y, t) = -2c \operatorname{sech}^2(\sqrt{c}(x - ct)), \quad (5.2.5)$$

$$w(x, y, t) = 0. \quad (5.2.6)$$

In order to investigate its stability we transform to a coordinate system that moves along

with the soliton by letting

$$(x, y, t) \mapsto \left(\frac{x+t}{\sqrt{c}}, \frac{y}{\sqrt{c}}, \frac{t}{c^{3/2}} \right),$$

$$u \mapsto cu, \quad v \mapsto cv, \quad w \mapsto cw.$$

and the resulting system is

$$0 = 4u_t - 4u_x + u_{xxx} - 3u_{xyy} - 3(uv)_x - 3(uw)_y, \quad (5.2.7)$$

$$u_x = v_x - w_y, \quad (5.2.8)$$

$$u_y = -w_x - v_y, \quad (5.2.9)$$

with stationary soliton solutions

$$u_0(x) = -2 \operatorname{sech}^2 x, \quad (5.2.10)$$

$$v_0(x) = -2 \operatorname{sech}^2 x, \quad (5.2.11)$$

$$w_0(x) = 0. \quad (5.2.12)$$

We now apply a sinusoidal perturbation with wavevector perpendicular to the direction of propagation. Add the perturbation to our stationary solutions (5.2.10) – (5.2.12),

$$u(x, y, t) = u_0(x) + \epsilon f(x) e^{iky + \gamma t}, \quad (5.2.13)$$

$$v(x, y, t) = v_0(x) + \epsilon g(x) e^{iky + \gamma t}, \quad (5.2.14)$$

$$w(x, y, t) = \epsilon h(x) e^{iky + \gamma t}. \quad (5.2.15)$$

Substituting equations (5.2.13) - (5.2.15) into (5.2.7) – (5.2.9) and assuming $\epsilon \ll k$ we

can neglect 2nd order and higher terms in f, g and h . Our system becomes (' denotes d/dx)

$$0 = 4\gamma f - 4f' + f''' + 3k^2 f' - 3(u_0 g)' - 3(v_0 f)' - 3iku_0 h \quad (5.2.16)$$

$$f' = g' - ikh, \quad (5.2.17)$$

$$ikf = -igk - h'. \quad (5.2.18)$$

We find that there are two stable and bounded solutions to equation (5.2.16) – (5.2.18), one for $k = 0$ and one for $k = 1$. That is, for $\gamma = 0$ (no growth) we find two solutions, one corresponding to $k = 0$ and one for $k = 1$

$$k = 0, \gamma = 0, \quad \begin{cases} f(x) = \text{sech}^2 x \tanh x \\ g(x) = \text{sech}^2 x \tanh x \\ h(x) = 0 \end{cases} \quad (5.2.19)$$

$$k = 1, \gamma = 0, \quad \begin{cases} f(x) = \text{sech}^3 x \\ g(x) = -\text{sech} x \tanh^2 x \\ h(x) = -i \text{sech} x \tanh x \end{cases} \quad (5.2.20)$$

Thus, we expect instability for $0 < k < 1$. We investigate this numerically and analytically.

5.2.2 Perturbation Analysis, $k = 0$

The analysis that follows is a linear approximation to the growth rate. We now assume k small and expand our quantities in k

$$\gamma = \gamma_1 k + \gamma_2 k^2 + \dots, \quad (5.2.21)$$

$$f = f_0 + k f_1 + k^2 f_2 + \dots \quad (5.2.22)$$

$$g = g_0 + k g_1 + k^2 g_2 + \dots \quad (5.2.23)$$

$$h = h_0 + k h_1 + k^2 h_2 + \dots \quad (5.2.24)$$

The task now is to substitute equations (5.2.21) – (5.2.24) into equations (5.2.16) – (5.2.18) and solve the resulting system of equations by setting each coefficient of k equal to 0.

In order to help verify our results we have developed a numerical approximation to γ based on the algorithms previously developed in [4, 50, 51]. The asymptotic assumption is that as $|x| \rightarrow \infty$, the perturbation functions f, g , and h all go to their geometrical optics limit.

For large $|x|$, since $u_0, v_0 \rightarrow 0$ as $|x| \rightarrow \infty$, the system (5.2.16)–(5.2.18) reduces to

$$0 = 4\gamma f - 4f' + f''' + 3k^2 f' \quad (5.2.25)$$

$$f' = g' - ikh, \quad (5.2.26)$$

$$ikf = -igk - h'. \quad (5.2.27)$$

Equation (5.2.25) can be rewritten as

$$0 = f''' - (4 - 3k^2)f' + 4\gamma f.$$

This is a 3rd order, constant coefficient differential equation and can be solved in the usual manner. The three solutions are $e^{p_1 x}$, $e^{-p_2 x}$ and $e^{p_3 x}$ where $p_i > 0$ for $i = 1, 2, 3$. For small k and γ we find $p_1 = 2 - \frac{\gamma}{2}$, $p_2 = 2 + \frac{\gamma}{2}$, and $p_3 = \gamma$, and so the zeroth order asymptotic

solution should go to e^{-2x} as $x \rightarrow \infty$ and either e^{2x} or e^0 as $x \rightarrow -\infty$.

Assuming x large and positive, equations (5.2.26) and (5.2.27) reduce to

$$-p_2 e^{-p_2 x} = g' - ikh, \quad (5.2.28)$$

$$ike^{-p_2 x} = -igk - h' \quad (5.2.29)$$

which, if we take the derivative of (5.2.28) and solve for h' , we can use equation (5.2.29) to solve for g . We then obtain

$$g'' - k^2 g = e^{-p_2 x} (p_2^2 + k^2)$$

with solution

$$g(x) = c_1 e^{-kx} + c_2 e^{kx} + \frac{p_2^2 + k^2}{p_2^2 - k^2} e^{-p_2 x}. \quad (5.2.30)$$

Similarly, we find for h ,

$$h(x) = d_1 e^{-kx} + d_2 e^{kx} + \frac{2p_2 ik}{p_2^2 - k^2} e^{-p_2 x}. \quad (5.2.31)$$

In order to have g and h decay to zero as $|x| \rightarrow \infty$ we must have that $c_1 = d_1 = c_2 = d_2 = 0$.

Solving the Zero Order System

Substituting equations (5.2.21) – (5.2.24) into equations (5.2.16) – (5.2.18) and setting the coefficients of the zero order term in k equal to 0, we obtain the following system,

$$0 = -4f_0' + f_0''' - 3(u_0g_0)' - 3(v_0f_0)' \quad (5.2.32)$$

$$f_0' = g_0', \quad (5.2.33)$$

$$0 = h_0' \quad (5.2.34)$$

We know that $v_0 = u_0$, and we are assuming all of our perturbed quantities are 0 in the limit. Therefore, we conclude $h_0 = 0$ and $f_0 = g_0$ and equation (5.2.32) becomes

$$0 = -4f_0' + f_0''' - 6(u_0f_0)',$$

or

$$\frac{d}{dx}Lf_0 = 0, \quad (5.2.35)$$

where

$$L := -4 + \frac{d^2}{dx^2} - 6u_0.$$

The solution to (5.2.35) is given by [4]

$$f_0 = \operatorname{sech}^2x \tanh x + B_0\Psi + C_0\xi, \quad (5.2.36)$$

where

$$\xi = \frac{1}{4}(3x\operatorname{sech}^2x \tanh x - 3\operatorname{sech}^2x + 1)$$

$$\Psi = \frac{1}{4} \cosh^2 x - \frac{5}{2}\xi.$$

Since $f_0 \rightarrow 0$ in the limit, we must have that B_0 and C_0 are 0, and so

$$f_0 = \operatorname{sech}^2x \tanh x.$$

In general,

$$L^{-1}R(x) = \phi_0(x) \int \frac{\int R(x'')\phi_0(x'')dx''}{\phi_0^2(x')} dx' \text{ mod } \phi_0(x) \quad (5.2.37)$$

for any function $R(x)$ that decays to 0 as $x \rightarrow \infty$. The $\text{mod}\phi_0(x)$ operation is to remove any extra ϕ_0 terms that may appear from the integration. These terms are unnecessary because they are the solution to the homogeneous problem $L\phi_0 = 0$.

Solving the First Order System

Going back to the expanded system (5.2.16) – (5.2.18), we set the coefficients of the first order term in k equal to 0, and obtain the following system,

$$0 = 4\gamma_1 f_0 - 4f_1' + f_1''' - 3(u_0 g_1)' - 3(v_0 f_1)' \quad (5.2.38)$$

$$f_1' = g_1', \quad (5.2.39)$$

$$2f_0 = ih_1' \quad (5.2.40)$$

Now, using $v_0 = u_0$ and that $f_1 = g_1$ we have

$$\frac{d}{dx} Lf_1 = -4\gamma_1 f_0, \implies Lf_1 = 2\gamma_1 \text{sech}^2 x + C_1. \quad (5.2.41)$$

The solution to (5.2.41) is

$$f_1(x) = -\frac{1}{2}\gamma_1(xf_0 - \text{sech}^2 x) + C_1\xi.$$

where $\xi = 3x\text{sech}^2 x \tanh x - 3\text{sech}^2 x + 1$. As before, equating C_1 to 0 results in a solution f_1 that vanishes at infinity. Note that γ_1 has yet to be determined. Using equation (5.2.40)

to solve for $h_1(x)$, the results for the first order system are

$$f_1(x) = -\frac{1}{2}\gamma_1(xf_0 - \operatorname{sech}^2x) \quad (5.2.42)$$

$$g_1(x) = -\frac{1}{2}\gamma_1(xf_0 - \operatorname{sech}^2x) \quad (5.2.43)$$

$$h_1(x) = i\operatorname{sech}^2x. \quad (5.2.44)$$

Solving the Second Order System

Collecting the coefficients of k^2 and setting them equal to 0 yields the following system,

$$0 = 4(\gamma_1f_1 + \gamma_2f_0) - 4f_2' + f_2''' + 3f_0' - 3(u_0g_2)' - 3(u_0f_2)' - 3iu_0h_1 \quad (5.2.45)$$

$$f_2' - g_2' = -ih_1, \quad (5.2.46)$$

$$2i(f_0 + kf_1) = -(h_1 + kh_2)'. \quad (5.2.47)$$

Equation (5.2.46) allows us to solve for g_2 in terms of f_2 and h_1 . The function h_1 is given in equation (5.2.44) and so integrating equation (5.2.46) shows $g_2 = f_2 - \tanh x + C$. Due to the asymptotic boundary conditions, $C = 1$ and $g_2 = f_2 - \tanh x + 1$. From this equation (5.2.45) becomes

$$0 = 4(\gamma_1f_1 + \gamma_2f_0) - 4f_2' + f_2''' - 6(u_0f_2)' + 3f_0' + 3(u_0(\tanh x - 1))' - 3iu_0h_1$$

Rewriting this in terms of the operator L and recalling that $h_1 = i\operatorname{sech}^2x$, we have

$$\frac{d}{dx}Lf_2 = -4(\gamma_1f_1 + \gamma_2f_0) - 3f_0' - 3(u_0(\tanh x - 1))' - 3u_0\operatorname{sech}^2x$$

and after integrating

$$\begin{aligned}
Lf_2 &= (4 - \gamma_1^2) \tanh x - \gamma_1^2 x \operatorname{sech}^2 x + (2\gamma_2 - 6) \operatorname{sech}^2 x \\
&\quad + 5 \operatorname{sech}^2 x \tanh x + C_2.
\end{aligned} \tag{5.2.48}$$

The solution to equation (5.2.48) is

$$\begin{aligned}
f_2 &= \left(\frac{1}{2} - \frac{\gamma_1^2}{8} \right) \sinh x \cosh x + \left(\frac{1}{2} - \frac{\gamma_1^2}{8} \right) \tanh x + \\
&\quad + \frac{1}{8} \gamma_1^2 x^2 \tanh x \operatorname{sech}^2 x - \frac{1}{4} \gamma_1^2 x \operatorname{sech}^2 x + (2\gamma_2 - 6) x \tanh x \operatorname{sech}^2 x \\
&\quad + (-2\gamma_2 + 6) \operatorname{sech}^2 x + \left(\frac{5\gamma_1^2}{64} + \frac{1}{48} \right) \tanh x \operatorname{sech}^2 x.
\end{aligned}$$

Both the $\tanh x$ term and the $\sinh x \cosh x$ term are divergent and they need to disappear to continue the analysis. In order to preserve the boundary condition that $f_2 \rightarrow 0$ as $x \rightarrow \infty$ let $\gamma_1^2 = 4$. This makes both terms vanish and we are left with

$$\begin{aligned}
f_2 &= \frac{1}{2} x^2 \tanh x \operatorname{sech}^2 x - x \operatorname{sech}^2 x + (2\gamma_2 - 6) x \tanh x \operatorname{sech}^2 x \\
&\quad + (-2\gamma_2 + 6) \operatorname{sech}^2 x + \frac{1}{3} \tanh x \operatorname{sech}^2 x, \\
g_2 &= f_2 - \tanh x + 1, \\
h_2 &= -i (x \operatorname{sech}^2 x + \tanh x - 1).
\end{aligned}$$

This has the desired asymptotic behavior, that is, $f_2, g_2, h_2 \rightarrow 0$ as $x \rightarrow \infty$. At this point it should be noted that the growth rate is shown to be positive and so *the soliton is unstable to transverse perturbations*. The analysis will continue to find a better approximation to the growth rate.

Solving the Third Order System

Collecting the coefficients of k^3 and setting them equal to 0 gives

$$0 = 3f_1' - 3iu_0h_2 - 3(u_0g_3)' - 3(u_0f_3)' - 4f_3' + f_3''' + 4f_0\gamma_3 + 4f_1\gamma_2 + 4f_2\gamma_1 \quad (5.2.49)$$

$$g_3' = f_3' + ih_2 \quad (5.2.50)$$

$$h_3' = -ig_2 - if_2. \quad (5.2.51)$$

Integrating equation (5.2.50) results in a solution for g_3 ,

$$\begin{aligned} g_3 &= f_3 + \int x \operatorname{sech}^2 x + \tanh x - 1 dx \\ &= f_3 + x(\tanh x - 1) + C_3 \end{aligned}$$

where it is necessary for $C_3 = 0$ in order to preserve the asymptotics. Since f_2 and g_2 have already been calculated, we can integrate equation (5.2.51) and we now have the solutions for h_3 and g_3 .

Using the solution for $g_3(x)$ (notice h_3 is not needed here), equation (5.2.49) becomes

$$\begin{aligned} \frac{d}{dx} Lf_3 &= (12\gamma_2 - 36) \operatorname{sech}^2 x - \left(\frac{17}{3} + 4\gamma_3 \right) \operatorname{sech}^2 x \tanh x + 15x \operatorname{sech}^2 x \tanh^2 x \\ &\quad - x \operatorname{sech}^2 - 4x^2 \operatorname{sech}^2 x \tanh x + (36 - 12\gamma_2) x \operatorname{sech}^2 x \tanh x, \end{aligned}$$

and upon integration,

$$\begin{aligned} Lf_3 &= (6\gamma_2 - 18) \tanh x + \left(\frac{1}{3} + 2\gamma_3 \right) \operatorname{sech}^2 x - 5x \tanh x \operatorname{sech}^2 x \\ &\quad + 2x^2 \operatorname{sech}^2 x + (6\gamma_2 - 18) (x \operatorname{sech}^2 x). \end{aligned}$$

Applying L^{-1} we find

$$\begin{aligned}
f_3 = & \frac{3}{12} (6\gamma_2 - 18) \sinh x \cosh x + \frac{1}{4} \left(\frac{1}{3} + 2\gamma_3 \right) \operatorname{sech}^2 x \tanh x (\coth x - x) \\
& \operatorname{sech}^2 x \tanh x \left(-\frac{x^3}{6} + \frac{1}{2} x^2 \coth x + \frac{x}{4} - \frac{\coth x}{4} \right) \\
& + (6\gamma_2 - 18) \left(\frac{1}{8} \tanh x - \frac{15}{192} \operatorname{sech}^2 x \tanh x \right) + \\
& + (6\gamma_2 - 18) \operatorname{sech}^2 x \tanh x \left(-\frac{x^2}{8} + \frac{1}{4} x \coth x \right).
\end{aligned}$$

The only divergent terms are the $\sinh x \cosh x$ and the $\tanh x$ terms. Both of these can be eliminated by letting

$$\gamma_2 = 3.$$

We already established that the soliton solution was unstable to transverse perturbations, but now we also have a quadratic approximation to the growth rate,

$$\gamma = 2k + 3k^2 + O(k^3).$$

5.2.3 Perturbation Analysis, $k = 1$

We need a transformation for k near 1 so that we can apply the same analysis as was done for $k = 0$. Let $\bar{k} = 1 - k$ so that $k^2 = 1 - 2\bar{k} + \bar{k}^2$. Now, we can expand about \bar{k} in equations (5.2.16) – (5.2.18). The NV system becomes

$$0 = 4\gamma f - f' + f''' - 6\bar{k}f' + 3\bar{k}^2 f' - 3(u_0 g)' - 3(u_0 f)' - 3i(1 - \bar{k})u_0 h \quad (5.2.52)$$

$$0 = g' - f' - i(1 - \bar{k})h, \quad (5.2.53)$$

$$0 = i(1 - \bar{k})f + ig(1 - \bar{k}) + h'. \quad (5.2.54)$$

Using equations (5.2.52) – (5.2.54) the zero order terms in k are collected and equated to 0. The zeroth order equation is

$$0 = -f_0' + f_0''' - 3(u_0 g_0)' - 3(u_0 f_0)' - 3iu_0 h_0, \quad (5.2.55)$$

$$f_0' = g_0' - ih_0, \quad (5.2.56)$$

$$if_0 = -ig_0 - h_0'. \quad (5.2.57)$$

Unlike the zero order case for $k = 0$, we are not able to reduce the zero order system for $k = 1$ to a single equation involving only one of the unknown functions. So far, a general solution to this system has been elusive. Various computer algebra software packages have also failed. However, the zeroth order equation is identical to the original perturbed system (5.2.16) – (5.2.18) with $k = 1$ and $\gamma = 0$ and so a solution is

$$f_0 = a \operatorname{sech}^3 x,$$

$$g_0 = -a \operatorname{sech} x \tanh^2 x,$$

$$h_0 = -ai \operatorname{sech} x \tanh x.$$

In order to proceed with the analysis, a general solution must be found. These efforts are ongoing. However, we can make a few observations. The zero order system can be written in terms of multiplicative operators,

$$0 = \frac{d}{dx} \mathcal{L} f_0 + \frac{d}{dx} \mathcal{G} g_0 + \mathcal{H} h_0, \quad (5.2.58)$$

$$g_0' - ih_0 - f_0' = 0, \quad (5.2.59)$$

$$ig_0 + if_0 + h_0' = 0, \quad (5.2.60)$$

where

$$\mathcal{L} := -1 + \frac{d^2}{dx^2} - 3u_0, \quad (5.2.61)$$

$$\mathcal{G} := -3u_0, \quad (5.2.62)$$

$$\mathcal{H} := -3iu_0. \quad (5.2.63)$$

One can show this is the homogeneous system for all orders of \bar{k} . What this means is at each order of \bar{k} we get this same system with inhomogeneities. Thus, if we solve the zero order system, we can solve this system we can solve all higher orders and find an approximation to the growth rate.

5.3 Numerical Estimation of the Growth Rate γ

Using the system (5.2.16) – (5.2.18) and the asymptotics developed on page 69 we find a numerical approximation to the growth rate γ . The algorithm was based on the algorithms developed in [4, 51]. Using Matlab's ODE45, the system is solved for a fixed k , and then refined by approximating a better γ . Once this γ is settled upon, the next k uses the previous γ as a starting point.

In order to use Matlab's ODE solver, we need boundary conditions and so we use the asymptotics developed earlier. Since the asymptotic behavior is ambiguous for $x \rightarrow -\infty$ we use the boundary condition at $x \rightarrow \infty$. Since $f(x) \rightarrow e^{-p_2x}$ as $x \rightarrow \infty$ we choose $f(x) = e^{-p_2x}$ as our initial condition. Recall $p_2 = 2 + \gamma/2$. When implemented on the

domain $[x_0, x_f]$, we take

$$\begin{aligned}
 f(x_f) &= e^{-p_2 x_f}, \\
 f'(x_f) &= -p_2 e^{-p_2 x_f}, \\
 f''(x_f) &= p_2^2 e^{-p_2 x_f}, \\
 g(x_f) &= \frac{p_2^2 + k^2}{p_2^2 - k^2} e^{-p_2 x_f}, \\
 h(x_f) &= \frac{2p_2 i k}{p_2^2 - k^2} e^{-p_2 x_f},
 \end{aligned}$$

as our initial conditions. To begin the algorithm, choose k near 0 and the first guess for γ will be $\gamma = 2k + 3k^2$. Then, for each k refine the approximation for γ .

For the results presented here, the domain for $k \in [0, 1]$ was partitioned with 100 points. The j^{th} element of k is denoted by $k_j = j/100$, where $j = 1, 2, \dots, 100$. Let γ_j^l be the l^{th} approximation of γ for a fixed k_j . Let f_k^l be the numerically computed value of $f(x_0)$ for the l^{th} iteration of γ and k_j . Recall, x_0 is the left hand endpoint of the domain of integration. Essentially, this method refines k and γ by trying to match the numerically calculated asymptotic behavior of f with the asymptotic behavior calculated analytically at $x = x_0$.

For each k_j , we compute γ_j iteratively. To obtain γ_j^{l+1} , the previous approximation γ_j^l is perturbed randomly by a small increment, usually between 2% - 5%. Then, the value f_k^{l+1} is calculated numerically. If $|f_k^{l+1}| < |f_k^l|$ for all $i \in \{1, 2, \dots, l\}$, then γ_j^{l+1} is kept as the best $l + 1$ approximation for γ_j . Otherwise, the integration is attempted again for a newly perturbed γ_j^{l+1} .

Many tests were run on the various parameters mentioned above to achieve the best graph for γ as a function of k . We first tested the percent of perturbation of γ , the left and right hand endpoints of integration (x_0 and x_f), the parameter j , which is the partition on k , and l , the number of γ tested per k . When testing the parameter l , it was found that if l is too large, the integration resulted in a trivial graph. The other tests were very stable in the sense

that small changes in the parameters caused small changes the graph. Movies of these tests can be found at my website. <http://www.math.colostate.edu/~croke/Research/research.html>

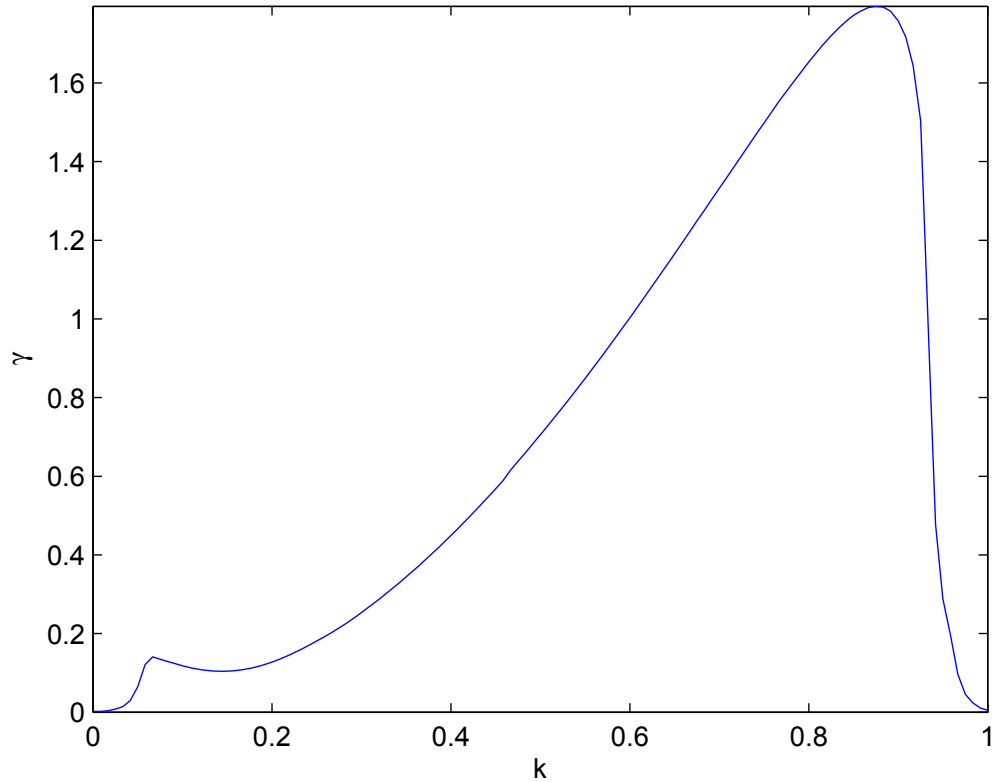


Fig. 5.1: Numerical Approximation for the Growth Rate γ

The graph of $\gamma(k)$ is presented in Figure 5.1. The bump seen in the bottom left hand corner is believed to be numerical error. The algorithm described above was used to reproduce the results shown in [4] for the ZK equation. The graphs I produced for the ZK equation matched the results in [4] but also sometimes contained bumps near the left and right hand values of k as seen in Figure 5.1.

5.4 Numerical Results Concerning the Instabilities of Soliton Solutions to the NV Equation

To investigate the instabilities of the NV equation with initial condition $u_{IC}(x, y, 0) = -2 \operatorname{sech}^2(x)$, we consider a transversely perturbed initial condition and compute its evolution numerically using the methods of chapter 4. We choose ϵ to be a small number and W_y be the length of the domain over which y is being computed. For the figures that follow, the spatial grid was $x \in [0, 50]$ and $y \in [0, 100]$. We define

$$u_p(x, y, 0) = \left(1 - \epsilon \cos \left(\frac{2\pi}{W_y} y \right) \right) (-2 \operatorname{sech}^2 x). \quad (5.4.1)$$

A typical value for ϵ is 0.01, giving a maximum of a 1% perturbation. Figure 5.2 shows the profile of the initial condition u_{IC} , and Figure 5.3 shows the profile of the perturbed initial condition, u_P .

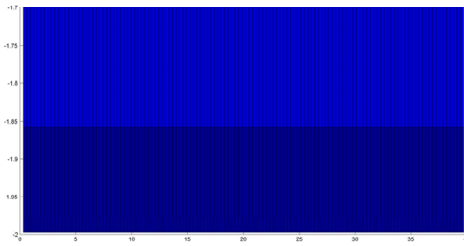


Fig. 5.2: Sech^2 Initial Condition

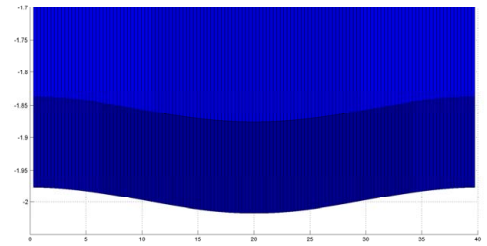


Fig. 5.3: Perturbed Sech^2 Initial Condition

Figure 5.4 shows u_p at $t = 0$ from an angle that shows the profile both laterally and transversely. The resulting evolution propagates uneventfully until it shows blow-up at approximately $t = 30.48$ time units as can be seen in Figure 5.5. A singularity forms where the maximum (in amplitude) was located in the initial condition $u_p(x, y, 0)$. This happens regardless of time step or grid size. Figure 5.6 shows a top view of the perturbed soliton at $t = 30.48$.

It remains a conjecture as to whether the feature in Figures 5.5 and 5.6 is an artifact of

the numerical solution or if these solutions have finite time blow-up. In [59] it was shown that there exists solutions to the NV equation that have finite time blow-up. Their analysis relies on the *binary Darboux transformation* established in [49]. Using this method they construct rational solutions that decay to 0 as $r \rightarrow \infty$, where $r = \sqrt{x^2 + y^2}$, but have finite time blow-up for $t \geq 29/12$. However, the singularities that are forming in Figures 5.5 and 5.6 change when the computational parameters change. For example, if the spatial grid is changed to $y \in [0, 50]$, the blow-up occurs at $t \approx 16.4$. If the time step changes, the time of blow-up also changes, though not as drastically. From the numerical evidence it seems probable that what we are seeing here is numerical blow-up.

In an effort to further investigate the perturbed solutions, the permissible amplitude was restricted, and the resulting evolution was observed. The perturbed soliton breaks into other coherent lumps at a time $t = t^* \approx 30.48$. For $t \geq t^*$ these new structures have been observed to continue to propagate undisturbed. This same behavior is seen in perturbed solutions to both the KP and ZK equations [24, 25]. For instance, in the pictures that follow, the amplitude was capped at -5. At each step, if the amplitude was less than -5, the value was reset to -5, otherwise it was left alone. The resulting evolution from performing this “capping” is seen in Figures 5.7 and 5.8. The four taller structures are stable and propagate as far as the numerical solver will take them.

Figures (5.9) – (5.18) show time snapshots the evolution of the perturbed soliton for $t = 5, 10, 15, 20, 25, 30, 35, 40, 45, 50$. Imposing a maximum on the amplitude gives rise to other coherent structures. The “capping” may be giving us the long-term behavior of the perturbed solitons, but the integrity of this result has not yet been determined.

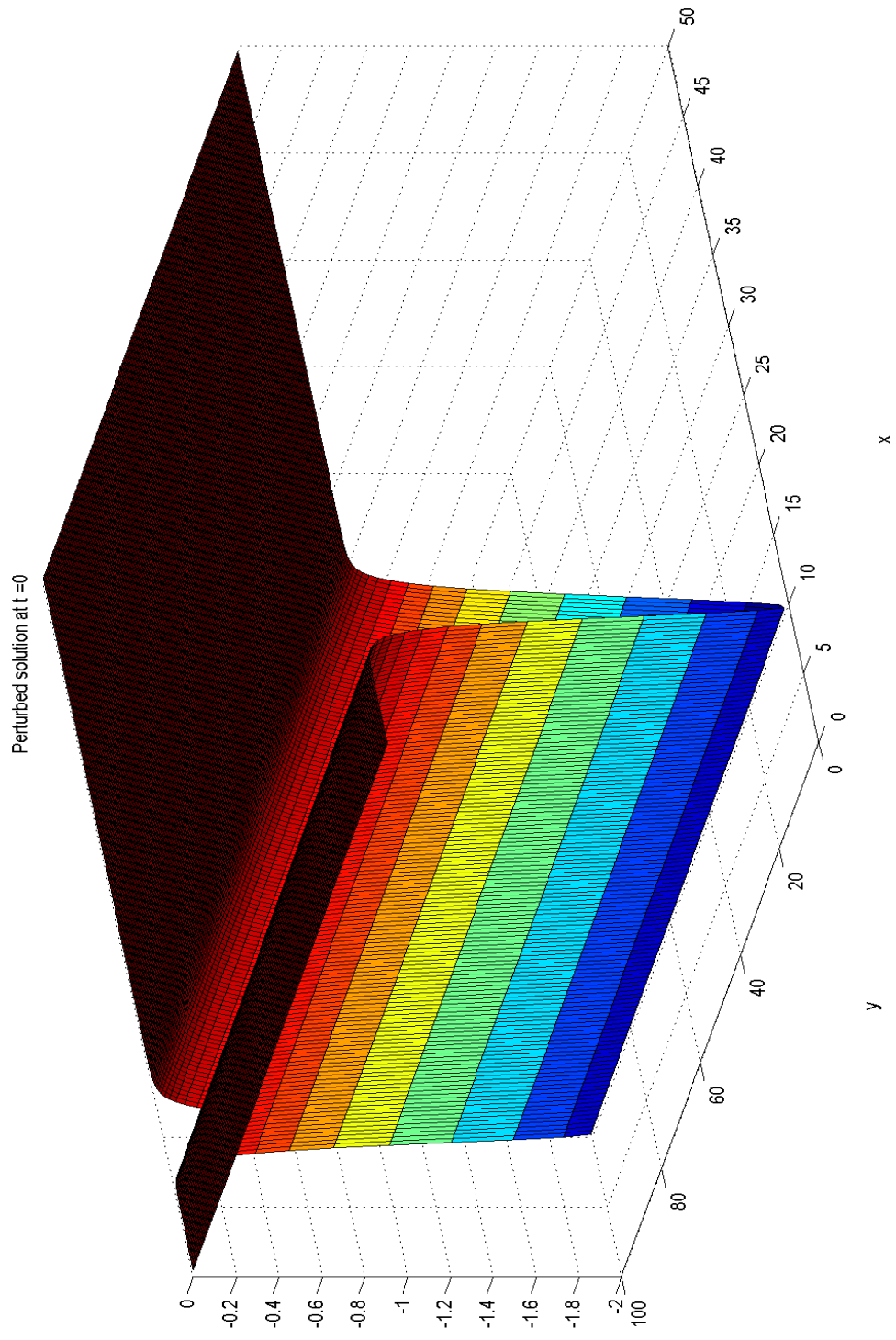


Fig. 5.4: Initial Condition, $u_p(x, y, 0) = -2 \operatorname{sech}^2(x)$

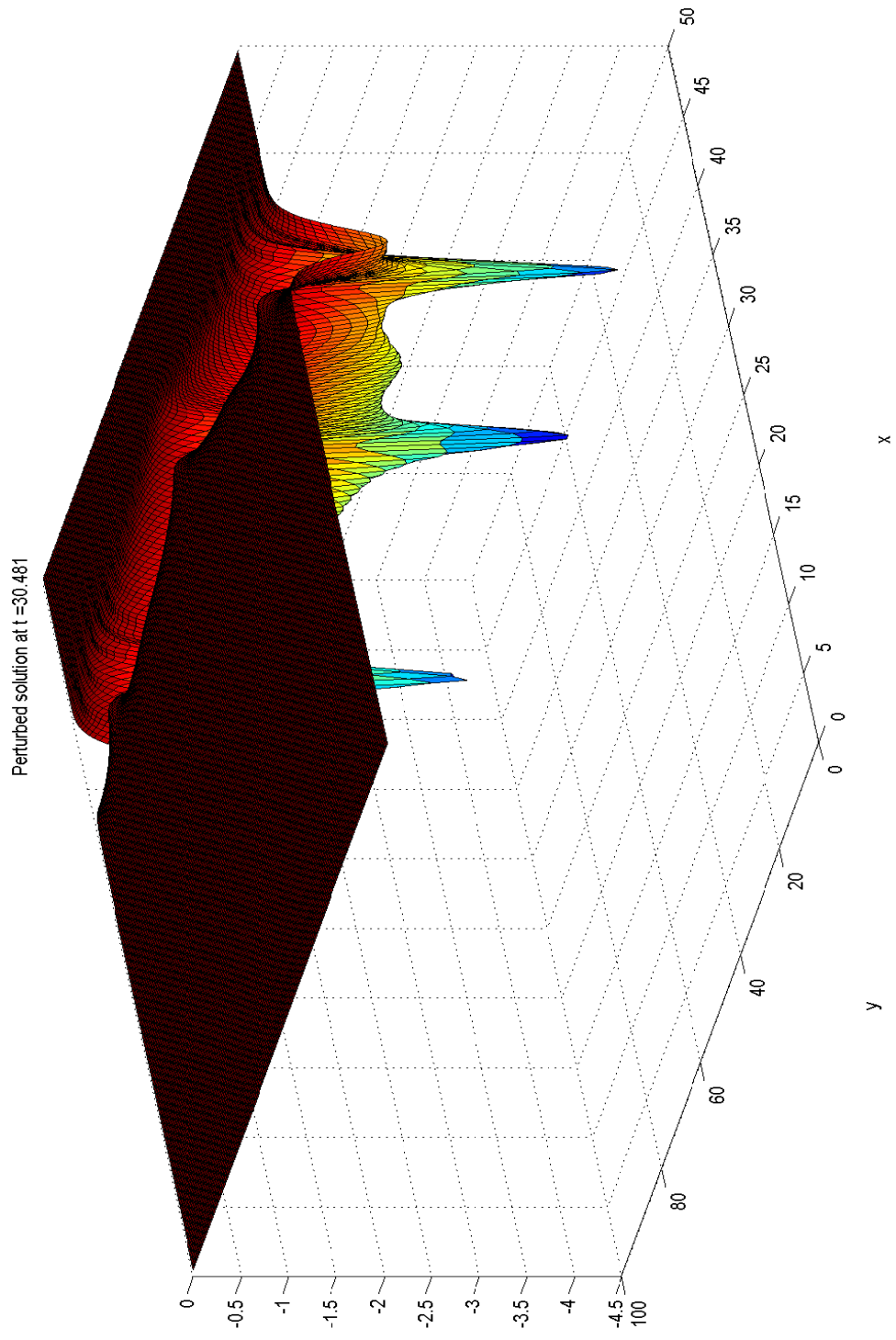


Fig. 5.5: Perturbed IC, $u_p(x, y, t)$ at $t = 30.48$.

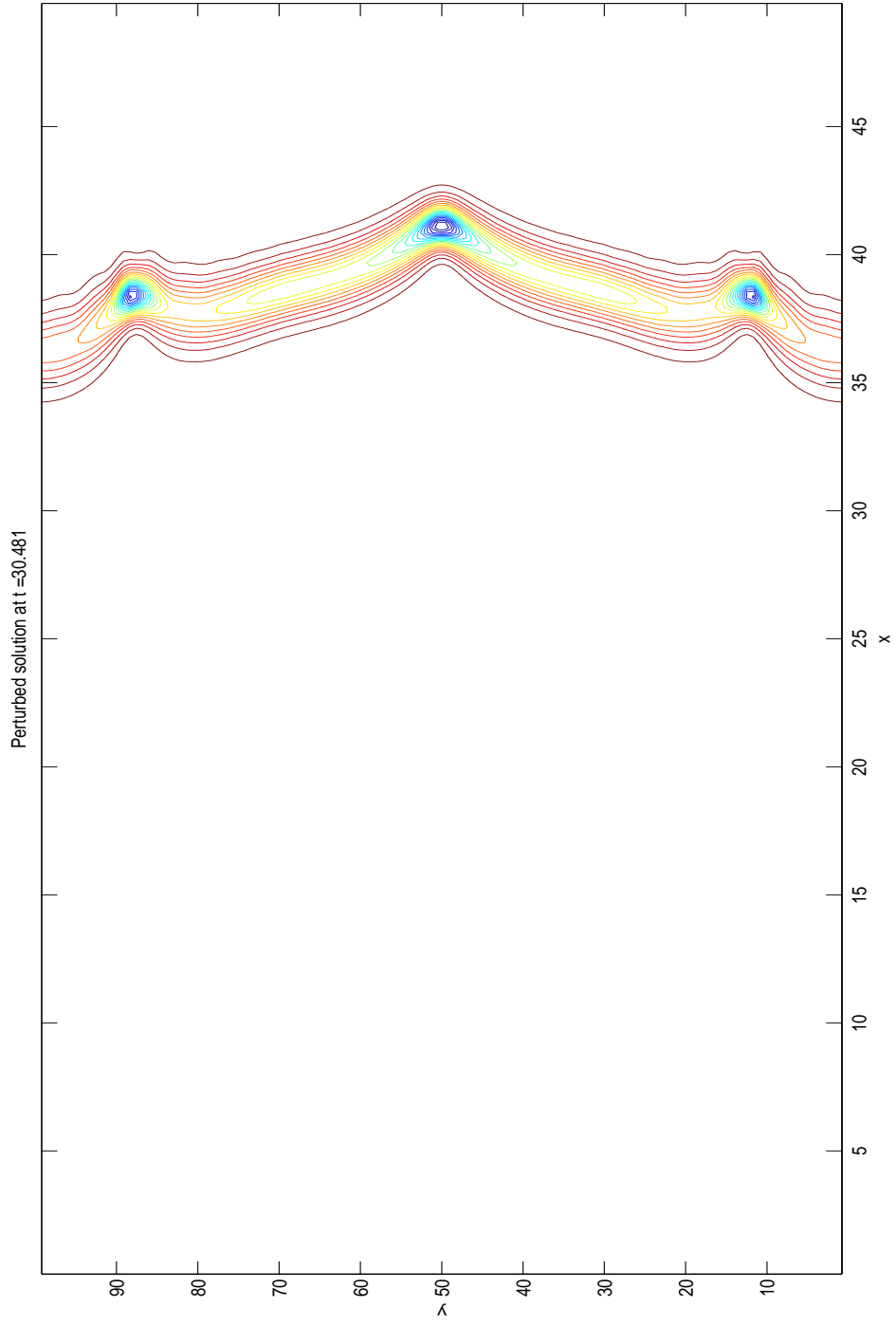


Fig. 5.6: Contour View of $u_p(x, y, t)$ at $t=30.48$

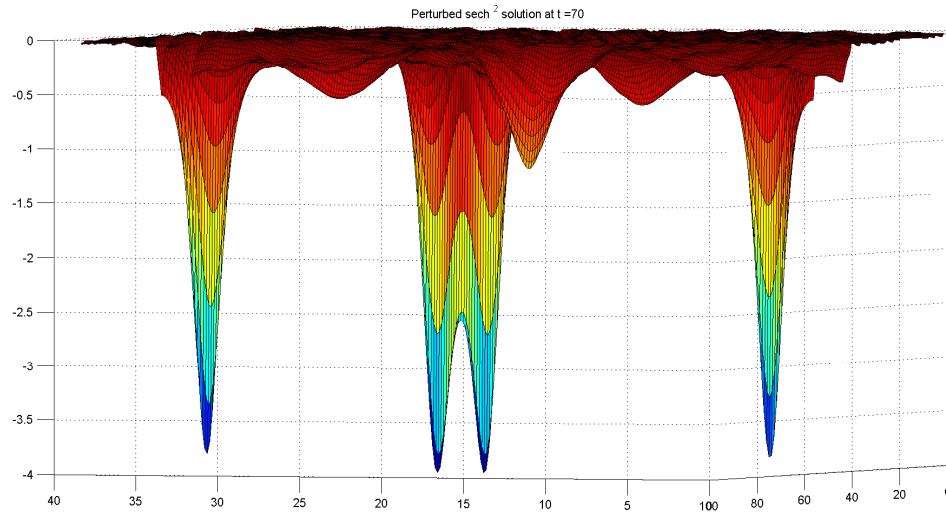


Fig. 5.7: $u_P(x, y, 70)$ with restricted amplitude throughout the evolution “capped” at -5.

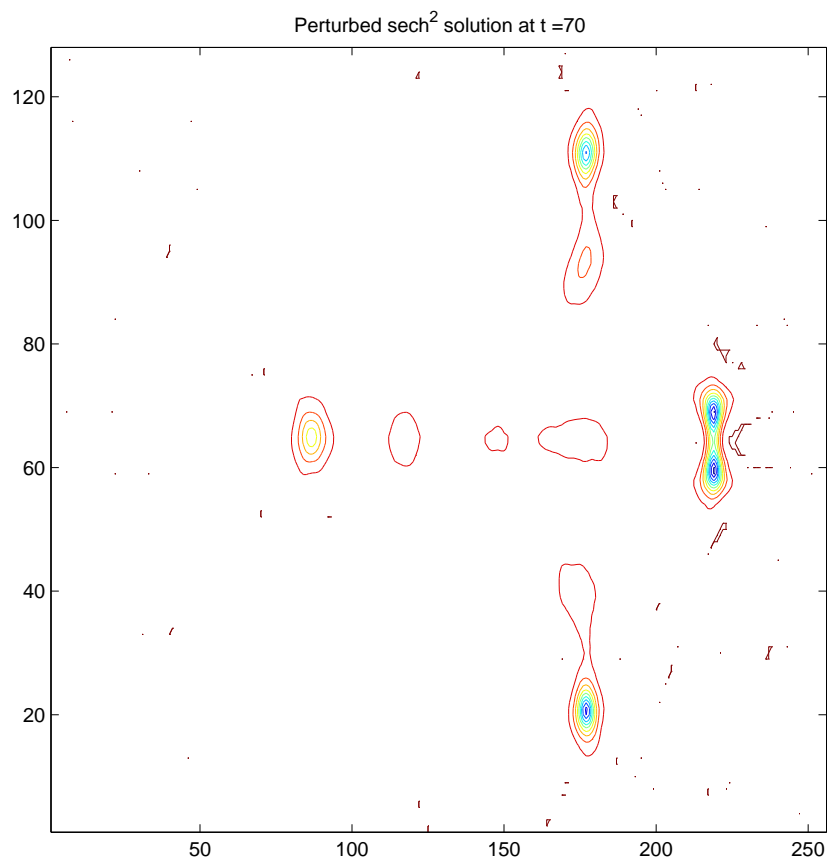


Fig. 5.8: $u_P(x, y, 70)$ with restricted amplitude throughout the evolution “capped” at -5, contour view.

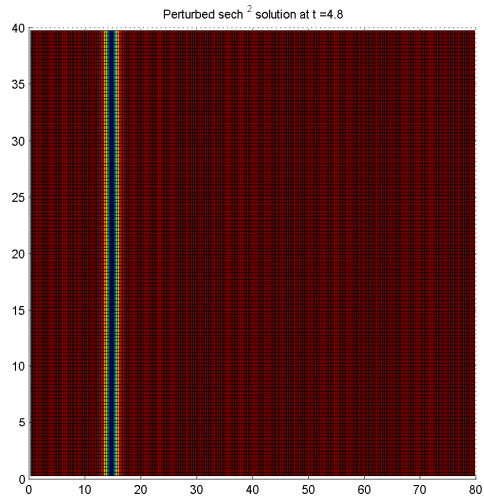


Fig. 5.9: Contour view, $t = 5$ with amplitude capping.

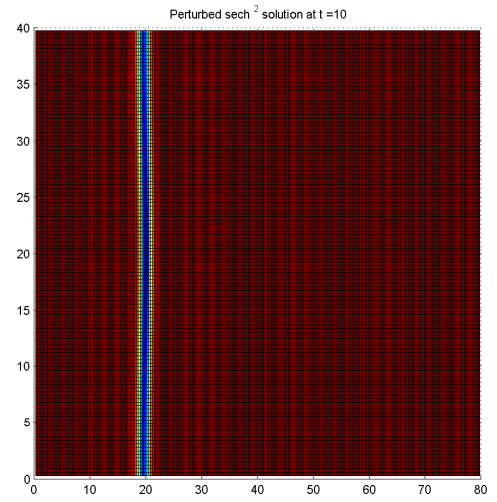


Fig. 5.10: Contour view, $t = 10$ with amplitude capping.

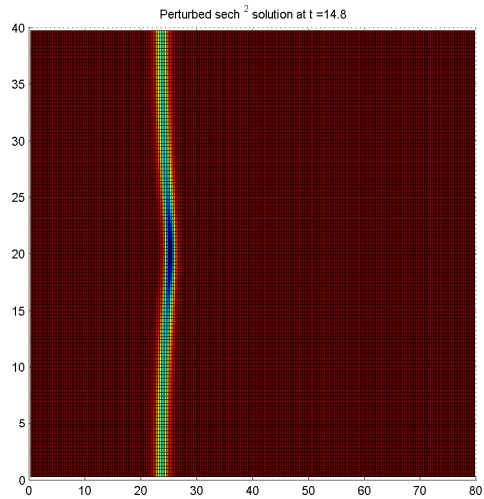


Fig. 5.11: Contour view, $t = 15$ with amplitude capping.

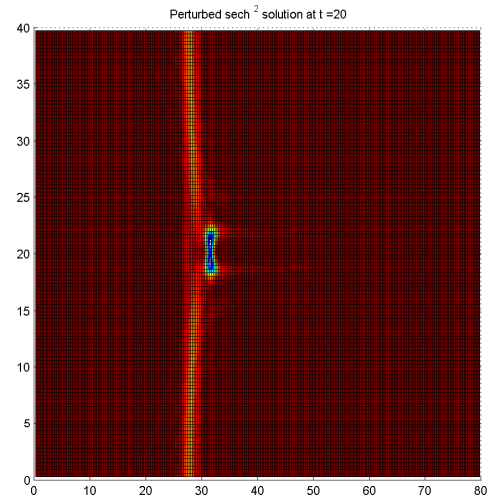


Fig. 5.12: Contour view, $t = 20$ with amplitude capping.

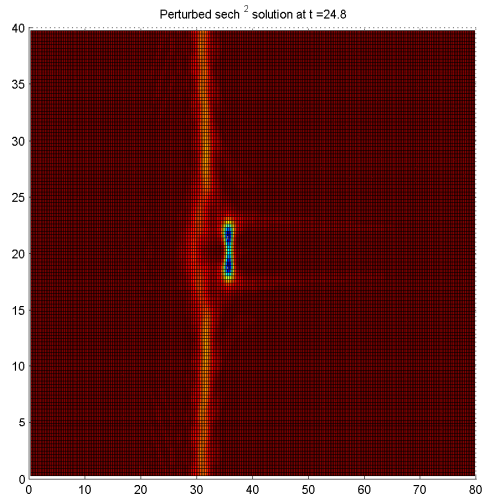


Fig. 5.13: Contour view, $t = 25$ with amplitude capping.

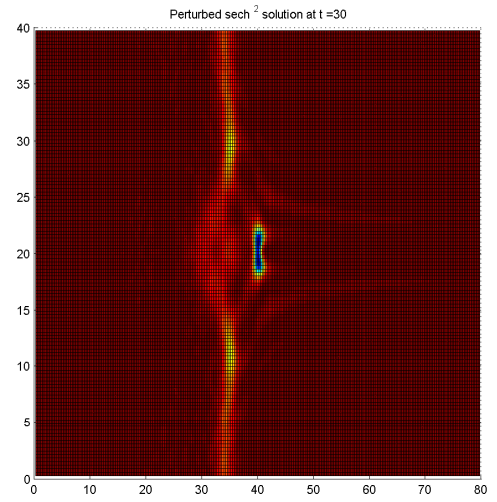


Fig. 5.14: Contour view, $t = 30$ with amplitude capping.

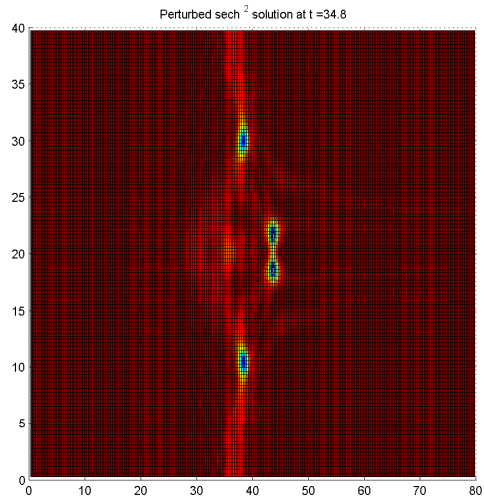


Fig. 5.15: Contour view, $t = 35$ with amplitude capping.

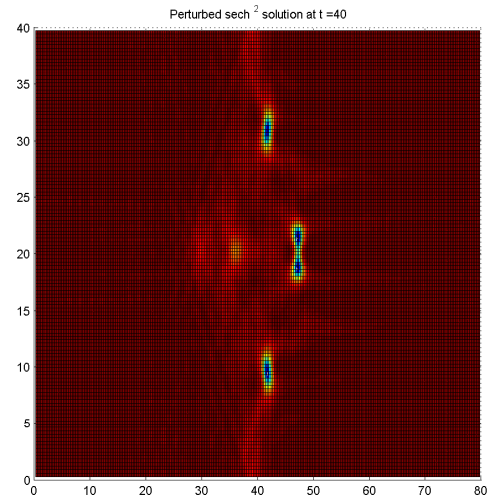


Fig. 5.16: Contour view, $t = 40$ with amplitude capping.

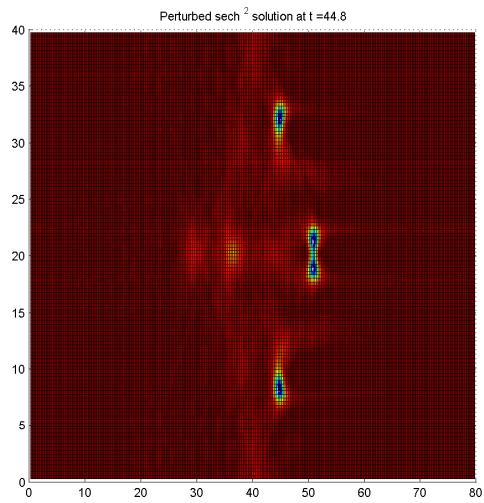


Fig. 5.17: Contour view, $t = 45$ with amplitude capping.

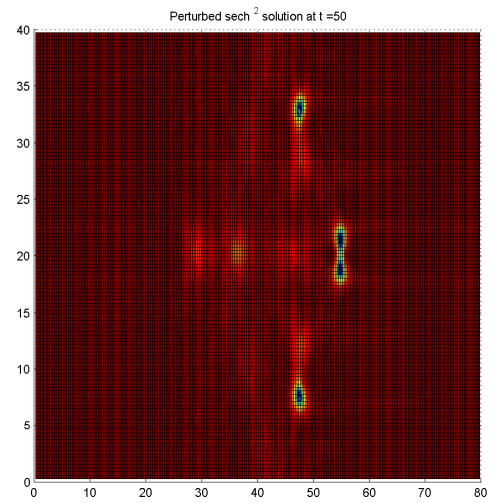


Fig. 5.18: Contour view, $t = 50$ with amplitude capping.

6. THE INVERSE SCATTERING METHOD FOR THE NV EQUATION

6.1 Numerical Verification of Recent Results Concerning the ISM for the NV Equation

Until very recently, the validity of the inverse scattering method for the NV equation had not been proven rigorously. A small presentation of previous results regarding the ISM for the NV equation is necessary to understand the usefulness of the numerical tests presented in this chapter.

Much of the material presented in section 6.1 has been taken from [42, 43, 44] unless otherwise cited. In order to stay consistent with the notation in the literature, we now use q to denote solutions to the NV equation instead of u . We begin with an important definition:

Definition 6.1.1. A compactly supported potential $q \in C_0^\infty(\mathbb{R}^2)$ is *of conductivity type* if $q = \gamma^{-1/2} \Delta \gamma^{1/2}$ for some real-valued $\gamma \in C^2(\mathbb{R}^2)$ satisfying $\gamma(x) \geq c > 0$ for all $x \in \Omega$ and $\gamma(x) \equiv 1$ for all $x \in \mathbb{R}^2 \setminus \Omega$.

Recall the D-bar formulation of the NV equation, now stated with the function q instead of u ,

$$q_t = \partial^3 q + \bar{\partial}^3 q + 3\partial(q\nu) + 3\bar{\partial}(q\bar{\nu}), \quad (6.1.1)$$

$$\bar{\partial}\nu = \partial q, \quad (6.1.2)$$

The study of equations (6.1.1) and (6.1.2) in the non-periodic setting via the inverse scattering method was initiated by Novikov and Veselov in [12] and continued by Tsai

[64, 65, 66]. They presented the following formal inverse scattering scheme for solving the Cauchy problem for (6.1.1) and (6.1.2):

$$\begin{array}{ccc}
 \mathbf{t}_0(k) & \xrightarrow{m_\tau := \exp(i\tau(k^3 + \bar{k}^3))} & \mathbf{t}_\tau(k) \\
 \uparrow \mathcal{T} & & \uparrow \mathcal{T} \\
 & \mathcal{Q} & \\
 & \downarrow & \\
 & & q_\tau^{\text{IS}}(z) \\
 q_0(z) & \xrightarrow{\text{nonlinear evolution (6.1.1)–(6.1.2)}} & q_\tau^{\text{NV}}(z),
 \end{array} \tag{6.1.3}$$

where \mathcal{T} and \mathcal{Q} stand for the direct and inverse nonlinear Fourier transform, respectively. Until a very recent result by Perry [56] it was not clear that one could use diagram (6.1.3) to solve the Novikov-Veselov equation using the linear evolution of the scattering data \mathbf{t}_τ . It was not clear if the following was true:

$$q_\tau^{\text{NV}} \stackrel{?}{=} q_\tau^{\text{IS}} := \mathcal{Q}(m_\tau \mathcal{T}(q_0)). \tag{6.1.4}$$

There was a question mark in formula (6.1.4) because of possible singularities in the scattering data. (It is not known how to define the operator \mathcal{Q} for singular argument functions.) Perry proved that equation (6.1.4) is true for a broad class of initial data q_0 that includes initial data of conductivity type.

First, we define the scattering transform and the operators \mathcal{T} and \mathcal{Q} in the context of the inverse conductivity problem. For this we must begin with the existence of exponentially growing solutions to the Schrödinger equation.

Let $q \in L^p(\mathbb{R}^2)$ for some $1 < p < 2$ and consider the Schrödinger equation

$$(-\Delta + q)\psi(\cdot, k) = 0 \tag{6.1.5}$$

where $k \in \mathbb{C} \setminus 0$ is a parameter. The existence of exponentially growing solutions of (6.1.5)

with asymptotic behavior $\psi(x, k) \sim e^{ikx}$ in the sense that

$$e^{-ikx}\psi(x, k) - 1 \in L^{\tilde{p}} \cap L^\infty(\mathbb{R}^2) \quad \text{for fixed } k \in \mathbb{C} \setminus 0, \quad \text{where } 1/\tilde{p} = 1/p - 1/2 \quad (6.1.6)$$

was established by Faddeev [21] and Nachman [52]. Points $x = (x_1, x_2)$ in the plane will be identified with $x = x_1 + ix_2 \in \mathbb{C}$. So $\exp(ikx) = \exp(i(k_1 + ik_2)(x_1 + ix_2))$ with $k \in \mathbb{C}$ and $x \in \mathbb{R}^2$. Defining $\mu(x, k) = e^{-ikx}\psi(x, k)$, μ satisfies the Lippmann-Schwinger equation

$$\mu = 1 - g_k * (q\mu) \quad (6.1.7)$$

where g_k is the Faddeev Green's function satisfying

$$g_k(x) := \frac{1}{(2\pi)^2} \int_{\mathbb{R}^2} \frac{e^{ix \cdot \xi}}{\xi(\bar{\xi} + 2k)} d\xi, \quad (-\Delta - 4ik\bar{\partial})g_k = \delta. \quad (6.1.8)$$

Exponentially growing solutions do not necessarily exist for all $k \in \mathbb{C}$. A point k is called a *non-exceptional point* of q if there is a unique solution of (6.1.5) satisfying (6.1.6). Otherwise k is called an *exceptional point* of q . If a potential q does not have exceptional points, one can define the scattering map $\mathcal{T} : q \mapsto \mathbf{t}$, taking the potential q to its *scattering transform* $\mathbf{t} : \mathbb{C} \rightarrow \mathbb{C}$ defined by

$$\mathbf{t}(k) = \int_{\mathbb{R}^2} e^{i\bar{k}\bar{x}} q(x) \psi(x, k) dx. \quad (6.1.9)$$

Under suitable assumptions the potential q can be recovered from its scattering transform \mathbf{t} via the inverse scattering map $\mathcal{Q} : \mathbf{t} \mapsto q$ defined by

$$(\mathcal{Q}\mathbf{t})(x) := \frac{i}{\pi^2} \bar{\partial}_x \int_{\mathbb{C}} \frac{\mathbf{t}(k)}{k} e_{-k}(x) \overline{\mu(x, k)} dk, \quad (6.1.10)$$

where $x \in \mathbb{R}^2$, dk denotes Lebesgue measure, and $e_{-k}(x) = e^{-i(kx + \bar{k}\bar{x})}$. The functions

$\mu(x, k)$ in (6.1.10) are determined by solving the $\bar{\partial}$ equation

$$\bar{\partial}_k \mu(x, k) = \frac{\mathbf{t}(k)}{4\pi k} e_{-k}(x) \overline{\mu(x, k)} \quad (6.1.11)$$

with fixed $x \in \mathbb{R}^2$ and assuming large $|k|$ asymptotics $\mu(x, \cdot) - 1 \in L^\infty \cap L^r(\mathbb{C})$ for some $2 < r < \infty$. The maps \mathcal{T} and \mathcal{Q} are often called the direct and inverse *nonlinear Fourier transforms*. Note also that a formula equivalent to (6.1.10) is given by Tsai in [66, formula (2.4)].

Now consider a time variable $\tau \geq 0$, and the diagram (6.1.3). Nachman shows in [52] that $\mathcal{T}q$ is well-defined for potentials of a conductivity type. In [42] the following extension of Nachmans work is proven:

Theorem 6.1.1. *Let $q \in C_0^\infty(\mathbb{R}^2)$ be of conductivity type. Then $q = \mathcal{Q}\mathcal{T}q$.*

New properties of the inverse scattering map \mathcal{Q} are also established in [42] through the following theorem.

Theorem 6.1.2. *Let $\mathbf{t} : \mathbb{C} \rightarrow \mathbb{C}$ satisfy $\mathbf{t}(k)/\bar{k} \in \mathcal{S}(\mathbb{C})$ and $\mathbf{t}(k)/k \in \mathcal{S}(\mathbb{C})$. Then the function $\mathcal{Q}\mathbf{t} : \mathbb{R}^2 \rightarrow \mathbb{C}$ given by (6.1.10) is well-defined and continuous. Furthermore,*

$$|(\mathcal{Q}\mathbf{t})(x)| \leq C\langle x \rangle^{-2}. \quad (6.1.12)$$

The smoothness results for $k^{-1}(\mathcal{T}q)(k)$ and $\bar{k}^{-1}(\mathcal{T}q)(k)$ and Theorem 6.1.2 can be used to show that the inverse scattering scheme (6.1.3) is well-defined for conductivity type initial potentials:

Corollary. *Let $q \in C_0^\infty(\mathbb{R}^2)$ be of conductivity type. Fix a positive odd integer n , let $\tau \geq 0$ and define $q_\tau : \mathbb{R}^2 \rightarrow \mathbb{C}$ by*

$$q_\tau := \mathcal{Q}(\mathbf{m}_\tau^{(n)}\mathcal{T}q).$$

Then $q_\tau(x)$ is continuous in x and belongs to $L^p(\mathbb{R}^2)$ for any $1 < p < 2$.

Note that there is no smallness assumption for the initial data in the Corollary.

The programs are already in place for computing solutions of the evolution equation by the inverse scattering method. The algorithm is as follows.

1. Define an initial potential q_0 of conductivity type and choose a sequence of evaluation times $\tau_0 = 0, \tau_1, \dots, \tau_N = T$.
2. Compute the bounded function $\mu_0(x, k)$ from the Lippmann-Schwinger equation (6.1.7).
3. Compute the scattering transform $\mathbf{t}_0(k)$ from (6.1.9), by numerical quadrature.

For $j = 1, \dots, N$

4. Set $t_{\tau_j}(k) = \exp(i\tau_j(k^3 + \bar{k}^3))\mathbf{t}_0$ on a finite grid in the complex k -plane.
5. Solve the integral form of the D-bar equation (6.1.11) for $\mu_{\tau_j}(x, k)$ by the solver developed in [35] where

$$\mu_{\tau_j}(x, k) = 1 + \frac{1}{(2\pi)^2} \int_{\mathbb{R}^2} \frac{\mathbf{t}_{\tau_j}(k')}{(k - k')\bar{k}'} e_{-x}(k') \overline{\mu_{\tau_j}(x, k')} dk'_1 dk'_2 \quad (6.1.13)$$

6. Solve for $q_{\tau_j}(x)$ from (6.1.10).

end

Recently, Perry [56] has proved that a solution to the modified Novikov–Veselov equation (mNV) with initial data of *conductivity-type* is a solution for the NV equation through a Muira-type map originally defined by Bogdonov [10]. The mNV is in the Davey-Stewartson hierarchy (DS II) and so it is shown that solutions to the DS II equation are solutions to the NV equation, greatly broadening the class of initial data and classical solutions to the NV equation.

The mNV and NV equations are related via the Muira map

$$\mathcal{M}(v) = 2\partial v + |v|^2 \quad (6.1.14)$$

where the domain of \mathcal{M} is the set $M = \{v \in \mathbf{S}(\mathbb{R}^2) | \partial v = \overline{\partial v}, \int v(z) dz = 0\}$. If $u(t)$ is a solution to the MNV equation and $u \in M$ then $\mathcal{M}(u(t))$ solves the Cauchy problem for NV with Cauchy data $2\partial u_0 + |u_0|^2$.

6.1.1 Comparing Two Types of Numerical Evolutions of Solutions to the NV Equation

Three examples are given in [44] that test the ISM for the NV equation against the FD difference method presented therein. Here, we choose to consider the second example, a high contrast example with an initial condition with high amplitude. This example will cause the nonlinear contribution to be strong in the evolution and therefore is a good test to see how the numerical method handles the nonlinearity. The initial data is constructed as follows.

Choose $0 < \rho < 1$ and let $F_\rho \in C_0^\infty(\mathbb{R})$ for $-\rho \leq x \leq \rho$ be given by

$$F_\rho(x) := e^{-\frac{2(\rho^2+x^2)}{(\rho+x)^2(\rho-x)^2}}, \quad (6.1.15)$$

and $F_\rho(x) = 0$ for $|x| > \rho$. We define γ by

$$\gamma(z) := (\alpha F_\rho(|z|) + 1)^2, \quad (6.1.16)$$

with $\rho = 0.95$, which gives a support of $[-\rho, \rho]$ for γ and q_0 . The Schrödinger potential q_0 outside the origin is given by

$$q_0(z) := \frac{\Delta \sqrt{\gamma(z)}}{\sqrt{\gamma(z)}} = \frac{\Delta F_\rho(|z|)}{F_\rho(|z|) + 1/\alpha}. \quad (6.1.17)$$

Note that $\gamma \equiv 1$ and $q \equiv 0$ for $|z| \geq \rho$. In the paper [44] example 1 is when $\alpha = 25$, and

example 2 is for $\alpha = 59$. Figure (6.1) shows the function defined by equation (6.1.17) from two points of view. We will compare the ISM evolution and the spectral evolution using these two points of view. Figures (6.2) – (6.4) compare the evolution at ten time steps, $t = 0.0001, 0.0002, \dots, 0.001$, at angle slightly above the xy -plane. Figures (6.5) – (6.9) compare the evolution at the same time steps for the contour plots and zoomed in for better detail.

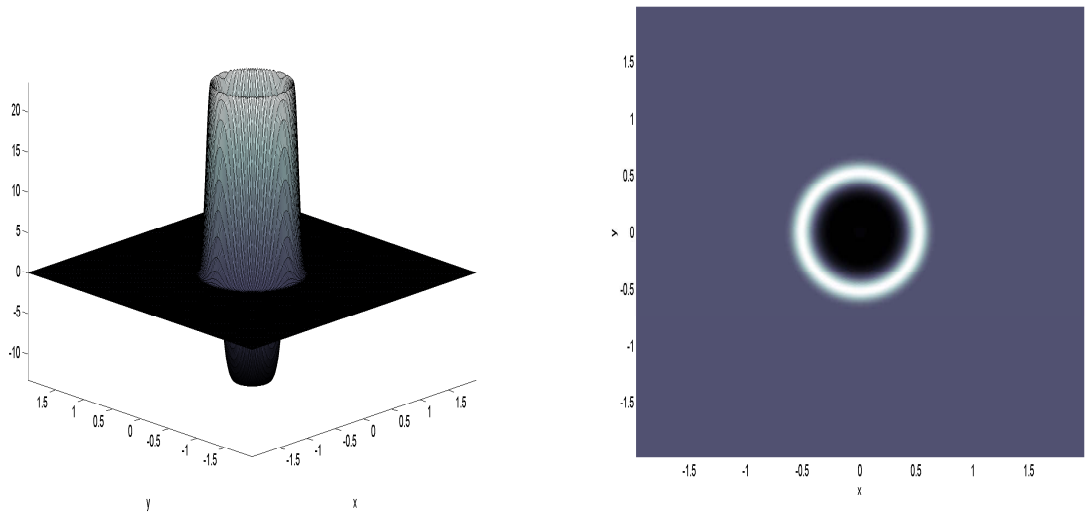


Fig. 6.1: The initial condition of conductivity type, equation (6.1.17)

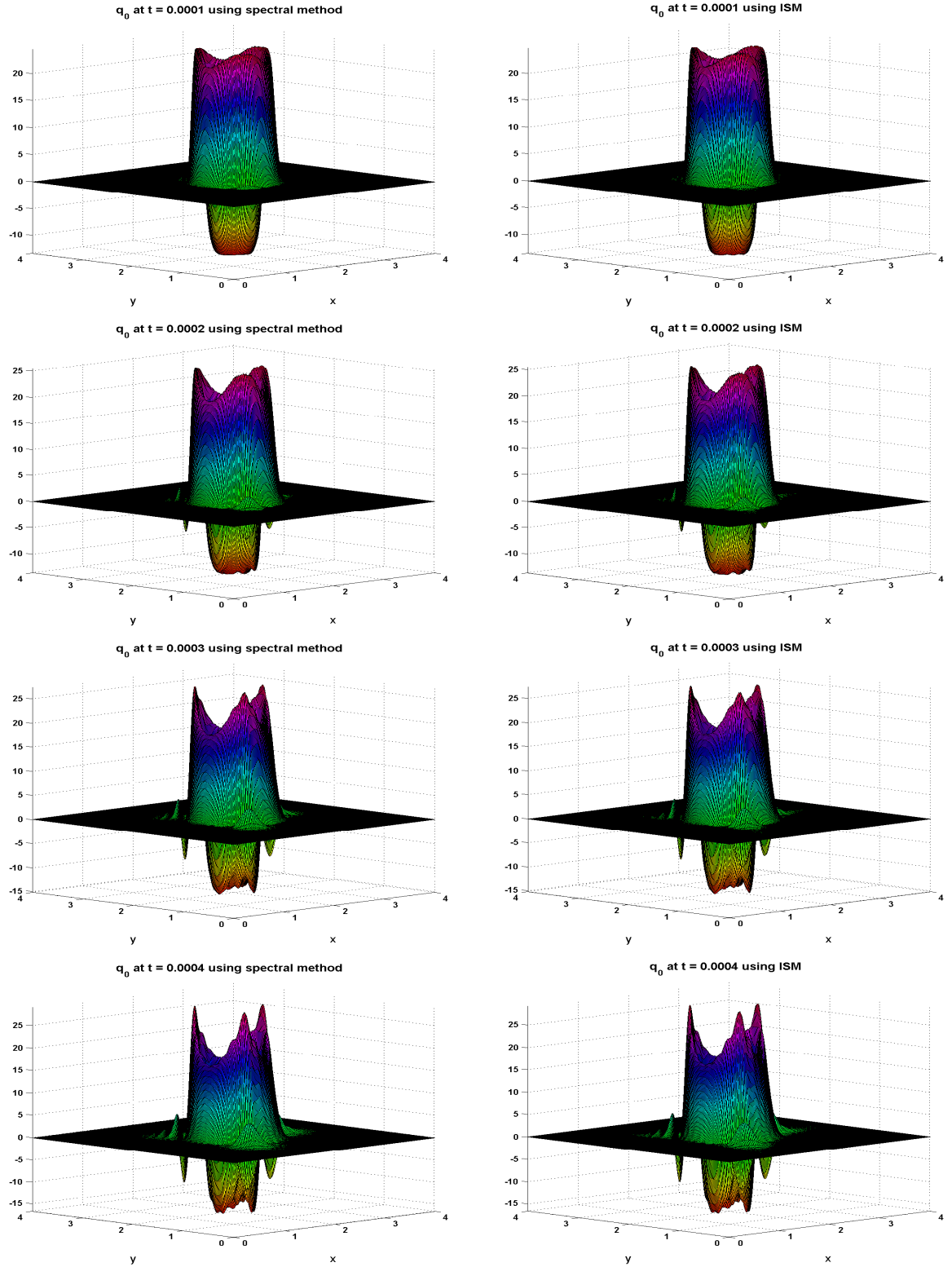


Fig. 6.2: Comparison of the Spectral Method with the ISM for times $\tau = 0.0001, 0.0002, 0.0003, 0.0004$. Left: Spectral Method, Right: ISM

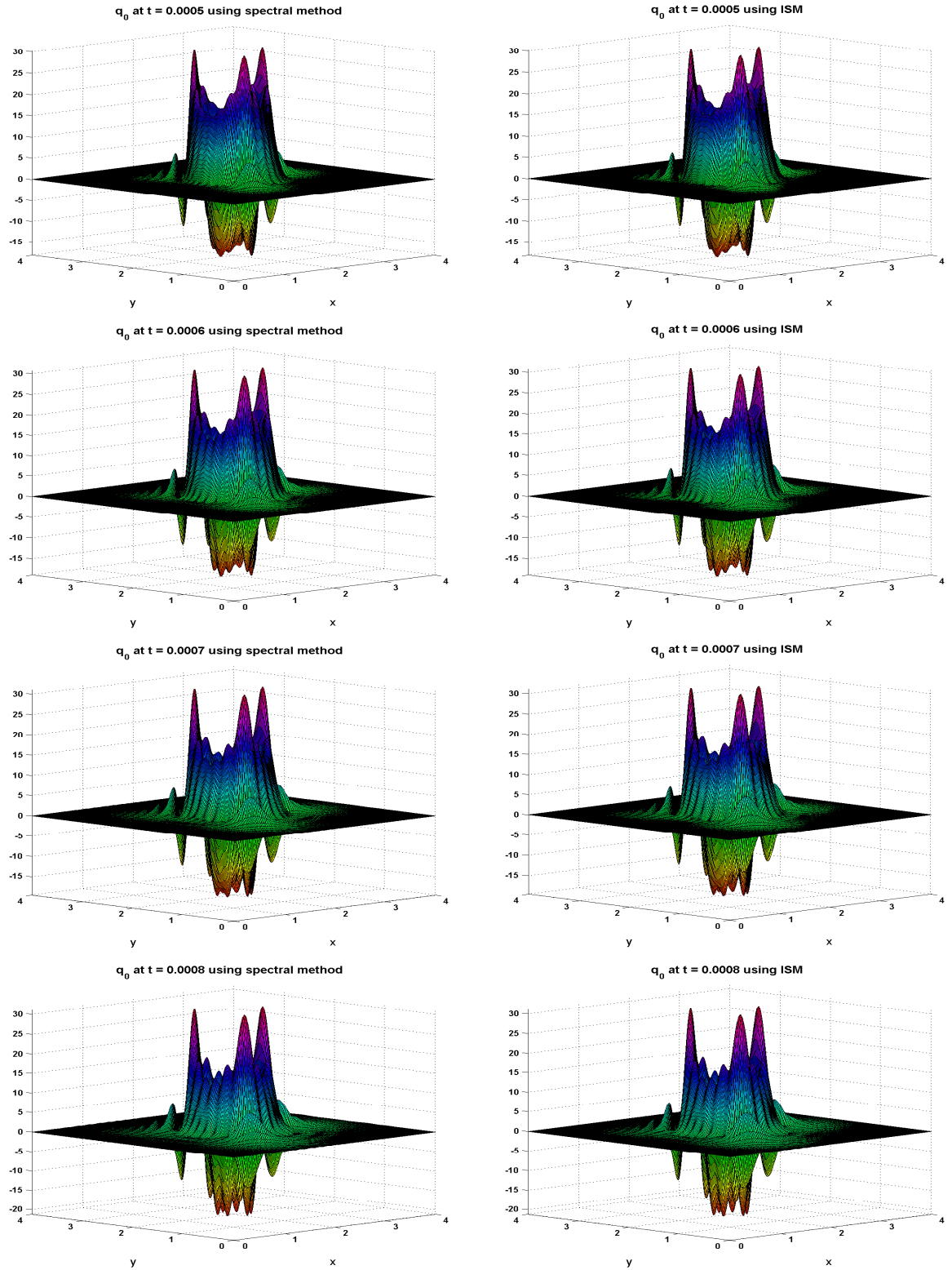


Fig. 6.3: Comparison of the Spectral Method with the ISM for times $\tau = 0.0005, 0.0006, 0.0007, 0.0008$. Left: Spectral Method, Right: ISM

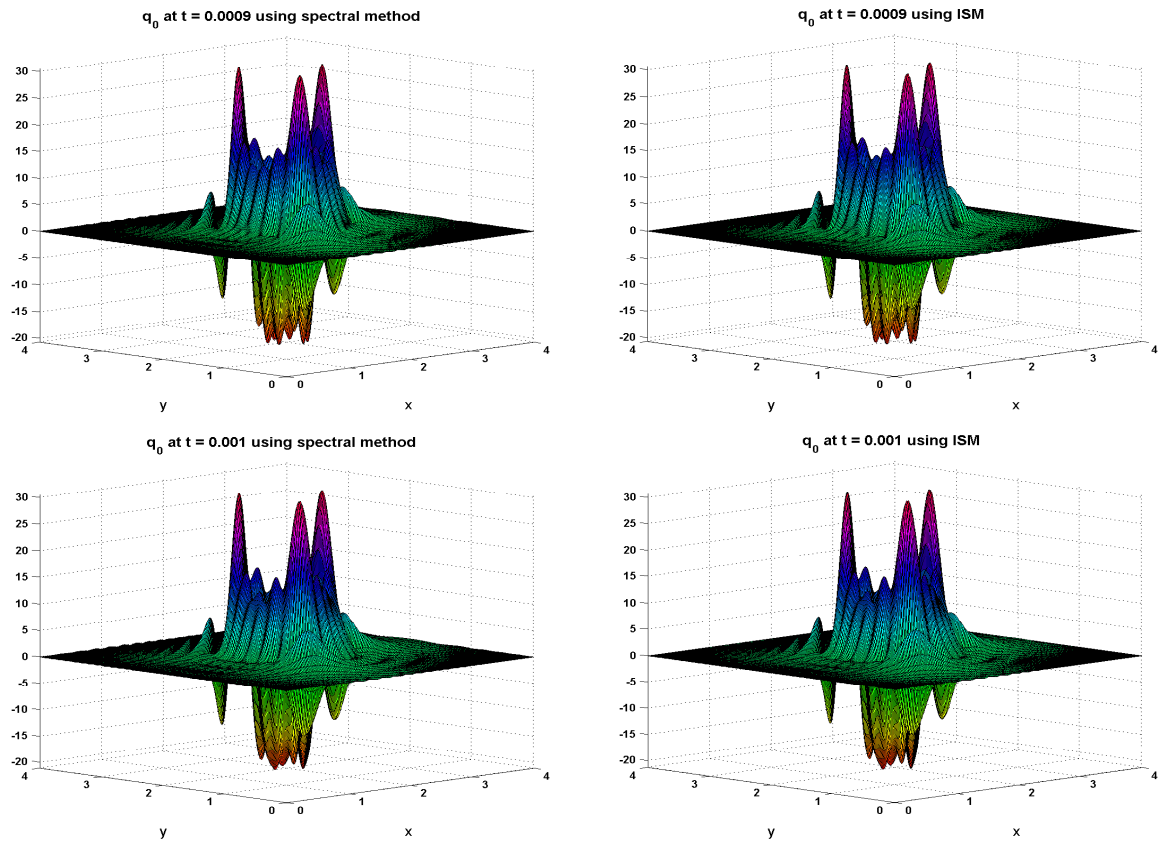


Fig. 6.4: Comparison of the Spectral Method with the ISM for times $\tau = 0.0009, 0.001$. Left: Spectral Method, Right: ISM

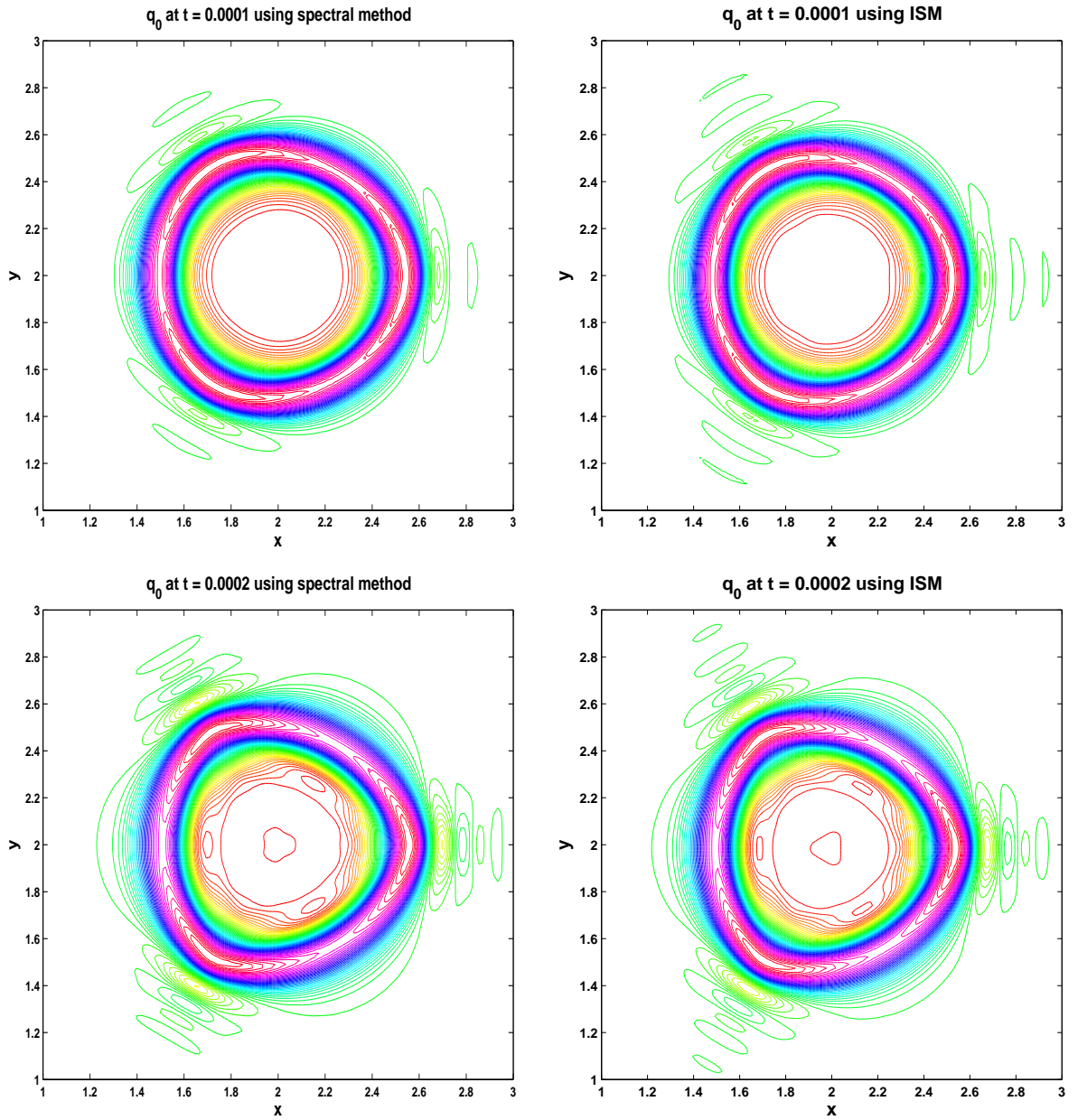


Fig. 6.5: Comparison of the Spectral Method with the ISM for times $\tau = 0.0001, 0.0002$, using contour plots

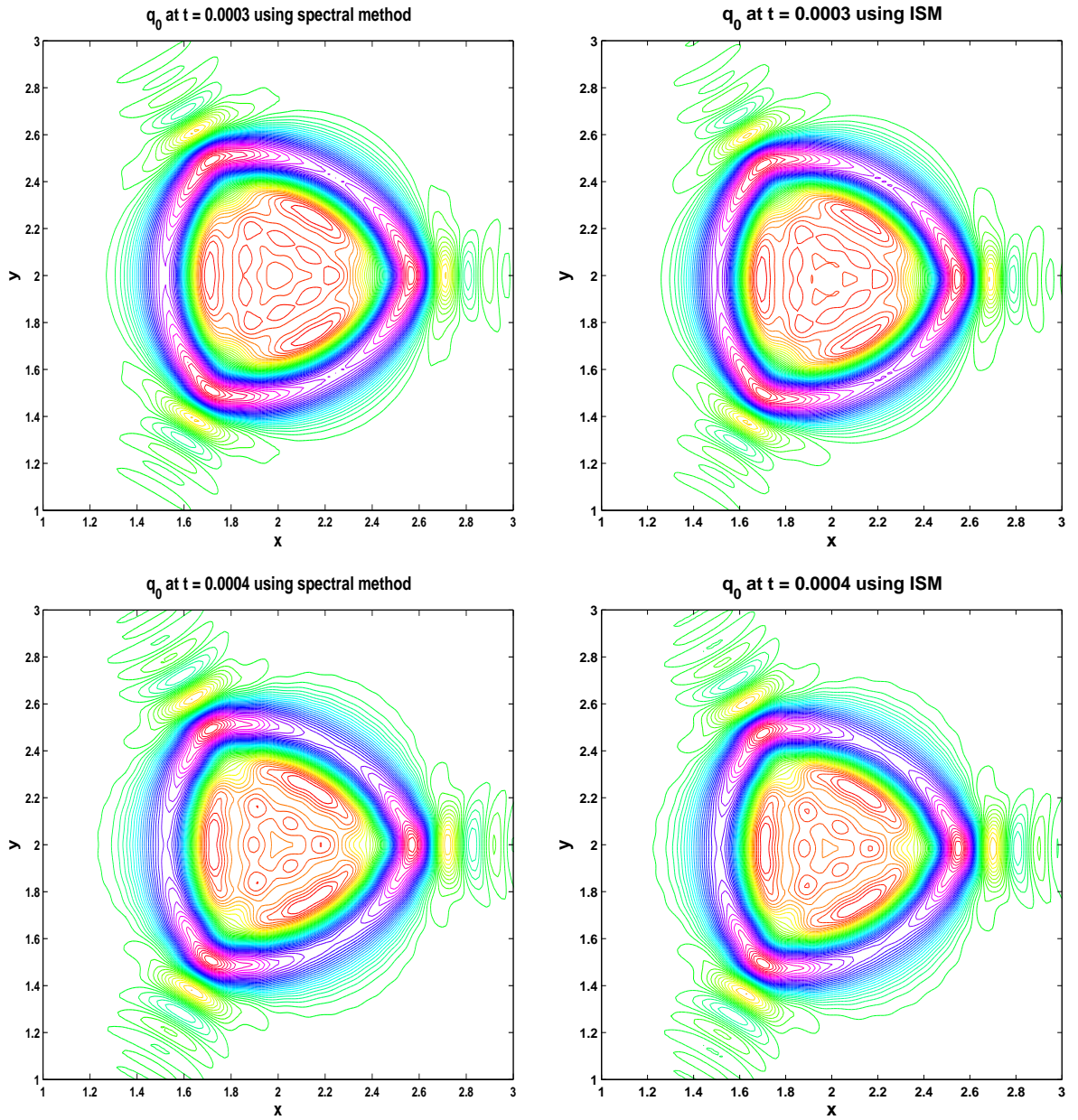


Fig. 6.6: Comparison of the Spectral Method with the ISM for times $\tau = 0.0003, 0.0004$ using contour plots

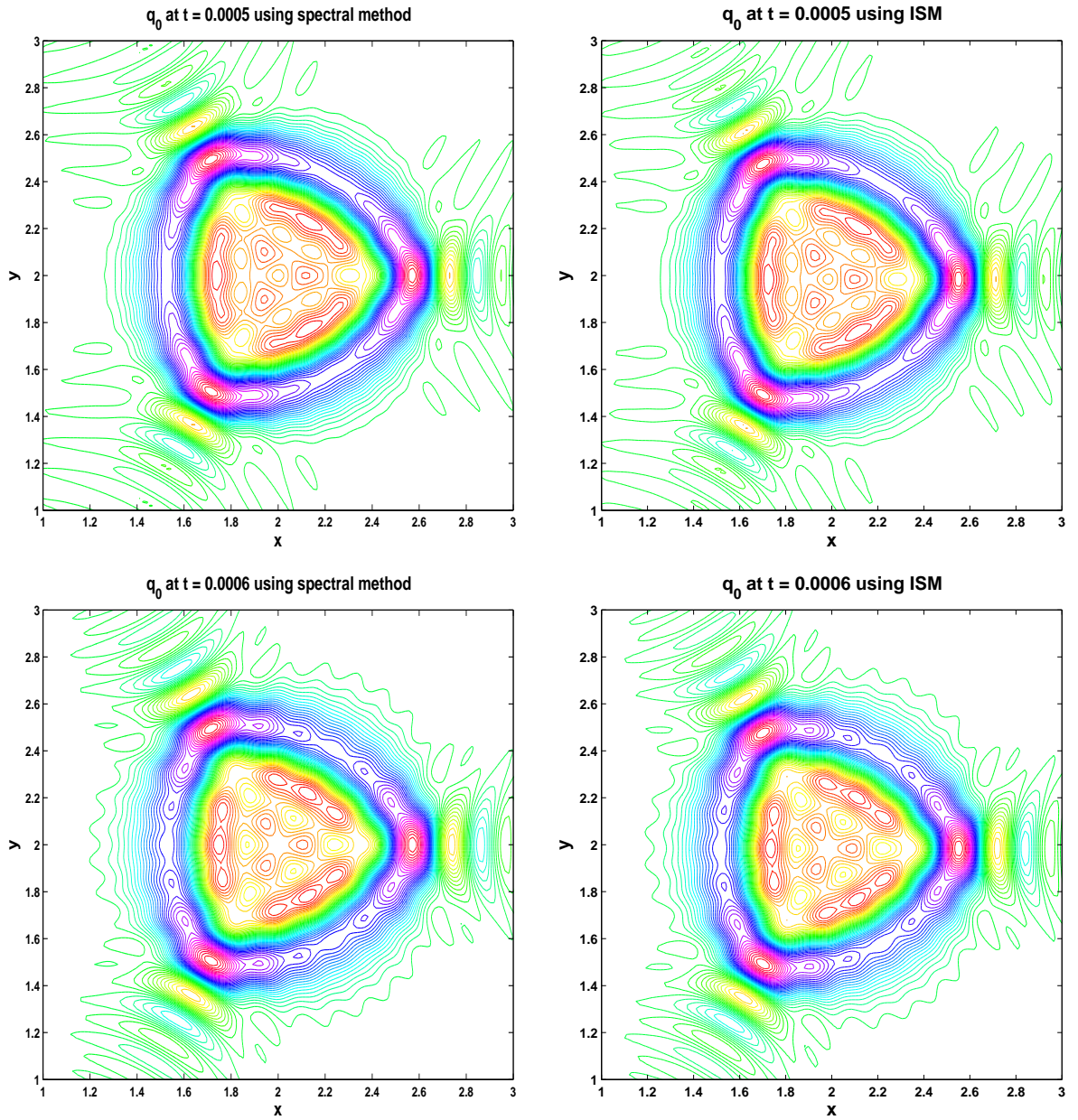


Fig. 6.7: Comparison of the Spectral Method with the ISM for times $\tau = 0.0005, 0.0006$, using contour plots

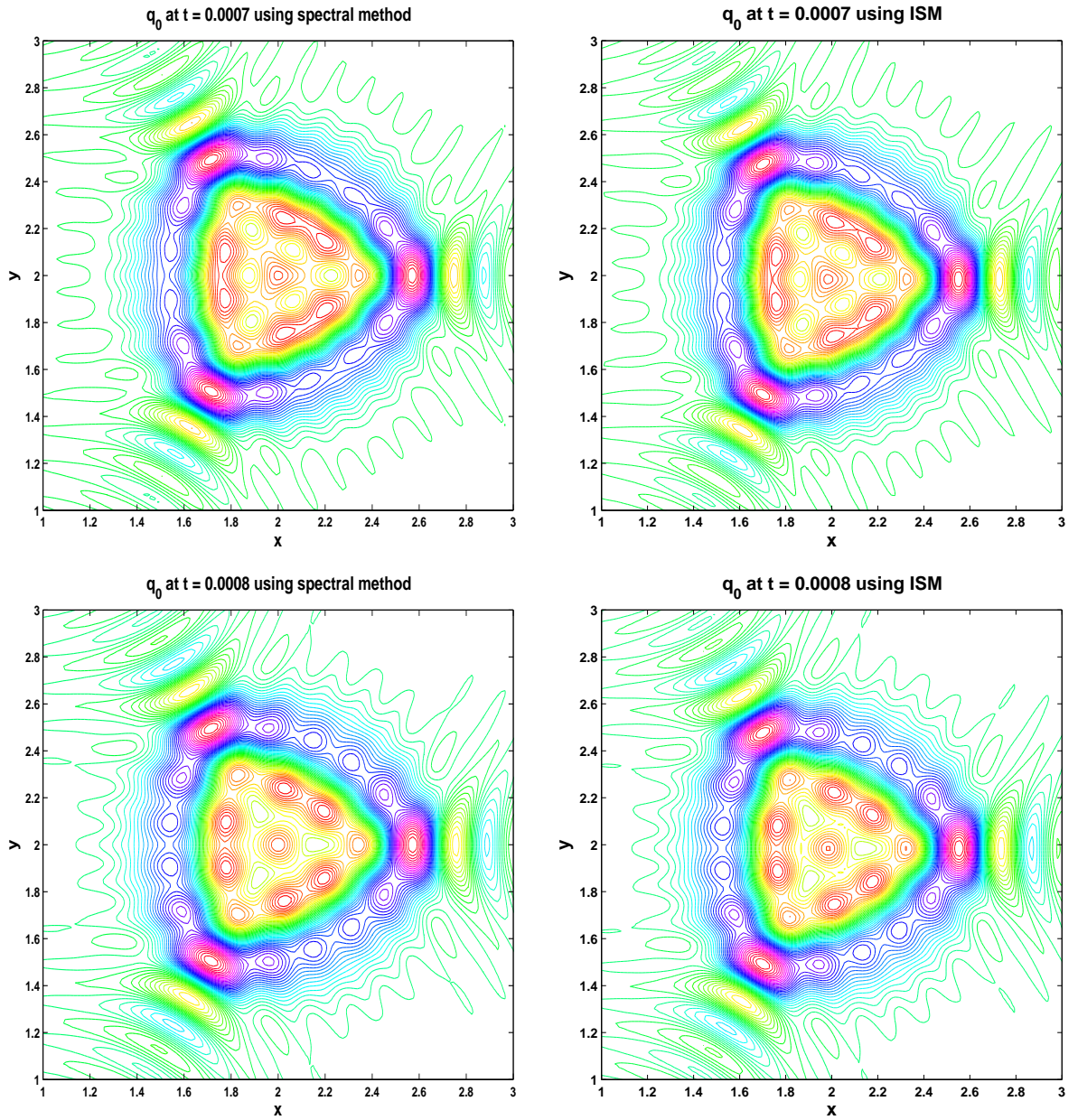


Fig. 6.8: Comparison of the Spectral Method with the ISM for times $\tau = 0.0007, 0.0008$ using contour plots

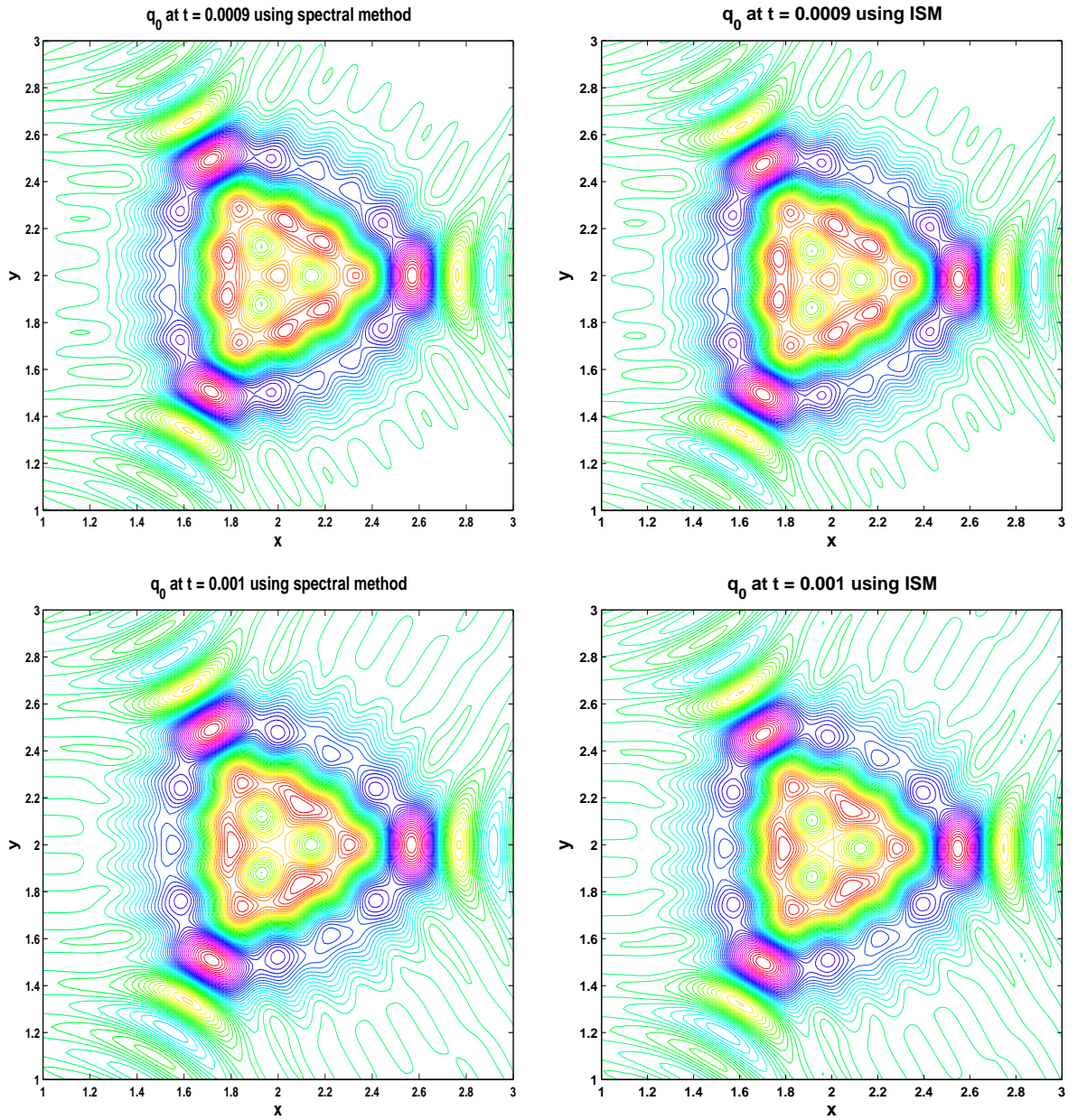


Fig. 6.9: Comparison of the Spectral Method with the ISM for times $\tau = 0.0009, 0.001$ using contour plots

6.2 Numerical Experiments Regarding the Soliton Conjecture of the IST for the NV Equation

The second set of computations presented in this chapter are experiments designed to investigate an important conjecture about soliton solutions to the NV equation.

It was shown in [52] that if q_0 is of conductivity-type, then there are no exceptional points in the scattering data:

Theorem 6.2.1. *Let q be a real-valued function in $L^p_\rho(\mathbb{R}^2)$, $1 < p < 2$, $\rho > 1$. The following are equivalent:*

- (a) $q = (\Delta\psi_0)/\psi_0$ for some $\psi_0 \in L^\infty(\mathbb{R}^2)$ with $\psi_0 \geq c_0 > 0$ a.e.
- (b) There are no exceptional points $\xi \in \mathbb{C}^2$ with $\xi^2 = 0$ and the scattering transform satisfies

$$|\mathfrak{t}(-2\xi_R, \xi)| \leq c|\xi|^\epsilon$$

for some $\epsilon > 0$ and all sufficiently small $\xi = \xi_R + \xi_I$ in Υ .

Note that condition (a) is simply that q is of conductivity-type. This result was extended later in [43] where it was shown that an evolved potential q_τ will have no exceptional points corresponding to it for radially symmetric initial conditions or initial conditions that correspond to an evolved radially symmetric initial condition. The conjecture is that this is true in general, that is, *initial conditions that evolve under the NV equation that did not begin with exceptional points will not have exceptional points at a later time.*

Theorem (6.2.1) leaves open the possibility that the scattering transform $\mathfrak{t}(k)$ could violate the decay condition (b) and that there could be other non-conductivity type potentials with no exceptional points. This is true and was recently proven in [56] where it is shown that there is a wider class of initial potentials that will not develop exceptional points. In other words, Perry showed that the ISM holds for initial conditions including, but not restricted to, conductivity-type.

Now, for initial conditions q_0 such that the ISM holds, the solution has a decay property that $q_\tau \rightarrow 0$ as $\tau \rightarrow \infty$. This, of course, will exclude soliton solutions. *Therefore, soliton solutions correspond to initial conditions where the ISM does not hold.* Thus, we have the following conjecture: Soliton solutions to the NV equation must correspond to initial data q_0 that has exceptional points.

As was proven in [43], the scattering transform is not well defined in this case, and so the ISM cannot be used to help investigate this conjecture. Therefore, the spectral method developed here can be used to test this conjecture. Indeed, using the spectral method, we have an initial condition that is not of conductivity-type that leads to soliton behavior. Let $\epsilon < 0$ and $\phi(z)$ be a compactly supported function of the Schwartz class.

In a personal communication it has come to our attention that the following has been proven. Potentials of the form

$$q_{NC} = q_{CT} + \epsilon\phi(z), \quad (6.2.1)$$

where $\epsilon < 0$ and ϕ is a test function, have exceptional points. The expectation is then that functions of the form (6.2.1) will produce solitonic behavior. We provide an example here.

Let $\epsilon = -5$. We construct a function that is 1 in most of the support of the function of conductivity type, and goes to 0 quickly near the unit disc. First, in order to build the test function we need to define a smoothing function. Let

$$s(t) = 1 - 10t^3 + 15t^4 - 6t^5. \quad (6.2.2)$$

The smoothing function $s(t)$ has the properties that $s(0) = 1$ and $s'(0) = s''(0) = s(1) = s'(1) = s''(1) = 0$. Now, we define a function $\sigma : \mathbb{C} \rightarrow \mathbb{C}$,

$$\sigma(z) = \begin{cases} 2 & 0 \leq |z| \leq 0.02, \\ 1 + s\left(\frac{|z|-0.02}{0.7}\right) & 0.02 \leq |z| \leq 0.072 \end{cases} \quad (6.2.3)$$

The argument for s in the definition of σ is chosen in such a way so that it is between 1 and 0. We define the test function, $T(t)$ as

$$T(z) = \begin{cases} 1 & 0 \leq t \leq 0.8, \\ s \left(\frac{|z|-0.8}{0.1} \right) & 0.8 \leq t \leq 0.9. \end{cases} \quad (6.2.4)$$

Our non-conductivity type potential is then

$$q_{NC}(z) = \sigma(z) + \epsilon T(z). \quad (6.2.5)$$

The initial condition described in equation (6.2.5) is seen in the top row of Figure (6.10).

As can be seen in the figures that follow, there are coherent structures that develop quite quickly. They are extremely stable and keep their amplitude and general form from $t = 0$ through $t = 0.5$. At $t \approx 5.5$ the evolution develops a singularity. It is believed this is numerical blow-up though this has not been proven.

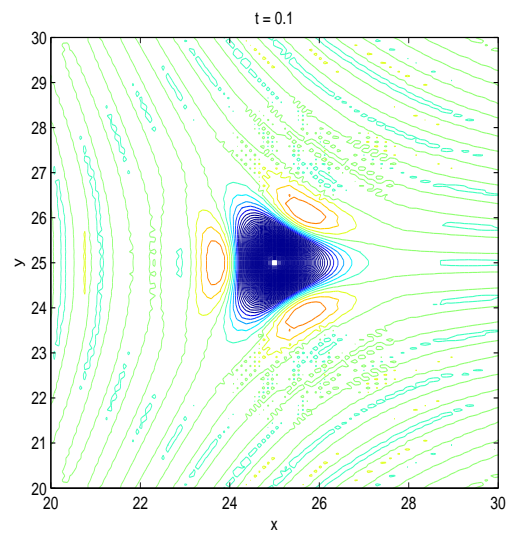
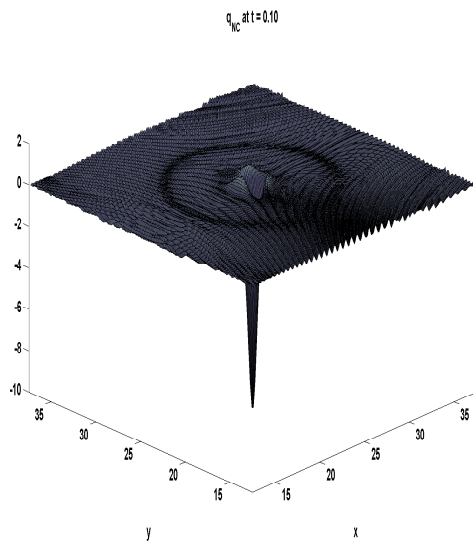
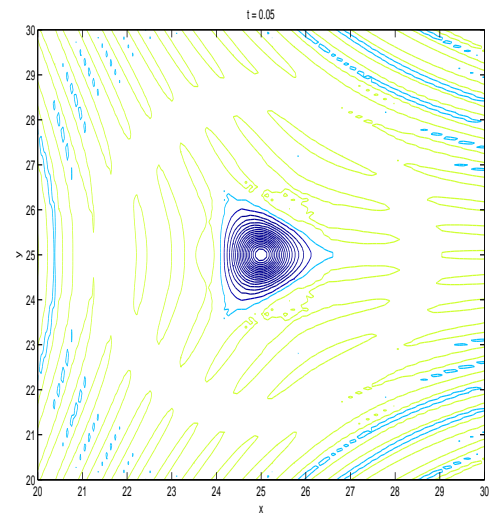
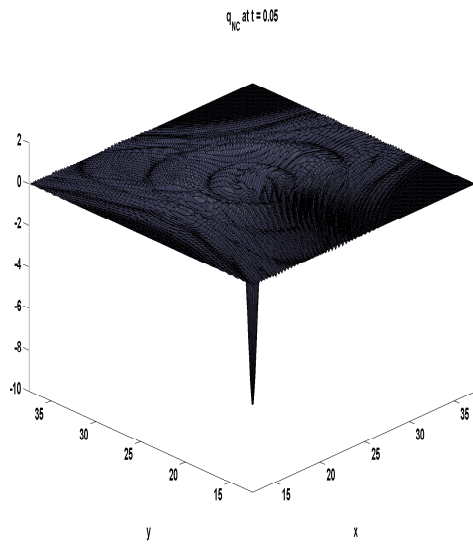
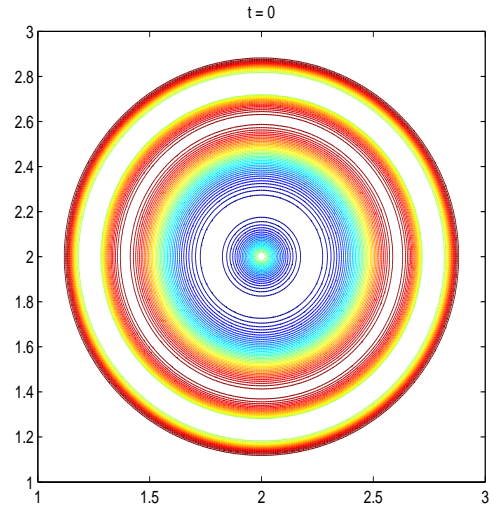
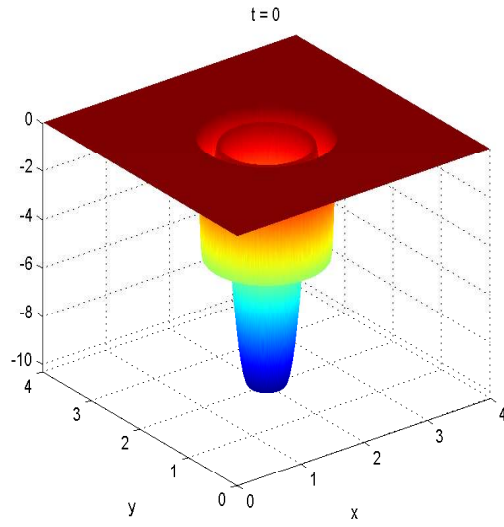


Fig. 6.10: Evolution of equation (6.2.5), q_{NC} , $t=0,0.05,0.1$

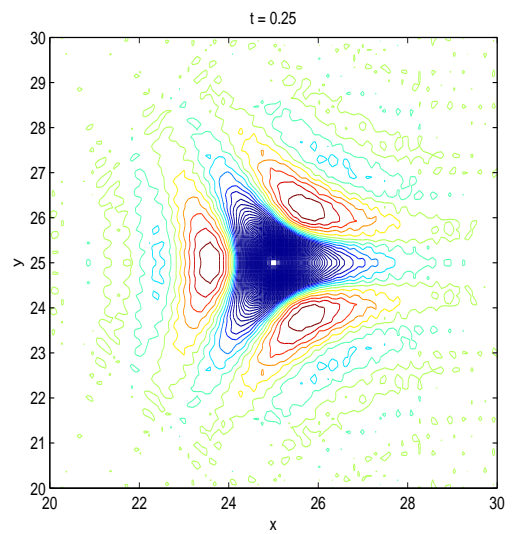
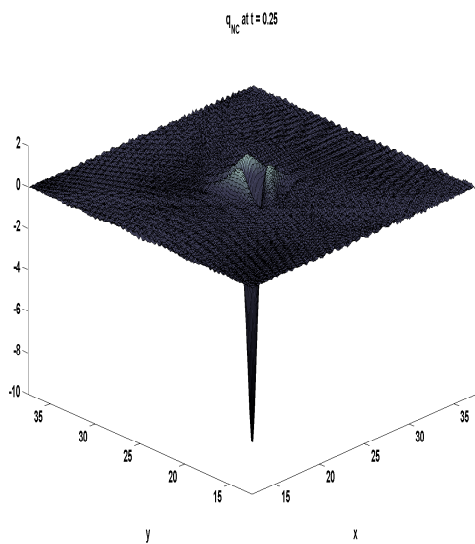
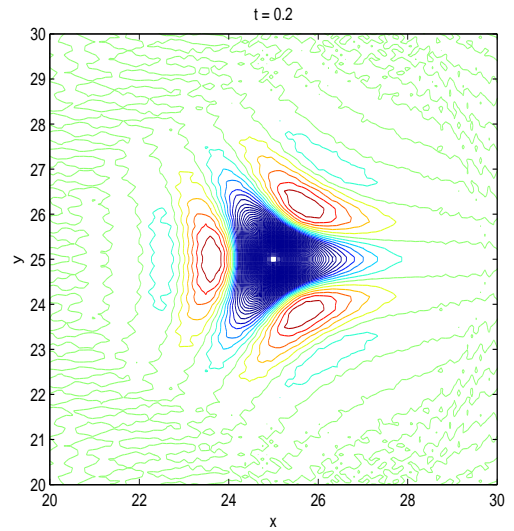
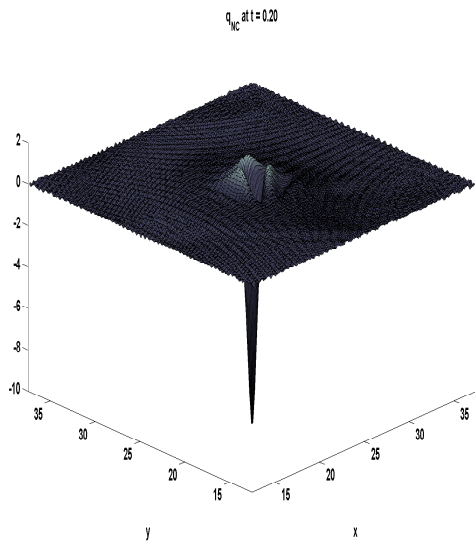
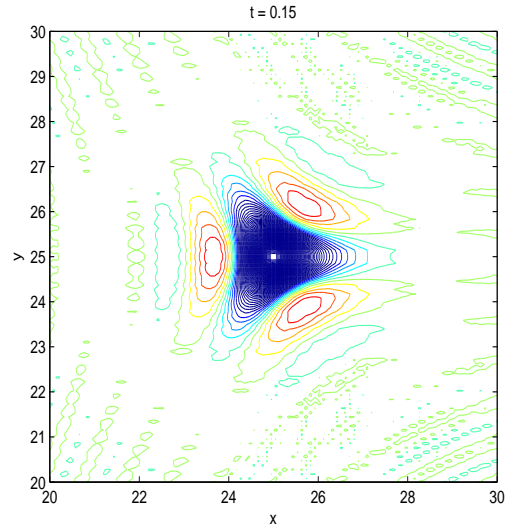
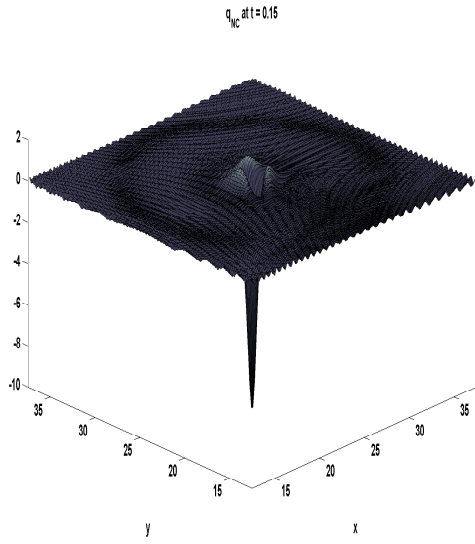


Fig. 6.11: Evolution of equation (6.2.5), q_{NC} , $t=0.15,0.2,0.25$

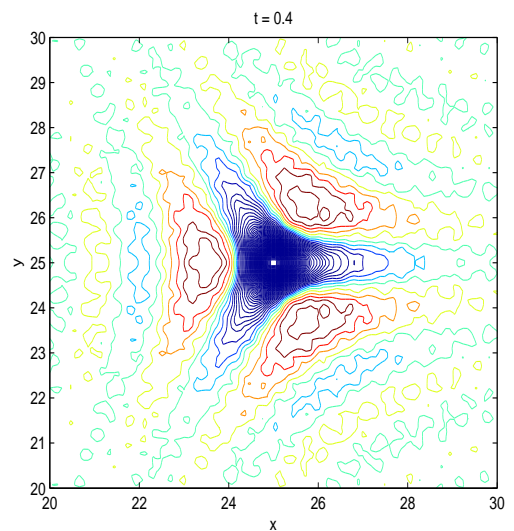
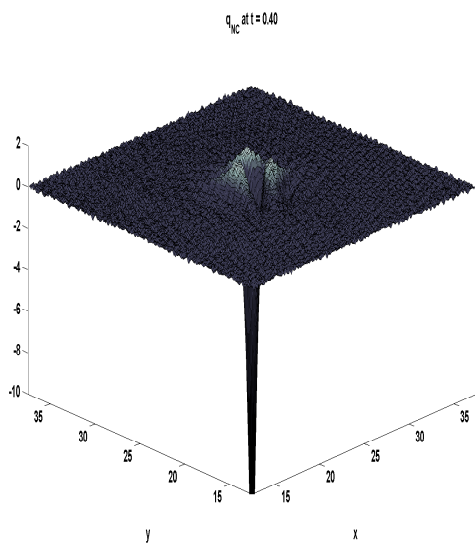
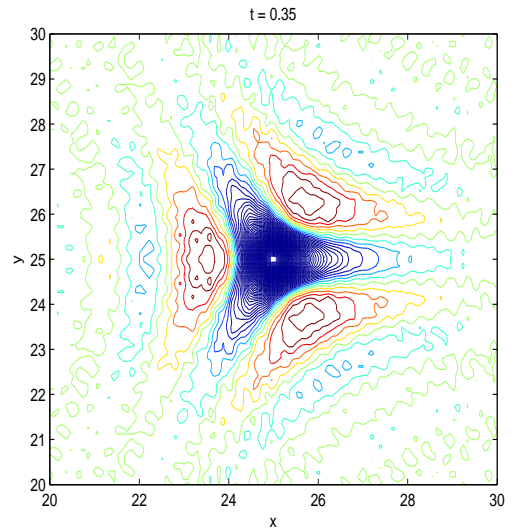
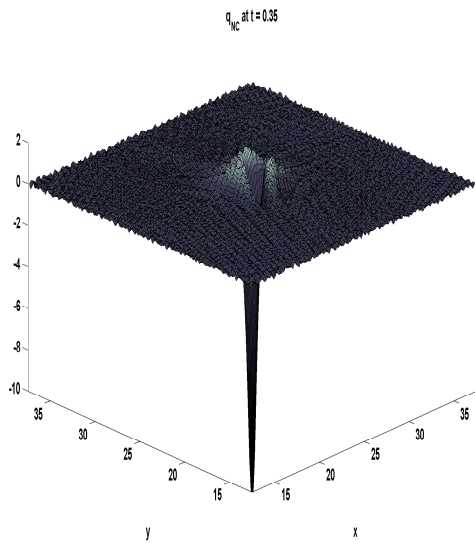
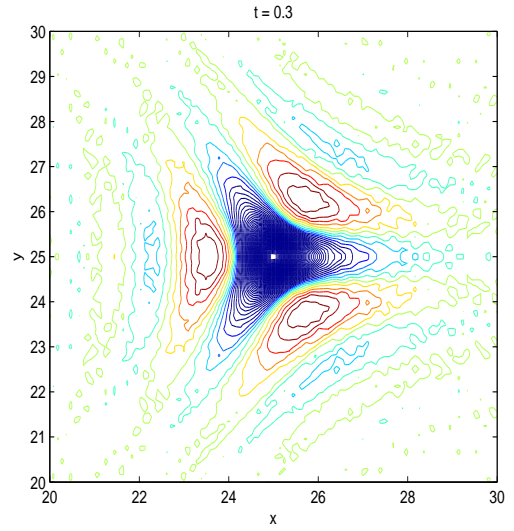
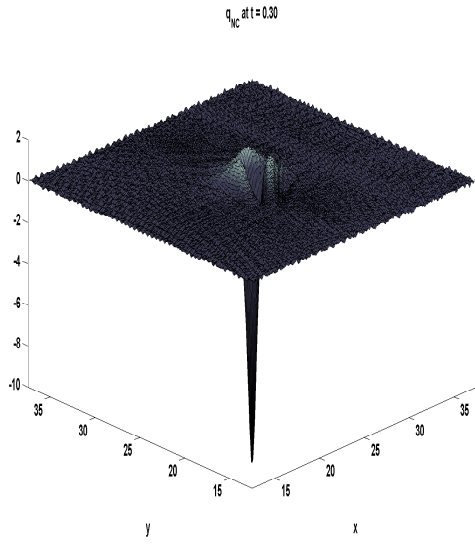


Fig. 6.12: Evolution of equation (6.2.5), q_{NC} , $t=0.3, 0.35, 0.4$

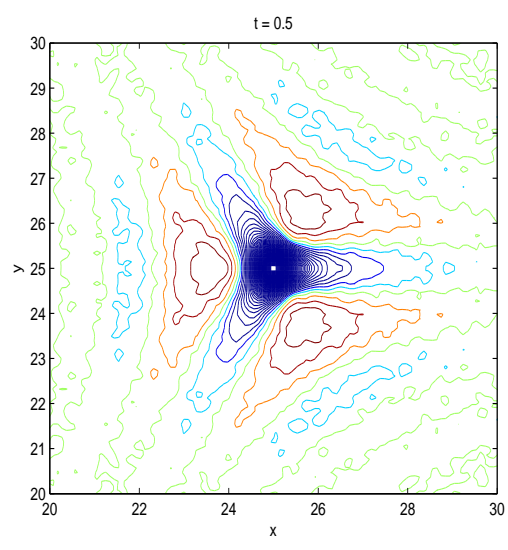
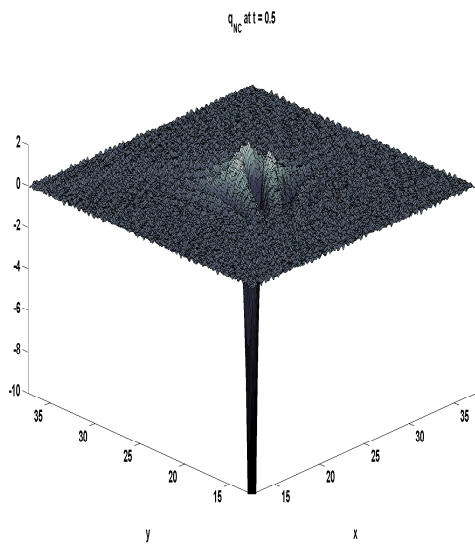
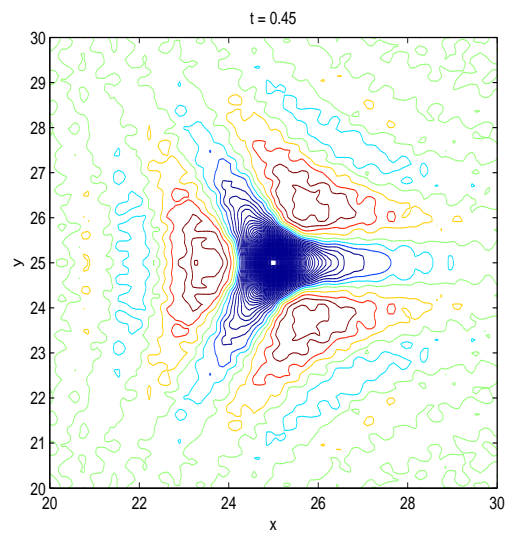
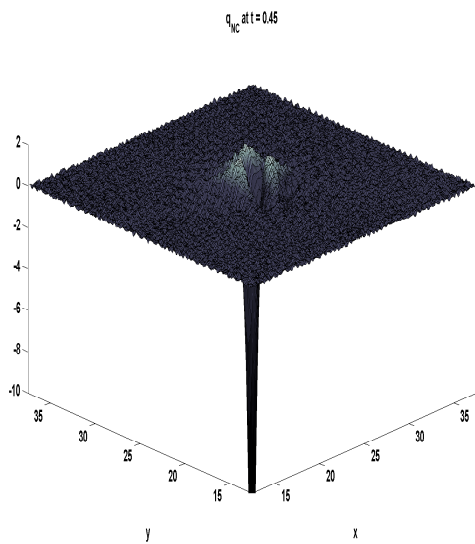


Fig. 6.13: Evolution of equation (6.2.5), q_{NC} , $t=0.45, 0.5$

7. CONCLUSIONS

The work presented here helps to give a fuller picture of the NV equation. The results are novel to the soliton community because there are few results that deal with soliton systems, or systems of NLPDE's that have soliton solutions.

In this thesis I have shown the existence of various types of soliton solutions to the NV equation, and developed methods to help find soliton solutions that are of use in the development of the ISM for the NV equation. I performed an analytical stability analysis for plane wave soliton solutions of KdV type of the NV equation.

To my knowledge **this is the first numerical implementation of a spectral method to a system of soliton NLPDE's**. Moving forward, there are a number of tasks that can be done to give a more complete picture of the NV equation including extending the stability results, applying the techniques here to more well known soliton equations, and investigating the long term behavior of the traveling wave solutions.

The stability analysis can be extended to perturbations at angles other than 90° and to multisoliton solutions. Here, only small k and $\theta = \frac{\pi}{2}$ were considered. Next, arbitrary k and arbitrary θ could be considered. An interesting question involving multisoliton solutions is what happens to perturbed solitons when they interact? It is possible that

$$\text{unstable soliton} + \text{stable soliton} = \text{unstable soliton} + \text{unstable soliton}$$

holds after interaction of the two solitons, a result observed for the ZK equation [31].

The numerical experiments have also lead to the observation that the solutions either blow up, or lead to other coherent structures. If the amplitudes are restricted it is seen that

coherent lump structures appear at long times. It has been observed that the ZK equation, under shorter wavelength perturbations, gives rise to cylindrical and spherical solitons [24, 25]. It would be interesting to see if the same phenomena occurs here.

The numerical code developed in this thesis was also used in conjunction with the pre-existing numerical implementation of the ISM to investigate the validity of more general sets of initial conditions than those introduced in [42] and [43]. In particular, I considered initial conditions of non conductivity-type that are rapidly decaying and computed their evolutions and have found strong numerical evidence of soliton solutions, supporting the conjecture of their existence, explained in Chapter 6.

The work in this dissertation is significant because it is the first thorough study of soliton solutions to the NV equation, an important equation because it is a soliton equation that is a system of PDE's and it is a generalization of KdV. There is no study of soliton stability for NV in the literature, and this work applies the direct K-method to a NLDPE system (NV). It has provided visual insight into the nature of solutions through numerical computations, and it provides a means to study conjectures about the integrability of NV and the ISM. I computed the evolution by the ISM and observed that it agrees to a high degree of accuracy with the results of the numerical code for the NV equation evolutions developed in this thesis.

BIBLIOGRAPHY

- [1] M. J. ABLOWITZ AND P. A. CLARKSON, Cambridge University Press, 1991.
- [2] M. J. ABLOWITZ, D. J. KAUP, A. C. NEWELL, AND H. SEGUR, *The inverse scattering transform-Fourier analysis for nonlinear problems*, Studies in Appl. Math., 53 (1974), pp. 249–315.
- [3] M. A. ALLEN AND PHIBANCHON, *Time evolution of perturbed solitons of modified Kadomtsev–Petviashvili equations*, Computational Science and its Applications, 2007. ICCSA 2007. International Conference on, (2007), pp. 20–23.
- [4] M. A. ALLEN AND G. ROWLANDS, *Determination of the growth rate for the linearized Zakharov-Kuznetsov equation*, Journal of Plasma Physics, 50 (1993), pp. 413–424.
- [5] ———, *On the transverse instabilities of solitary waves*, Physics Letters A, 235 (1997), pp. 145 – 146.
- [6] R. BEALS AND R. R. COIFMAN, *Multidimensional inverse scattering and nonlinear partial differential equations.*, AMS, 43 (1985), pp. 45–70.
- [7] T. B. BENJAMIN, *The stability of solitary waves*, Proceedings of the Royal Society of London. A. Mathematical and Physical Sciences, 328 (1972), pp. 153–183.
- [8] T. B. BENJAMIN AND J. E. FEIR, *The disintegration of wave trains on deep water part 1. theory*, Journal of Fluid Mechanics, 27 (1967), pp. 417–430.

- [9] X.-H. (BENN)WU AND J.-H. HE, *Exp-function method and its application to nonlinear equations*, Chaos, Solitons & Fractals, 38 (2008), pp. 903 – 910.
- [10] L. V. BOGDANOV, *The Veselov-Novikov equation as a natural generalization of the Korteweg-de Vries equation*, Teoret. Mat. Fiz., 70 (1987), pp. 309–314.
- [11] L. V. BOGDANOV, B. G. KONOPELCHENKO, AND A. MORO, *Symmetry constraints for real dispersionless Veselov–Novikov equation*, Preprint (arXiv:nlin.SI/0406023 v1 14 Jun 2004), (2004).
- [12] M. BOITI, J. P. LEON, M. MANNA, AND F. PEMPINELLI, *On the spectral transform of a Korteweg-deVries equation in two spatial dimensions*, Inverse Problems, 2 (1986), pp. 271–279.
- [13] R. M. BRADLEY, *Electromigration-induced soliton propagation on metal surfaces*, Phys. Rev. E, 60 (1999), pp. 3736–3740.
- [14] T. J. BRIDGES, *Transverse instability of solitary-wave states of the water-wave problem*, Journal of Fluid Mechanics, 439 (2001), pp. 255–278.
- [15] P. J. CAUDREY, *The inverse problem for a general $n \times n$ spectral equation*, Phys. D, 6 (1982/83), pp. 51–66.
- [16] P. G. DRAZIN, *Solitons*, vol. 85 of London Mathematical Society Lecture Note Series, Cambridge University Press, Cambridge, 1983.
- [17] P. G. DRAZIN AND R. S. JOHNSON, *Solitons: an introduction*, Cambridge Texts in Applied Mathematics, Cambridge University Press, Cambridge, 1989.
- [18] S. EL-WAKIL AND M. ABDOU, *Modified extended tanh-function method for solving nonlinear partial differential equations*, Chaos, Solitons & Fractals, 31 (2007), pp. 1256 – 1264.

- [19] S. EL-WAKIL, M. ABDOU, AND A. HENDI, *New periodic and soliton solutions of nonlinear evolution equations*, Applied Mathematics and Computation, 197 (2008), pp. 497 – 506.
- [20] P. G. ESTEVEZ AND S. LEBLE, *A wave equation in 2+1: Painleve analysis and solutions*, Inverse Probl., 11 (1995), p. 925.
- [21] L. D. FADDEEV, *Increasing solutions of the schrödinger equation*, Sov. Phys. Dokl, 10 (1966), pp. 1033–1035.
- [22] B. F. FENG, T. KAWAHARA, AND T. MITSUI, *A conservative spectral method for several two-dimensional nonlinear wave equations*, Journal of Computational Physics, 153 (1999), pp. 467 – 487.
- [23] P. FRYCZ AND E. INFELD, *Self-focusing of nonlinear ion-acoustic waves and solitons in magnetized plasmas. part 3. Arbitrary-angle perturbations, period doubling of waves*, J. Plasma Phys., 41 (1989), pp. 441–446.
- [24] P. FRYCZ AND E. INFELD, *Spontaneous transition from flat to cylindrical solitons*, Phys. Rev. Lett., 63 (1989), pp. 384–385.
- [25] P. FRYCZ, E. INFELD, AND J. C. SAMSON, *Spontaneous transition from flat to spherical solitons*, Phys. Rev. Lett., 69 (1992), pp. 1057–1060.
- [26] G. GALLAVOTTI, ed., *The Fermi-Pasta-Ulam problem*, vol. 728 of Lecture Notes in Physics, Springer, Berlin, 2008. A status report.
- [27] C. S. GARDNER, J. M. GREENE, M. D. KRUSKAL, AND R. M. MIURA, *Method for solving the Korteweg–deVries equation*, Phys. Rev. Lett., 19 (1967), pp. 1095–1097.
- [28] R. HANG-YU, *Reflection and reconnection interactions of resonant dromions*, Phys. Scr., 75 (2007), p. 201.

- [29] R. HIROTA, *Exact N -soliton solutions of the wave equation of long waves in shallow-water and in nonlinear lattices*, J. Math. Phys., 14 (1973), pp. 810–814.
- [30] E. INFELD, *Self-focusing of nonlinear ion-acoustic waves and solitons in magnetized plasmas*, J. Plasma Phys., 33 (1985), pp. 171–182.
- [31] E. INFELD AND P. FRYCZ, *Self-focusing of nonlinear ion-acoustic waves and solitons in magnetized plasmas. part 2. Numerical simulations, two-soliton collisions*, J. Plasma Phys., 37 (1987), pp. 97–106.
- [32] E. INFELD AND G. ROWLANDS, *Nonlinear waves, solitons and chaos*, Cambridge University Press, Cambridge, second ed., 2000.
- [33] E. INFELD, G. ROWLANDS, AND A. SENATORSKI, *Instabilities and oscillations of one and two-dimensional Kadomtsev-Petviashvili waves and solitons*, Proc R Soc A, 455 (1999), pp. 4363–4381.
- [34] B. KADOMTSEV AND V. PETVIASHVILI, *On the stability of solitary waves in weakly dispersing media*, Soviet Physics Doklady, 15 (1970), pp. 539–+.
- [35] K. KNUDSEN, J. L. MUELLER, AND S. SILTANEN, *Numerical solution method for the dbar-equation in the plane*, J. Comp. Phys., 198 (2004), pp. 500–517.
- [36] B. KONOPELCHENKO AND A. MORO, *Geometrical optics in nonlinear media and integrable equations*, J. Phys. A, 37 (2004), pp. L105–L111.
- [37] ———, *Integrable equations in nonlinear geometrical optics*, Stud. Appl. Math., 113 (2004), pp. 325–352.
- [38] D. KORTEWEG AND G. VRIES, *On the change of form of long waves advancing in a rectangular canal, and on a new type of long stationary wave*, Philos. Mag. Ser., 5 (1895), pp. 422–443.

- [39] N. A. KUDRYASHOV, *Seven common errors in finding exact solutions of nonlinear differential equations*, Communications in Nonlinear Science and Numerical Simulation, 14 (2009), pp. 3507 – 3529.
- [40] E. KUZNETSOV, M. SPECTOR, AND G. FAL’KOVICH, *On the stability of nonlinear waves in integrable models*, Physica D: Nonlinear Phenomena, 10 (1984), pp. 379 – 386.
- [41] H. LAN AND K. WANG, *Exact solutions for some nonlinear equations*, Physics Letters A, 137 (1989), pp. 369 – 373.
- [42] M. LASSAS, J. L. MUELLER, AND S. SILTANEN, *Mapping properties of the nonlinear Fourier transform in dimension two*, Communications in Partial Differential Equations, 32 (2005), pp. 591–610.
- [43] M. LASSAS, J. L. MUELLER, S. SILTANEN, AND A. STAHEL, *The Novikov-Veselov Equation and the Inverse Scattering Method, Part I: Analysis*, ArXiv e-prints, (2011).
- [44] ———, *The Novikov-Veselov Equation and the Inverse Scattering Method, Part II: Computation*, Preprint, (2011).
- [45] P. LAX, *Integrals of nonlinear equations of evolution and solitary waves*, Comm. Pure Appl. Math., 21 (1968), pp. 467–490.
- [46] S.-Y. LOU, C.-L. CHEN, AND X.-Y. TANG, *(2+1)-dimensional $(m + n)$ -component akns system: Painlevé integrability, infinitely many symmetries, similarity reductions and exact solutions*, Journal of Mathematical Physics, 43 (2002), pp. 4078–4109.
- [47] S.-Y. LOU AND J. LU, *Special solutions from the variable separation approach: the Davey - Stewartson equation*, J. Phys. A: Math. Gen., 29 (1996), pp. 4209–4215.

- [48] S. Y. LOU AND X. Y. TANG, *Methods of Nonlinear Mathematical Physics*, 32, Science Press, Beijing, 2002.
- [49] V. B. MATVEEV AND M. A. SALLE, *Darboux transformations and solitons*, Springer Series in Nonlinear Dynamics, Springer-Verlag, Berlin, 1991.
- [50] S. MUNRO AND E. J. PARKES, *The derivation of a modified Zakharov-Kuznetsov equation and the stability of its solutions*, J. Plasma Phys., 62 (1999), pp. 305–317.
- [51] ———, *Stability of solitary-wave solutions to a modified Zakharov-Kuznetsov equation*, J. Plasma Phys., 64 (2000), pp. 411–426.
- [52] A. I. NACHMAN, *Global uniqueness for a two-dimensional inverse boundary value problem*, Annals of Mathematics, 143 (1996), pp. 71–96.
- [53] J. NICKEL, V. S. SEROV, AND H. W. SCHURMANN, *Some elliptic traveling wave solutions to the Novikov–Veselov equation*, Progress In Electromagnetics Research, 61 (2006), pp. 323–331.
- [54] S. P. NOVIKOV AND A. P. VESELOV, *Finite-zone, two-dimensional, potential Schrödinger operators. explicit formulas and evolution equations*, Sov. Math. Dokl, 30 (1984), pp. 558–591.
- [55] ———, *Two-dimensional Schrödinger operator: inverse scattering transform and evolutionary equations*, Physica D, 18 (1986), pp. 267–273.
- [56] P. A. PERRY, *Miura maps and inverse scattering for the Novikov–Veselov equation*, ArXiv e-prints:1201.2385, (2012).
- [57] G. ROWLANDS, *Stability of non-linear plasma waves*, Journal of Plasma Physics, 3 (1969), pp. 567–576.
- [58] I. SHINGAREVA AND C. LIZARRAGA-CELAYA, *Solving Nonlinear Partial Differential Equations with Maple and Mathematica*, Springer, 2011.

- [59] I. TAIMANOV AND S. TSARËV, *On the Moutard transformation and its applications to spectral theory and soliton equations*, Journal of Mathematical Sciences, 170 (2010), pp. 371–387. 10.1007/s10958-010-0092-x.
- [60] X. TANG AND Z. LIANG, *Variable separation solutions for the (3+1)-dimensional Jimbo-Miwa equation*, Phys. Lett. A, 351 (2006), pp. 398 – 402.
- [61] X.-Y. TANG AND S.-Y. LOU, *A variable separation approach to solve the integrable and nonintegrable models: coherent structures of the (2+1)-dimensional KdV equation*, Commun. Theor. Phys. (Beijing), 38 (2002), pp. 1–8.
- [62] X.-Y. TANG AND S.-Y. LOU, *Multi-linear variable separation approach to nonlinear systems*, Front. Phys. China, 4 (2009), pp. 235–240.
- [63] X.-Y. TANG, S.-Y. LOU, AND Y. ZHANG, *Localized excitations in (2+1)-dimensional systems*, Phys. Rev. E, 66 (2002), p. 046601.
- [64] T. TSAI, *Nonlinear evolutions of the Schrödinger operator in \mathbb{R}^2* , PhD thesis, Yale University, (1989).
- [65] ———, *The Schrödinger operator in the plane*, Inverse Problems, 9 (1993), pp. 763–787.
- [66] ———, *The associated evolution equations of the Schrödinger operator in the plane*, Inverse Problems, 10 (1994), pp. 1419–1432.
- [67] M. WANG AND X. LI, *Extended f -expansion method and periodic wave solutions for the generalized Zakharov equations*, Physics Letters A, 343 (2005), pp. 48 – 54.
- [68] A. WAZWAZ, *Multiple soliton solutions for the (2+1)-dimensional asymmetric Nizhnik-Novikov-Veselov equation*, Nonlinear Analysis: Theory, Methods & Applications, 72 (2010), pp. 1314 – 1318.

- [69] G. B. WHITHAM, *Non-linear dispersive waves*, Proceedings of the Royal Society of London. Series A, Mathematical and Physical Sciences, 283 (1965), pp. 238–261.
- [70] ———, *Variational methods and applications to water waves*, Proceedings of the Royal Society of London. Series A, Mathematical and Physical Sciences, 299 (1967), pp. 6–25.
- [71] Z. YAN, *New jacobi elliptic function solutions of $(2 + 1)$ – dimensional complex nonlinear integrable system*, Int J. Modern Phys C, (2003), p. 277.
- [72] S. YUE LOU AND G. JIONG NI, *The relations among a special type of solutions in some $(d+1)$ -dimensional nonlinear equations*, J. Math. Phys., 30 (1989), pp. 1614–1620.
- [73] N. J. ZABUSKY, *Fermi–Pasta–Ulam, solitons and the fabric of nonlinear and computational science: History, synergetics, and visiometrics*, Chaos: An Interdisciplinary Journal of Nonlinear Science, 15 (2005), p. 015102.
- [74] V. E. ZAKHAROV AND A. B. SHABAT, *Exact theory of two-dimensional self-focusing and one-dimensional self-modulation of waves in nonlinear media*, Sov. Phys. JETP, 34 (1972), pp. 62–69.
- [75] S.-L. ZHANG AND S.-Y. LOU, *Variable separation and derivative-dependent functional separable solutions to generalized KdV equations*, Commun. Theor. Phys. (Beijing), 40 (2003), pp. 401–406.
- [76] C.-L. ZHENG, J.-P. FANG, AND L.-Q. CHEN, *New variable separation excitations of $(2+1)$ -dimensional dispersive long-water wave system obtained by an extended mapping approach*, Chaos, Solitons & Fractals, 23 (2005), pp. 1741 – 1748.
- [77] C.-L. ZHENG, H.-P. ZHU, AND L.-Q. CHEN, *Exact solution and semifolded struc-*

tures of generalized Broer-Kaup system in (2+1)-dimensions, Chaos, Solitons & Fractals, 26 (2005), pp. 187 – 194.